Glasnik hemičara i tehnologa Bosne I Hercegovine

Bulletin of the Chemists and Technologists of Bosnia and Herzegovina

Print ISSN: 0367-4444
Online ISSN: 2232-7266

45

December 2015.

Prirodno-matematički fakultet Sarajevo
Faculty of Science Sarajevo

Glasnik hemičara i tehnologa Bosne I Hercegovine

Bulletin of the Chemists and Technologists of Bosnia and Herzegovina

Print ISSN: 0367-4444
Online ISSN: 2232-7266

45

December 2015.

Prirodno-matematički fakultet Sarajevo
Faculty of Science Sarajevo

Glasnik hemičara i tehnologa Bosne i Hercegovine

Print ISSN: 0367-4444
Online ISSN: 2232-7266

Bulletin of the Chemists and Technologists of Bosnia and Herzegovina

Zmaja od Bosne 33-35, BA-Sarajevo
Bosnia and Herzegovina
Phone: +387-33-279-918
Fax: +387-33-649-359
E-mail: glasnik@pmf.unsa.ba
glasnikhtbh@gmail.com

REDAKCIJA / EDITORIAL BOARD

Časopis izlazi polugodišnje, a kompletna tekst verzija objavljenih radova je dostupna na http://www.pmf.unsa.ba/hemija/glasnik.

The journal is published semiannual, and full text version of the papers published are available free of cost at http://www.pmf.unsa.ba/hemija/glasnik.

Citiran u *Chemical Abstracts Service*.

Cited by *Chemical Abstracts Service*.

www.cas.org

Citiran u *EBSCO Host*.

Cited by *EBSCO Host*.

Glasnik hemičara i tehnologa Bosne i Hercegovine

Bulletin of the Chemists and Technologists of Bosnia and Herzegovina

Print ISSN: 0367-4444
Online ISSN: 2232-7266

2015
Issue *45*

CONTENT / SADRŽAJ

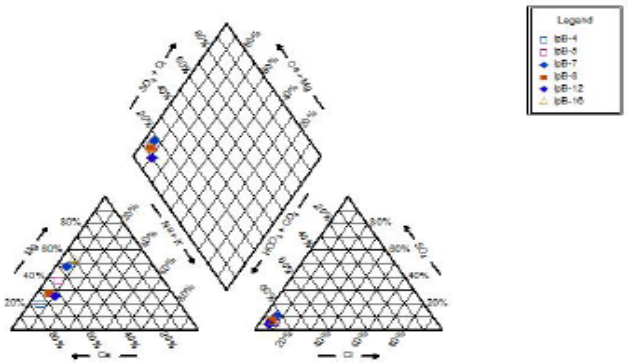

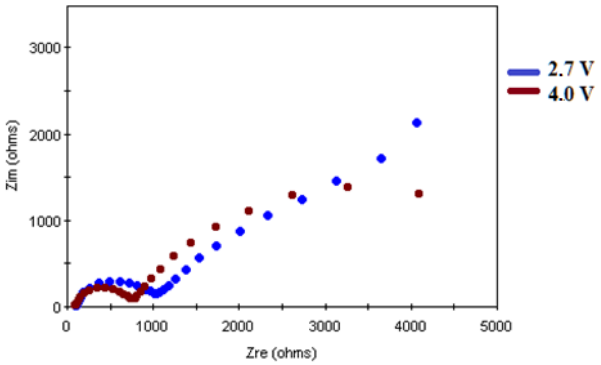

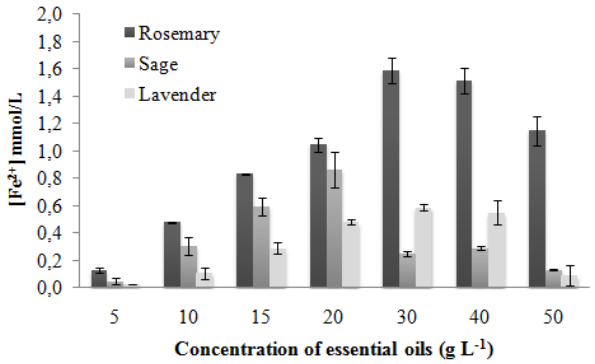

Water samples	Gross alpha activity (Bq/g)	Gross beta activity (Bq/g)
1	0.019	0.00318
2	0.00115	0.177
3	0.0112	0.0584
4	0.034	0.0123
5	0.00439	0.105

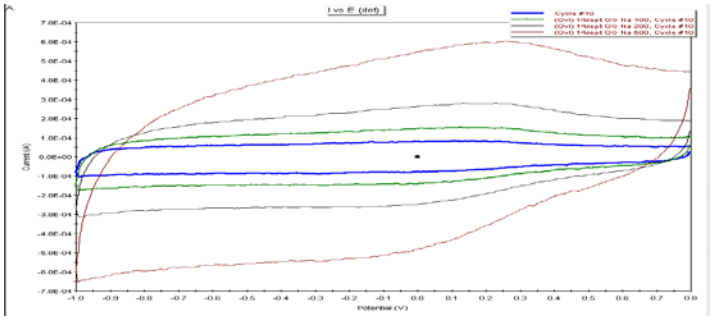

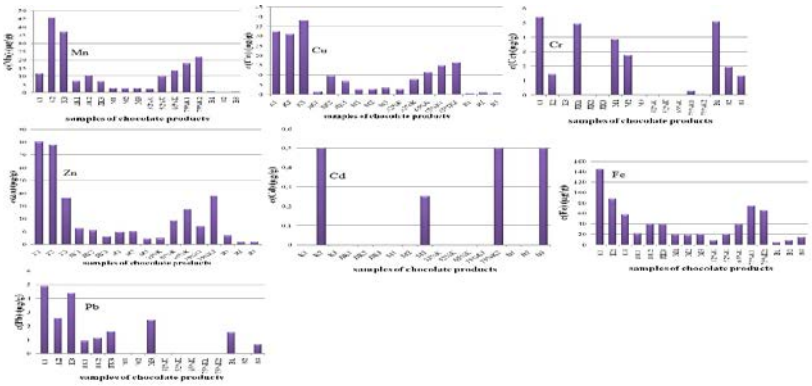

Item No.	1	2	3	4	5	6	7	8	9	10
f (%) TK 8th grade-1	59.6	35.1	42.8	9.1	72.9	51.6	25.4	50.9	36.6	33.4
f (%) TK 8th grade-2	45.6	33.3	45.7	31.5	85.1	56.1	29.8	73.7	64.9	44.2

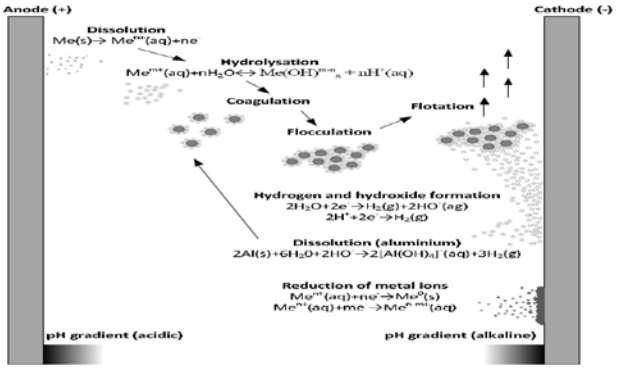

Editorial

Sarajevo is not the only capital city suffering from air pollution during the winter period. The European Environment Agency reported that a significant proportion of Europe's population lives in areas, especially cities, where exceedances of air quality standards occur: ozone, nitrogen dioxide and particulate matter (PM) pollution pose serious health risks. Heavy fog and smog are not uncommon in Sarajevo which lies in a valley surrounded by mountains. The problem becomes more serious in winter when many residents burn coal or wood for heating.

The World Health Organization estimates that over 7 million deaths annually caused by respiratory disease, cardiovascular disease and cancer can be attributed to air pollution globally. In many cities, breathing has become dangerous - particularly in cities, and this will worsen with increasing climate change.

A historic international climate agreement was signed at the COP21 (21st annual session of the Conference of the Parties) United Nations climate summit in Paris by negotiators from 195 countries. The agreement is designed to reduce greenhouse gas emissions and limit the average rise in global temperatures to 2 degrees Celsius above pre-industrial times.

Many of the steps needed to prevent climate change have positive health benefits. For example, increased use of public transport instead of personal cars in industrialized countries will reduce greenhouse gas emissions. It will also improve air quality and lead to better respiratory health and fewer premature deaths. Furthermore, the increase in physical activity from walking may lead to less obesity and fewer obesity-related illness. The sooner these steps are taken, the greater their impact will be on public health.

Editors

Glasnik hemičara i tehnologa Bosne i Hercegovine

Bulletin of the Chemists and Technologists of Bosnia and Herzegovina

2015

45

1-8

Print ISSN: 0367-4444
Online ISSN: 2232-7266

UDC: _____

Original Scientific Article

Bis(iminato)ruthenates(III): Correlation of Half-wave Potential and Hydrolysis Constant with Electronic Effects of Substituent

Zahirović A., Turkušić E., Kahrović E.*

Laboratory for Inorganic Chemistry, Department of Chemistry, Faculty of Science, University of Sarajevo, Zmaja od Bosne 35, 71 000 Sarajevo, Bosnia and Herzegovina

Article info
Received: 10/11/2015
Accepted: 01/12/2015

Keywords:
Ruthenium
Schiff base
Substituent effect
Cyclic voltammetry
Spectroscopy

***Corresponding author:**
E-mail: emira_kahrovic@yahoo.com
Phone: +387-33-279-910

Abstract: Influence of electronic effects of substituent on Schiff base ligands, derived from salicylaldehyde and 5-substituted salicylaldehydes with 2-aminophenole, on half-wave potential and hydrolysis constants of Sodium bis(iminato)ruthenates(III) hemitriethylamine solvate was investigated by cyclic voltammetry and electronic spectroscopy. New complex, Sodium bis[*N*-(2-oxy-κO-phenyl)salicylideneimine-$\kappa^2 N,O$(1-)]ruthenate(III) hemitriethylamine solvate was prepared and characterized on the basis of infrared and electron spectroscopy, MALDI-TOF/TOF mass spectrometry and ruthenium content. Cyclic voltammograms of complexes in organic solvents demonstrate quasi-reversible one-electron process with pronounced reducing power of Ru(II). Appling Hammet equation for half-wave potential of complexes we found that substituents conduct electronic density *via* X-C_6H_3-O-Ru-O-C_6H_3-X bonds. Electron spectroscopy was used to investigate behavior of complexes under physiological conditions and showed that hydrolysis occur. Constants of hydrolysis were determined spectrophotometrically using kinetics of pseudo-first order.

INTRODUCTION

During the last fifty years chemistry of ruthenium complexes is in focus of research in at least two fields: (i) bioinorganic chemistry, due to biological activity of compounds which exhibit antitumor (Rademaker-Lakhai *et al.*, 2004; Kahrović, 2011) and antibacterial properties (Jayabalakrishnan *et al.*, 2002), (ii) material science, due to potential usage as catalysts (Scholl *et al.*, 1999), (bio)sensors (Zhang *et al.*, 2008) and solar cells based materials (Wang *et al.*, 2003). Concerning the biological activity of ruthenium based compounds there are two important factors that strongly control their activity, reduction potential and hydrolysis ability. It is found that well-known antimetastatic drug, NAMI-A named Imidazolium *trans*-[tetrachloro(dimethyl--sulfoxide-κS)(imidazole-κN)ruthenate(III)] reaches its maximum activity after reduction *in situ*, which indicates significance of reduction potential on activity of Ru compounds (Sava *et al.*, 2002). On the other hand, activity of another clinically important compound ICR, indazole analog of NAMI-A, is dependent on hydrolysis of acido-ligand, demonstrating that kinetics of ligand substitution is also essential factor for biological activity of these metallofaramaceutics (Vargiu *et al.*, 2008). In the frame of our investigation on ruthenium compounds we report here on the effect of the substituent on Scfiff bases in bis(iminato)ruthenium(III) complexes on redox potentials and constants of hydrolysis, as essential in design and development of new potential anticancer drugs.

EXPERIMENTAL

Materials and methods

All chemicals were commercially available, analytical grade of purity, and used without further purification. Tetraethylammonium perchlorate was prepared from bromide salt as previously described (Kolthoff *et al.*, 1957). Complexes Sodium bis[*N*-(2-oxy-*κO*-phenyl)-5-substituted-salicylideneimine-κ^2*N*,*O*(1-)]ruthenate(III) hemitriethylamine solvate, hereinafter Na[Ru(*N*-R-5-X-salim)$_2$] × ½ Et_3N, where Et_3N= triethylamine, R = C_6H_4O and X = Cl, Br or NO_2 were prepared by published procedure (Kahrović *et al.*, 2014). Purity was checked by FTIR and electronic spectra. Complex in which X = H was prepared on the basis of the same general procedure and was characterized by infrared and electron spectroscopy, MALDI/TOF-TOF (matrix assisted laser desorption / ionization – time of flight) mass spectrometry, FA AAS (flame atomization atomic absorption spectroscopy) and cyclic voltammetry.

Synthesis of N-(2-hydroxyphenyl)salicylideneimine

Ligand *N*-(2-hydroxyphenyl)salicylideneimine, here in after *N*-RH-5-H-salimH (R = C_6H_4O) was prepared according to published procedure (Ligtenbarg *et al.*, 1999). *Yield*: 0.33 g (80 %).

Synthesis of Na[Ru(N-R-5-H-salim)$_2$] × ½ Et_3N

Ruthenium trichloride hydrate (Ru content 40 – 42%) (0.5 mmol, 0.13 g) was dissolved in absolute ethanol (5 mL) and ethanol mixture (40 mL) of *N*-(2-hydroxyphenyl)salicylideneimine (1 mmol, 0.21 g) and triethylamine (1 mmol, 0.13 mL) was added dropwise. Brownish solution was heated in rotary evaporator with constant stirring during 4 hours at 70°C changing its color to dark green. After the mixture was cooled to room temperature aqueous solution (0.5 mL) of NaCl (0.5 mmol, 0.03 g) was added to precipitate anionic complex. Weakly crystalline dark green powder of compound was obtained after reducing volume of solvent to half and cooling the mixture in ice. Product was filtered off, washed with ethanol (2 × 5 mL), water (2 × 5 mL) and petrol ether (2 × 5 mL). Recrystallization was made from mixed solvent ethanol:dichloromethane 1:1 v/v and complex was dried in vacuum desiccator. *Yield*: 0.12 g (78%).

Anal. Calc. for $NaRuC_{26}H_{18}N_2O_4 \times ½\ C_6H_{15}N$: Ru 16.93. *Found*: Ru: 16.55. MALDI-TOF/TOF MS *m / z* 100 %: 524.0306 $[C_{26}H_{18}N_2O_4Ru]^-$. IR (KBr) ν_{max}/ cm^{-1}: 1597 vs (C=N), 1288 m (C-O). IR (CsI) ν_{max}/ cm^{-1}: 393 w (Ru-O), 460 w (Ru-N). UV / Vis [CH_2Cl_2, λ_{max} / nm]: 334, 395 and 578 (ε / M^{-1} cm^{-1}): 9982, 13109 and 5397, respectively.

Physical measurements

Determination of ruthenium content was performed by flame atomization atomic absorption spectroscopy (FA AAS) on Varian AA 240 Z atomic absorption spectrophotometer by already reported procedure using standard curve method from DMSO solution (Rowston *et al.*, 1970).

Electron spectra measurements were performed on Perkin Elmer spectrophotometer Lambda 35. Electron spectrum of complex Na[Ru(*N*-R-5-H-salim)$_2$] × ½ Et_3N was recorded in dichloromethane in range from 200 to 700 nm. Hydrolysis of complexes of general formula Na[Ru(N-R-5-X-salim)$_2$] × ½ Et_3N were monitored spectrophotometrically for one hour recording spectra in three minute-intervals under physiological conditions, in Tris-HCl (Tris(hydroxymethyl)aminomethane) buffer pH 7.40 and in the presence of 150 mM NaCl. Complexes were initially dissolved in small volume of DMSO (dimethylsulfoxide) and then diluted to required concentration. Constants of hydrolysis were determined graphically by kinetics of pseudo-first order.

IR spectra were obtained on Perkin Elmer BX FTIR using KBr pallets technique in range 4000 – 400 cm^{-1}.

Electrochemical measurements were performed on Potentiostat /galvanostat Autolab 12 in 2.00 mL self-made three electrode electrochemical cell using glassy carbon electrode as working electrode, platinum wire as counter electrode and Ag/AgCl as reference electrode. Salt bridge with saturated KCl was used to minimize liquid junction potential. Cyclic voltammograms were recorded in DMF/$NaClO_4$ (dimethylformamide) in potential range -1.1 to 0.0 V and in MeCN/Et_4NClO_4 (acetonitrile) in range -1.1 to -0.5 V, both with scan rate of 0.3 Vs^{-1}. Working electrode was polished prior to measurements with 1 μm diamond paste.

Mass spectrum was obtained on a matrix–assisted laser desorption / ionization – Time – of – flight MALDI-TOF/TOF mass spectrometer (4800 Plus MALDI TOF/TOF analyzer, Applied Biosystems Inc., Foster City, CA, USA) equipped with Nd:YAG laser operating at 355 nm with firing rate 200 Hz in the negative ion reflector mode. 1600 shots per spectrum was taken with mass range 10−1500 Da, focus mass 500 Da and delay time 100 ns. Small amount of sample (on pipette tip) was resuspended in 10 μl of DHB (2,5-dihydroxybenzoic acid) MALDI matrix (5 mg/mL; dissolved in 50/50 acetonitrile/water, *v*/*v*) and 1 μl was spotted on MALDI plate. The spectrum was internally calibrated providing measured mass accuracy within 5 ppm of theoretical mass. Riboflavin and 3-aminosalicylic acid were used as internal calibrants in negative ion mode.

RESULTS AND DISCUSSION

Synthesis and spectroscopic characterization

Na[Ru(*N*-R-5-H-salim)$_2$] × ½ Et_3N was prepared as a part of homologous series of Na[Ru(*N*-R-5-H-salim)$_2$] × ½ Et_3N, where X = H, Cl, Br, NO_2 using procedure previously published by our team. Ruthenium(III) chloride and ligand were mixed in molar ratio 1:2 to

ensure replacement of all six positions on octahedrally coordinated Ru(III) with two tridentate dibasic Schiff base ligands. Anionic complex was precipitated by adding concentrated aqueous solution of sodium chloride. Air stable weakly crystalline dark green compound is insoluble in water and soluble in common polar organic solvents such as CH_2Cl_2, DMSO, DMF, MeCN, acetone etc.

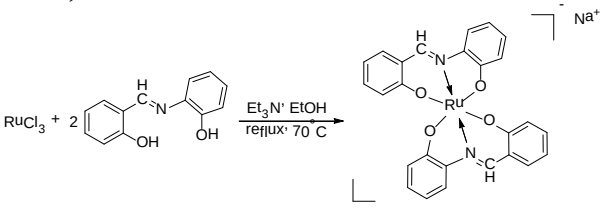

Figure 1. Synthesis of complex

The characterization is based on FA AAS, MALDI-TOF/TOF mass spectrometry, infrared and electron spectroscopy. Mass spectrum showed molecular ion (M^-) at *m/z* (100%) = 524.0306 confirming existence of $[C_{26}H_{18}N_2O_4Ru]^-$. Formulation of complex as Na[Ru(*N*-R-5-H-salim)$_2$] × ½ Et_3N was supported by FA AAS determination of ruthenium content.

Strong sharp absorption band positioned at 1632 cm^{-1} in IR spectrum of free ligand is attributed to CH=N stretching vibrations. After coordination the frequency was moved to lower wavenumber, and appears in spectrum of complex at 1597 cm^{-1} confirming coordination of ligand *via* azomethine nitrogen. On the other hand, phenolic C-O stretching vibration after coordination is shifted from 1276 cm^{-1} in ligand to 1288 cm^{-1} in spectrum of complex. Hypsochromic shift of 12 cm^{-1} is a result of the fact that C-O(Ru) bond is stronger than C-O(H) bond and confirms coordination *via* deprotonated oxygen atom. If a shift of CH=N and C-O bonds vibrations is taken as a rough measure of bond strength then new weak absorption bands in spectrum of complex positioned at 460 and 393 cm^{-1} can be ascribed to Ru-N and Ru-O bonds, respectively.

Absorption bands located in electronic spectrum of ligand and complex around 230 nm belong to intraligand aromat $\pi\rightarrow\pi^*$ transitions. Weakly defined absorption band at 270 nm is spectrum of ligand is attributed to $n\rightarrow\pi^*$ transition on phenolic oxygen and after coordination is shifted to 293 nm. Bathochromic shift of 23 nm is consequence of weaker localization of electron density (less covalent bond) in O-Ru compared to O-H bond and is in good correlation with infrared spectrum and coordination of ligand *via* deprotonated oxygen atom. Significant localization of electron pair of azomethine nitrogen after coordination is in correlation with 20 nm hypsochromic shift of the band located in spectrum of ligand at 354 nm. Broad absorption at 395 nm in spectrum of complex, which is not found in spectrum of ligand is ascribed to ligand metal charge transfer (LMCT). Weak absorption at 578 nm in spectrum of complex is assigned to *Lapport* forbidden spin allowed $t_{2g}^5\rightarrow t_{2g}^4e_g^1$ transition of low spin Ru(III).

Electrochemical behavior: Cyclic voltammetry studies

Cyclic voltammetry was used to investigate and correlate electrochemical properties of complexes with electronic effect of substituent on Schiff base ligand. Since the possibility of reduction *in vivo* is one of the most important parameters in design of new ruthenium based anticancer compounds due possibility to be activated through mechanism known as reduction *in situ*, determination of redox potentials is ultimate. Cyclic voltammograms of complexes in DMF/$NaClO_4$ and MeCN/Et_4NClO_4 showed quasi-reversible redox reaction and pronounced reduction character of Ru(II) in Ru(III)/Ru(II) pair. Although the ratio of cathodic and anodic current is nearly 1, separation of peaks is significantly higher than theoretically expected 59 mV for one-electron processes, 0.141 to 0.183 V in MeCN and 0.537 to 0.683 V in DMF. Reversibility in MeCN is improved compared to DMF, which can be ascribed to better coordinating properties of DMF. Quite negative values of half-wave electrode potential, -0.804 to -0.824 V in MeCN and -0.482 to -0.560 V in DMF correlate with O_4N_2 coordination environment of Ru(III). Small electronegative oxygen atom is hard in character and prefers binding with harder Ru(III) compared to Ru(II). On contrary, azomethine nitrogen is softer in character and stabilizes lower oxidation state. Since there are four atoms of oxygen in primary coordination sphere, Ru(III) is significantly stabilized making reduction significantly harder, which results with very negative $E_{1/2}$ values. Cyclic voltammograms are shown in Fig. 2. and data obtained from them are collected in Table 1.

Table 1. Data from cyclic voltammograms of Na[Ru(*N*-R-5-X-salim)$_2$] × ½ Et_3N in DMF / $NaClO_4$ and MeCN / Et_4NClO_4

	MeCN / Et_4NClO_4				DMF / $NaClO_4$			
X	E_c / V	E_a / V	$E_{1/2}$ / V	ΔE_p / V	E_c / V	E_a / V	$E_{1/2}$ / V	ΔE_p / V
H	-0.900	-0.725	-0.812	0.175	-0.828	-0.291	-0.560	0.537
Cl	-0.895	-0.712	-0.804	0.183	-0.814	-0.250	-0.532	0.564
Br	-0.883	-0.742	-0.812	0.141	-0.826	-0.240	-0.533	0.586
NO_2	-0.915	-0.734	-0.824	0.181	-0.823	-0.140	-0.482	0.683

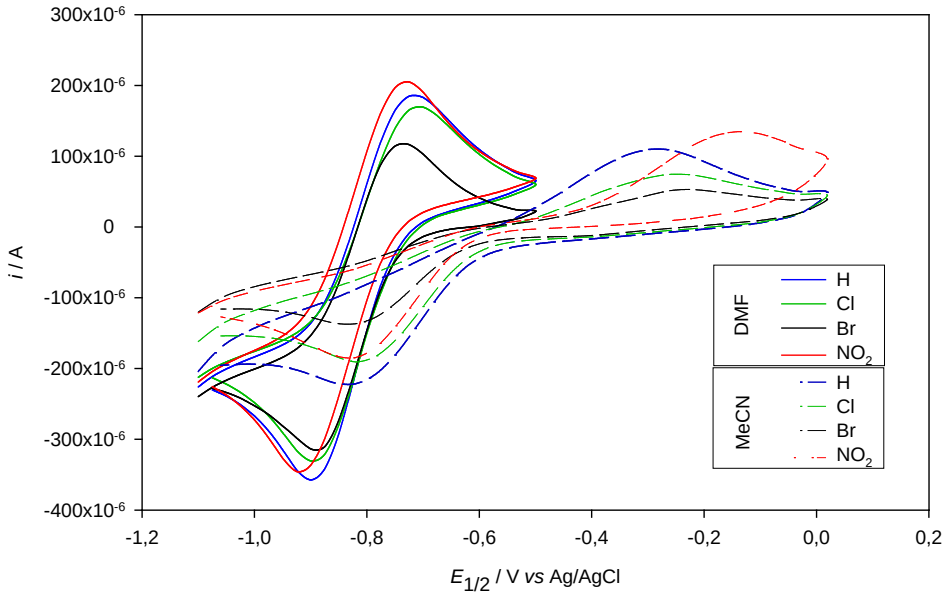

Figure 2. Cyclic voltammograms of Na[Ru(*N*-R-5-X-salim)$_2$] × ½ Et$_3$N in DMF / NaClO$_4$ and MeCN / Et$_4$NClO$_4$

Half-wave potential of a system involving metal complex is determined by many factors such as electronic effects of ligand, stereochemical characteristics of redox couples, degree of solvation, temperature and metal oxidation state.

If we consider electronic effects of ligand as a factor determining redox potential of a metal complex we can discuss about two ways that substituents affect electronic density. Electron withdrawing substituents on ligand system decrease electron density making reduction easier over oxidation and electron donating substituents facilitate oxidation over reduction. Changes in electron density are the result of two opposite ways of electron transport through σ bonds (inductive effect) and π bonds (resonance effect) of an aromatic system.

In the case of complex containing *N*-(2-hydroxyphenyl)5-nitrosalicylideneimine in MeCN, the most negative value, $E_{1/2}$ = -0.915 V, corresponds with strong electron withdrawing properties of nitro group, as a consequence of negative resonance effect and decrease of electron density on aromatic ring.

Character of halogen substituents is determined by two opposite effects: negative inductive effect due to their electronegativity and positive resonance effect due to three lone electron pairs. Since resonance effect is stronger than inductive, overall result is partial including of lone pair electrons in delocalization through aromatic ring resulting in more positive values of half wave potentials of halogen derivatives compared to hydrogen- and nitro-homologues. Bromo substituent has more diffused and weakly bonded lone pair electrons then chloro-derivate which results in more positive value of $E_{1/2}$.

Correlation of electronic effects of substituent on ligand system and half-wave potential was made on the basis of *Hammet* equation:

$$\Delta E = \rho \times \sigma \quad (\mathbf{1})$$

where ΔE is difference between the redox potential of the complex containing substituted and unsubstituted ligand respectively, ρ is constant which measures the sensitivity of the redox potential to the electronic effects of the substituents and σ is *Hammett* parameter which assigns a numerical value to the electronic effects of the substituents and normally refer to the inductive electronic effects of the substituents in *metha* or *para* positions of aromatic rings. Our model consider that substituent is in *metha* position to azomethine and in *para* position to phenol oxygen, as it is shown in Fig. 3.

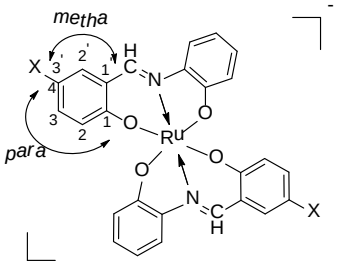

Figure 3. Position of substituent X according to azomethine group (*metha* position) and phenolic oxygen (*para* position) in complex anion [Ru(*N*-R-5-X-salim)$_2$]$^-$.

Table 2. *Hammet* values of constant in *metha* and *para* position of substituent X and half-potential values for Na[Ru(*N*-R-5-X-salim)$_2$] × ½ Et$_3$N in DMF/NaClO$_4$

X	σ_{metha}	σ_{para}	$E_{1/2}$ / V
H	0.00	0.00	-0.560
Cl	+ 0.37	+ 0.23	-0.532
Br	+ 0.39	+ 0.23	-0.533
NO_2	+ 0.78	+ 0.71	-0.482

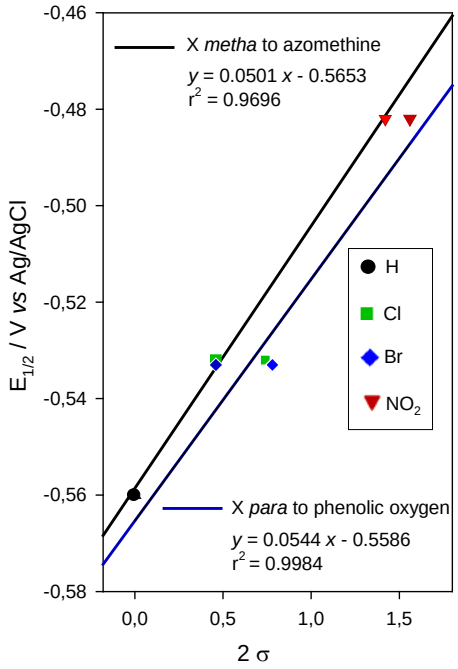

Figure 4. Dependence of half-wave potential for Na[Ru(*N*-R-5-X-salim)$_2$] × ½ Et$_3$N in DMF/NaClO$_4$ on electronic effects of substituent X: Substituent is in *para* position according to phenolic oxygen (blue line) and *metha* position according to azomethine group (black line).

Diagram shown in Fig. 4. demonstrates linear correlation between $E_{1/2}$ and substituent in position 5- on salicylaldehyde part of Schiff base. Correlation coefficient of linear regression (Zanello, 2003) suggests that substituents conduct electronic density *via* X-C$_6$H$_3$-O-Ru-O-C$_6$H$_3$-X bonds (r^2 = 0.9984), but conduction *via* X-C$_6$H$_3$-CH=N-C$_6$H$_3$-X bonds (r^2 = 0.9639) is also not *a priori* excluded. Linearity is not found in the case of less solvating MeCN.

Behavior in solution: Hydrolysis by electronic spectroscopy studies

Taking into account that substituents affect electron density of aromatic system we investigated correlation between rate of hydrolysis of bis(iminato)ruthenates(III) under physiological solution with substituent X in [Ru(*N*-R-5-X-salim)$_2$]$^-$. Since Ru(III) is an inert low spin t_{2g}^5 system and complexes Na[Ru(*N*-R-5-X-salim)$_2$] × ½ Et$_3$N absorb in UV/Vis region of electromagnetic spectrum, electron spectroscopy was used for hydrolysis studies. Study of hydrolysis in physiological solution is essential since ligand-water exchange reaction is of great importance for potential biological properties of the drugs.

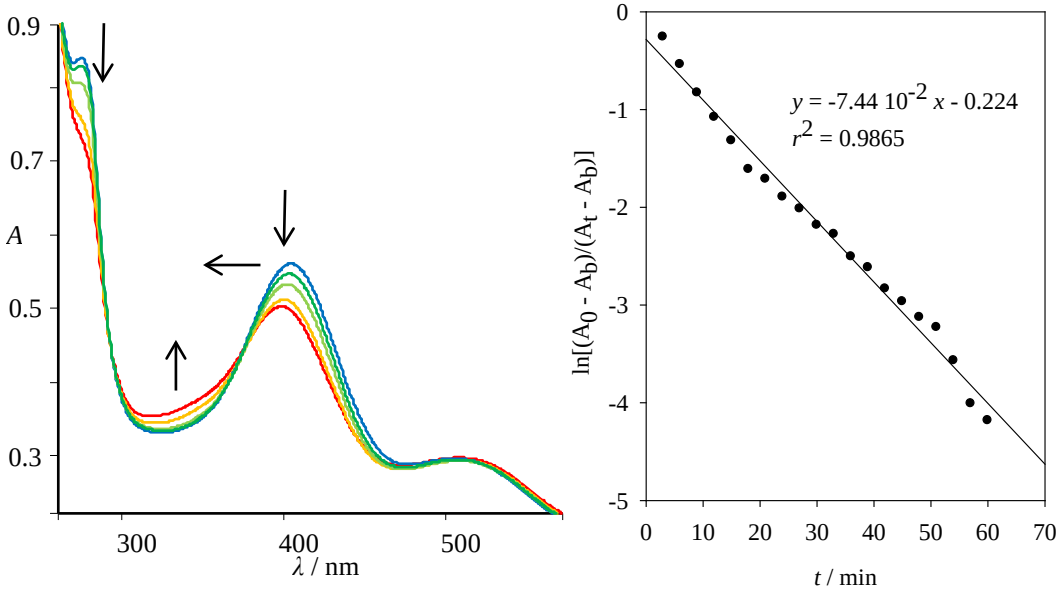

Figure 5. Left: Hydrolysis of Na[Ru(*N*-R-5-Cl-salim)$_2$] × ½ Et$_3$N during an hour. Right: Graphical determination of hydrolysis constant of Na[Ru(*N*-R-5-Cl-salim)$_2$] × ½ Et$_3$N by kinetics of pseudo-first order.

Isosbestic points in hydrolytic profile of complex compounds undoubtedly confirm simultaneous existence of two species in solution as a result of hydrolysis. Ligand to metal charge transfer bands centered near 400 nm are characterized with moderate hypochromism and hypsochromic shift, which correlates with entrance of hydroxyl ion (pH 7.40) in primary coordination sphere. Since the hydrolysis of 10^{-5} M complex compounds was performed in 0.1 M buffered system, keeping concentration of hydroxyl ions constant, rate of hydrolysis is only dependent on complex making this reaction of pseudo-first order. Hydrolysis constants were determined graphically using equation:

$$k = 1/t \times \ln[(A_0 - A_\infty)/(A_t - A_\infty)] \quad (2)$$

where A_0 is the absorbance at the beginning, A_t absorbance in time t and A_∞ is absorbance after $10t_{1/2}$.

Table 3. Hydrolysis constants of complexes Na[Ru(*N*-R-5-X-salim)$_2$] × ½ Et$_3$N under physiological conditions at 294 K measured at LMCT

X	λ / nm	10^{-2} k_H / min^{-1}
H	395	8.31
Cl	416	7.44
Br	404	4.99
NO_2	377	4.60

Hydrolysis constants of complexes have 10^{-2} min^{-1} magnitude. Measured values of k_H suggest that 5-X-substituent on Schiff bases has impact on hydrolysis constant of complexes, which decrease in order H > Cl > Br > NO_2. There are few theoretically possible pathways for hydrolysis of Na[Ru(*N*-R-5-X-salim)$_2$] × ½ Et$_3$N (Fig. 6.)

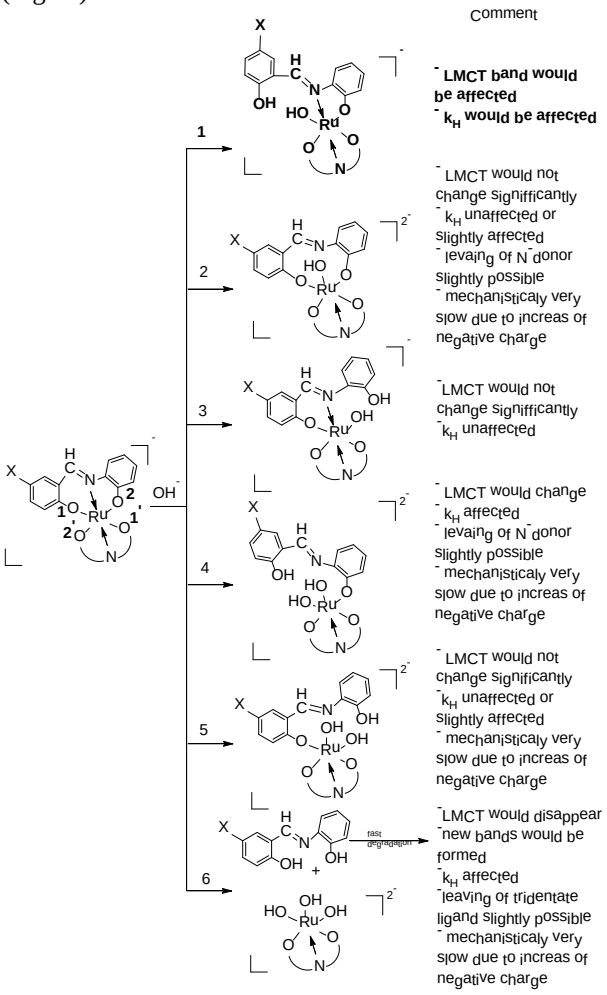

Figure 6. Possible pathways for hydrolysis of complex with short comments. Second ligand molecule was omitted for clarity.

Regarding comments from Fig. 6 hydrolysis occur most probably by pathway 1. Few factors might be determining for k_H values in the case of studied complexes: (i) strength of Ru-O bond, (ii) size of ligand, (iii) electronic effect of substituent. All other parameters that can affect k_H were kept constant (ionic strength, temperature, charge or basic octahedral geometry of complex etc.). The change in vibration frequency of C-O bond in free and bound ligand is rough measure of Ru-O bond strength. Significant change in vibration frequency of C-O bond means weak Ru-O bond and *vice versa*. Change in stretching vibrations of C-O bond for H, Cl, Br and NO_2 are 12, 15, 16 and 19 cm^{-1}, respectively (Kahrović *et al.*, 2014), meaning that strength of Ru-O(1) bond increases in order H < Cl < Br < NO_2. This is in excellent correlation with the fact that strengthening of Ru-O(1) bond leads to decrease of k_H value. Size of ligand increases in order H < Cl < Br ~ NO_2 while constant of hydrolysis decrease. This can be interpreted in the light of solvatation theory, meaning that the degree of solvation decreases with increasing of particle size. Moving from H- to NO_2 derivative of [Ru(*N*-R-5-X-salim)$_2$]$^-$, the number of nucleophile species (OH^-) available in second coordination sphere for binding to the metal atom decreases resulting in decrease of k_H value.

Variation of hydrolysis constants for different 5-X-substituents shows that the entry of OH^- nucleophile into the first coordination sphere of metal center occurs on account of breaking of Ru-O bond that comes from salicylaldehyde part of Schiff bases thus supporting pathway 1(Fig. 6.) for hydrolysis.

Obviously not only effects of substituents are responsible for k_H values of complexes, rather overall effect concerning Ru-O bond strength, size of ligand and electronic effects of substituents are determining for k_H.

The constant of hydrolysis and half wave potentials confirm that Ru(III) complexes Na[Ru(*N*-R-5-X-salim)$_2$] × ½ Et$_3$N are sufficiently inert toward hydrolysis at physiological condition, also might be stable toward different reducing agents, e.g. ascorbic acid or glutathione in biological environment, which recommend these complexes for further studies.

CONCLUSION

A new complex of ruthenium(III) with Schiff base derived from salicylaldehyde and 2-aminophenole was prepared as a homologue of Na[Ru(*N*-R-5-X-salim)$_2$] × ½ Et$_3$N, where X = Cl, Br, NO_2, published by our team recently. The compound is characterized using different spectroscopic and spectrometric techniques. Low spin ruthenium(III) is octahedrally chelated with two dibasic tridentate Schiff base ligands. Four complexes named Sodium bis[*N*-(2-oxy-κO-phenyl)-5-substituted salicylideneimine-$\kappa^2 N,O$(1-)]ruthenate(III) hemitriethylamine solvate were investigated using electron spectroscopy and cyclic voltammetry to study correlation between electronic effects of substituent on Schiff base ligand of complexes and half-wave potential and rate of hydrolysis. We found that ability of hydrolysis and reduction potential can be tuned up by manipulations of substituent on ligand system, which can be very useful in design of new anticancer drugs with required well defined properties.

REFERENCES

Jayabalakrishnan, C., Natarajan, K. (2002). Ruthenium (II) carbonyl complexes with tridentate Schiff bases and their antibacterial activity. *Transition Metal Chemistry*, *27 (1),* 75-79.

Kahrovic, E. (2011). Chemical feature of inorganic compounds as anticancer agents. *HealthMED, 5(5),* 1112-1116.

Kahrovic, E., Zahirovic, A., Turkusic, E. (2014). Calf Thymus DNA Intercalation by Anionic Ru (III) Complexes Containing Tridentate Schiff Bases Derived from 5-X-Substituted Salicyladehyde and 2-Aminophenol. *Journal of Chemistry and Chemical Engeenering*, *8*, 335-343.

Kolthoff, I. M., Coetzee, J. F. (1957). Polarography in Acetonitrile. 1 I. Metal Ions which Have Comparable Polarographic Properties in Acetonitrile and in Water. *Journal of the American Chemical Society*, *79 (4),* 870-874.

Ligtenbarg, A. G., Hage, R., Meetsma, A., Feringa, B. L. (1999). Hydrogen bonding properties and intermediate structure of N-(2-carboxyphenyl) salicylidenimine. *Journal of the Chemical Society, Perkin Transactions 2 (4),* 807-812.

Rademaker-Lakhai, J. M., van den Bongard, D., Pluim, D., Beijnen, J. H., Schellens, J. H. (2004). A phase I and pharmacological study with imidazolium-trans-DMSO-imidazole-tetrachlororuthenate, a novel ruthenium anticancer agent. *Clinical Cancer Research*, *10 (11),* 3717-3727.

Rowston, W. B., Ottaway, J. M. (1970). The Determination of Ruthenium by Atomic Absorption Spectrophotometry. *Analytical Letters*, *3 (8),* 411-417.

Sava, G., Bergamo, A., Zorzet, S., Gava, B., Casarsa, C., Cocchietto, M., Mestroni, G. (2002). Influence of chemical stability on the activity of the antimetastasis ruthenium compound NAMI-A. *European Journal of Cancer*, *38 (3),* 427-435.

Scholl, M., Ding, S., Lee, C. W., Grubbs, R. H. (1999). Synthesis and Activity of a New Generation of Ruthenium-Based Olefin Metathesis Catalysts Coordinated with 1, 3-Dimesityl-4, 5-dihydroimidazol-2-ylidene Ligands .*Organic Letters*, *1 (6),* 953-956.

Vargiu, A. V., Robertazzi, A., Magistrato, A., Ruggerone, P., Carloni, P. (2008). The hydrolysis mechanism of the anticancer ruthenium drugs NAMI-A and ICR investigated by DFT-PCM calculations. *The Journal of Physical Chemistry B, 112 (14),* 4401-4409.

Wang, P., Zakeeruddin, S. M., Moser, J. E., Nazeeruddin, M. K., Sekiguchi, T., Grätzel, M. (2003). A stable quasi-solid-state dye-sensitized solar cell with an amphiphilic ruthenium sensitizer and polymer gel electrolyte. *Nature materials*, *2* (*6),* 402-407.

Zanello, P. (2003). *Inorganic electrochemistry: theory, practice and applications*. Royal Society of Chemistry.

Zhang, J., Qi, H., Li, Y., Yang, J., Gao, Q., & Zhang, C. (2008). Electrogenerated chemiluminescence DNA biosensor based on hairpin DNA probe labeled with ruthenium complex. *Analytical chemistry*, *80* (*8),* 2888-2894.

Summary/Sažetak

Uticaj elektronskih efekata supstituenata na Šifovim bazama kao ligandima, izvedenim iz salicilaldehida i 5-supstituiranih saliciladehida i 2-aminofenola, na polutalasni potencijal i konstante hidrolize odgovarajućih Natrij bis(iminato)rutenata(III) hemitrietilamin solvata je ispitan cikličkom voltametrijom i elektronskom spektroskopijom. Novi kompleks Natrij bis[*N*-(2-oksi-κO-fenil)salicilidenimin-$\kappa^2 N,O$(1-)]rutenat(III) hemitrietilamin je pripremljen i okarakterisan na bazi infracrvene i elektronske spektroskopije, MALDI-TOF/TOF masene spektrometrije i sadržaja rutenija. Ciklički voltamogrami kompleksa u organskim rastvaračima demonstitraju kvazi-reverzibilan jednoelektronski proces sa izraženom reducirajućom sposobnosti Ru(II). Primjenom Hametove jednačine na polutalsne potencijale kompleksa našli smo da supstituenti utiču na pomijeranje elektronske gustoće preko X-C_6H_3-O-Ru-O-C_6H_3-X veza. Elektronska spektroskopija je korištena za ispitivanje ponašanja kompleksa u fiziološkim uslovima i pokazala je da se dešava hidroliza. Konstante hidrolize su određene spektrofotometrijski na osnovu kinetike pseudo-prvog reda.

Glasnik hemičara i tehnologa Bosne i Hercegovine

Bulletin of the Chemists and Technologists of Bosnia and Herzegovina

2015

45

Print ISSN: 0367-4444

UDC: _____

Online ISSN: 2232-7266

Original Scientific Article

9-12

Antioxidant potential of selected traditional plant-based beverages in Bosnia and Herzegovina

Marjanović, A.[a, *], Đedibegović, J.[a], Brčaninović, M.[a], Omeragić, E.[a], Čaklovica, F.[b], Dobrača, A.[a], Šober, M.[a]

[a]*Faculty of Pharmacy, University of Sarajevo, Zmaja od Bosne 8, Sarajevo, BiH*

[b]*Faculty of Veterinary Medicine, University of Sarajevo, Zmaja od Bosne 90, Sarajevo, BiH*

Article info
Received: 11/06/2015
Accepted: 03/12/2015

Keywords:
Antioxidants
Elder
Blackberry
Pomegranate
Boza
Juniper

***Corresponding author:**
E-mail: aca1902@gmail.com
Phone: 00-387-33-586178
Fax: 00-387-33-586178

Abstract: The main aim of our work was to determine antioxidant capacity of some traditional non-alcoholic beverages in Bosnia and Herzegovina. Eight samples of traditionally prepared beverages were tested by DPPH and FRAP assay. Total phenolic content was determined by Folin-Ciocalteau method and anthocyanidines by Vanilin-HCl method. Total phenolic content was in range of 74.31 mg TEA/L (elder juice with lemon) to 3 365.35 mg TEA/L (pomegranate juice). Anthocyanidines content ranged from 125.27 mg/L (elder juice without lemon) to 1899.08 mg/L (traditionally prepared blackberry juice). Pomegranate juice exhibited the strongest activity against DPPH radicals (75.29% inhibition). The DPPH determined antioxidant capacity showed positive correlation with total phenolic content as well as with flavonoids content. FRAP assay showed stronger antioxidant capacity for most of the samples, compared to ascorbic acid standard. The analyzed traditionally prepared beverages showed strong antioxidant capacity which was even more pronounced than in the commercial juice.

INTRODUCTION

Oxidative stress is deemed to play important role in many acute and chronic diseases (Polimeni *et al.*, 2015; Cobb and Cole, 2015). The burden of chronic diseases like cardiovascular, neurodegenerative diseases and cancer is constantly rising, and so does the research in the field of antioxidants (Pisoschi and Pop, 2015). Antioxidants and functional food containing antioxidants gain rising popularity among consumers (Lobo *et al.*, 2010). Consequently, the market of the functional food with these compounds is rapidly growing. On the other hand, some traditional food is also high in antioxidants, but their use is deprived by the rising number of commercial products. This trend can affect the dietary habits since the consumers are oriented to processed instead of homemade food. The health professionals and authorities should be more devoted to the research of traditional, non-processed food, its functional properties and promotion of its consumption. The main aim of our work was to determine antioxidant capacity of some traditional non-alcoholic beverages in BiH.

EXPERIMENTAL

Eight samples of traditionally prepared beverages (elder juice, elder and lemon juice, juniper berries juice, juniper berries and lemon juice, blackberry juice, pomegranate juice, and boza) were obtained from the home production (home-made products) and from the local market (commercial products).

The antioxidative effects of fruit juices were determined using the 2,2-Diphenyl-1-picryl hydrazyl (DPPH) assay as previously described (Huang *et al.*, 2005; Gorjanović *et al.*, 2013). An aliquot (50 μL) of samples diluted in destiled water (1:9 v/v) was mixed with 2 mL of freshly prepared DPPH methanolic solution (20 mg/L). The absorbance was measured at 517 nm after 16 minutes. The percent of

inhibition was calculated according to Yen and Duh (1994) using Equation 1.

$$\% \text{ inhibition} = A_{k.r(os)} - A_{uz(16\ min)} / A_{k.r(os)} \times 100 \quad (1)$$

$A_{k.r(os)}$= absorbance of control (blank) measured at 0 minutes
$A_{uz(16\ min)}$= absorbance of sample measured at 16 minutes

The IC50 was also calculated and results were expressed as v/v% in comparison to the DPPH. The antioxidant capacity was also measured by ferric reducing antioxidant power (FRAP) assay. The Fe(III)-TPTZ (2,4,6-tripyridyl-s-triazine) complex is used as an oxidant, which reduces to Fe(II)-TPTZ in the presence of antioxidant compound. An aliquot (50 μL) of samples were mixed with 1,5 mL of freshly prepared FRAP reagent (0.3 mol/L acetic buffer pH 3.6, 0.01 mol/L TPTZ and 0.02 mol/L $FeCl_3$ in ratio 10:1:1). The resulting blue colour was measured at 593 nm at 0 and 4 minutes, and the mean absorbance was recorded. The results were expressed as FRAP values (mmol/l Fe^{+2}) and compared to the standard antioxidants (Benzie and Strain, 1996). Pure compounds (cathechine, ascorbic acid and trolox) were used as control standards in both assays.
In addition, total phenolic content was determined by Folin-Ciocalteau method described previously by Slinkard and Singleton (1999). Sample aliquot (20 μL) was added to the portion of FC reagent (100 μL) and 1.58 mL of distilled water, after 8 minutes 300 μl 20% Na_2CO_3 aqueous solution was added and incubated at 40^0C for 30 minutes. The absorbance was measured at 765 nm and used for calculation of total phenolic content.
The PVPP bound phenolic compounds (flavonoids) were determined according to Makkar *et al.* (1993). Two milliliters of samples were mixed with 100 mg of insoluble, crosslinked PVPP. The tubes were vortexed and left for 15 min at 4°C. The non-adsorbed phenolics were determined in the aliquots of supernatant by the same procedure used for total phenolics. The content of PVPP bound phenolics was calculated as the difference between total and non-adsorbed phenolics. The results were expressed as mg tannic acid equivalents (TAE) per liter. Anthocyanidines content was determined by Vanilin-HCl method based on reaction of vaniline with meta-substituted A ring of flavanols resulting in formation of chromophore (Sun *et al.*, 1998). The absorption was measured at 500 nm and results were calculated as catehine content (mg/L). The anthocyanidines absorbance was calculated by Equation 2.

$$A = (A_S - A_b) - (A_c - A_0) \quad (2)$$

A_S – absorbance of test sample
A_b- absorbance of sample containing 0 mg of catechin
A_c – absorbance of control solution
A_0 – absorbance of control solution containing 0 mg of catechin

The calculated absorbances were used for determination of the anthocyanidines content from the external calibration plot. All the reagents were of analytical grade and supplied from Fluka and Sigma Aldrich.

RESULTS AND DISCUSSION

The calibration curves were linear in range of 50-1000 mg/L TAE (R^2=0.999) and in range 20-300 mg/L of catechin (R^2=0.998) (Table 1).
Total phenolic content was in range of 74.31 mg TAE/L (elder juice) to 3365.35 mg TAE/L (pomegranate juice) (Table 2). The presented phenolics content respondes to one liter of native sample, which is used as purchased in case of samples 6 (commercial blackberry juice), 8 and 9 (two boza samples), while the rest of sampes are usually diluted with water (1:10) prior to consumption. Taking this factor in count, the highest total phenolic content (820.53 mg TAE/L) was in sample 6 (commercial blackberry juice), and the lowest (7.43 mg TAE/L) in sample 1 (elder and lemone juice). The PVPP bound phenolics were dominant in elder juices (samples 1 and 2), commercial blackberry juice (sample 6) and pomegranate juice (sample 7). The oposite case was found in boza samples (samples 8 and 9). Anthocyanidines content ranged from 125.27 mg/L (elder and lemon juice) to 1899.08 mg/L (traditionally prepared blackberry juice) in native samples (Table 2). Taking into account the dilution factor, the highest antocyanidine content was found in boza samples (samples 8 and 9) and commercial blackberry juice (sample 6).

Table 1: Absorbances of tannic acid (total phenolic content) and catechin (anthocyanidines) series of standards

	Total phenolic content		Anthocyanidines	
Standard	mg TAE/L	A_{765nm}	mg/L catechin	A_{500nm}
1	50	0.16	20	0.007
2	100	0.19	50	0.009
3	150	0.20	100	0.014
4	250	0.25	200	0.022
5	500	0.37	250	0.027
6	1000	0.58	300	0.032

Table 2: Content of total phenolic compounds (TP), PVPP bound phenolics (PVPP b), PVPP non-adsorbed phenolics (PVPP nb) and anthocyanidines (AN) in samples

Sampl.	TP (mg TAE/L)	PVPP b (mg TAE/L)	PVPP nb (mg TAE/L)	AN (mg/L catechin)
1	74.31	58.09	16.22	147.72
2	136.87	91.60	45.27	125.27
3	360.28	180.97	179.31	237.53
4	317.84	194.37	123.47	293.67
5	2505.19	1172.95	1332.24	1899.08
6	820.53	547.37	273.16	540.65
7	3365.35	2223.01	1142.34	1322.98
8	273.15	98.30	174.85	956.04
9	210.59	51.39	159.20	1539.83

1 – Elder; 2 - Elder and lemon; 3 - Juniper berries; 4 - Juniper berries and lemon; 5 - Blackberry homemade; 6 - Blackberry commercial;
7 – Pomegranate; 8 - Boza 1; 9 - Boza 2.

Pomegranate juice exhibited the strongest activity against DPPH radicals (75.29 % inhibition), followed by traditionally prepared blackberry juice (42.86 % of inhibition) with their IC50 values of 5.5 % (v/v) and 6.4 % (v/v), respectively (Figure 1).

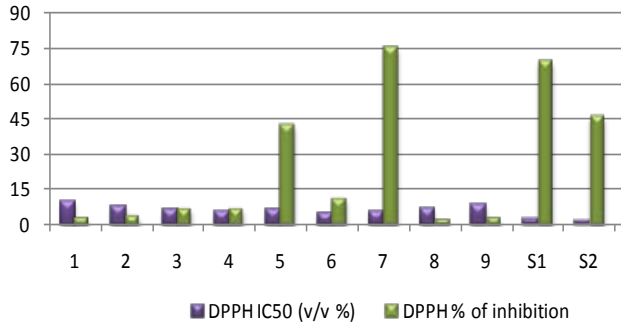

Figure 1: Antioxidant activity by DPPH assay (1 – Elder; 2 - Elder and lemon; 3 - Juniper berries; 4 - Juniper berries and lemon; 5 - Blackberry homemade; 6 - Blackberry commercial; 7 – Pomegranate; 8 - Boza 1; 9 - Boza 2; S1 – Ascorbic acid; S2 – Catechin; S3 – Trolox)

The DPPH antioxidative activity of sample 7 (pomegranate juice) was higher than for the ascorbic acid and catechine pure compounds, and slightly lower than for Trolox. The samples 1 (elder juice) and 2 (elder and lemon juice), as well as two boza samples (samples 8 and 9) showed lowest DPPH% of inhibition and highest IC50 values. FRAP assay showed stronger antioxidant capacity for most of the samples, compared to ascorbic acid standard (Figure 2).

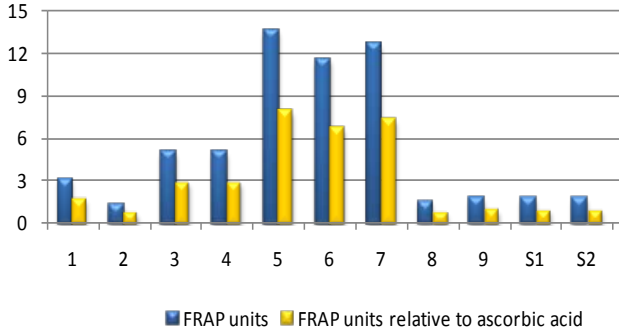

Figure 2: Antioxidant activity by FRAP assay (1 – Elder; 2 - Elder and lemon; 3 - Juniper berries; 4 - Juniper berries and lemon; 5 - Blackberry homemade; 6 - Blackberry commercial; 7 – Pomegranate; 8 - Boza 1; 9 - Boza 2; S1 – Ascorbic acid; S2 – Catechin; S3 – Trolox)

The FRAP antioxidative activity of samples 5 (blackberry homemade juice), 6 (blackberry commercial juice) and 7 (pomegranate juice) was approximately five times higher than for the pure standard compounds. The lowest antioxidative capacity was recorded for samples 1 (elder juice) and 2 (elder and lemon juice), as well as for the two boza samples (samples 8 and 9). This is in good agreement with the DPPH assay results.

The DPPH determined antioxidant capacity showed positive correlation with total phenolic content as well as with flavonoids content (Figure 3).

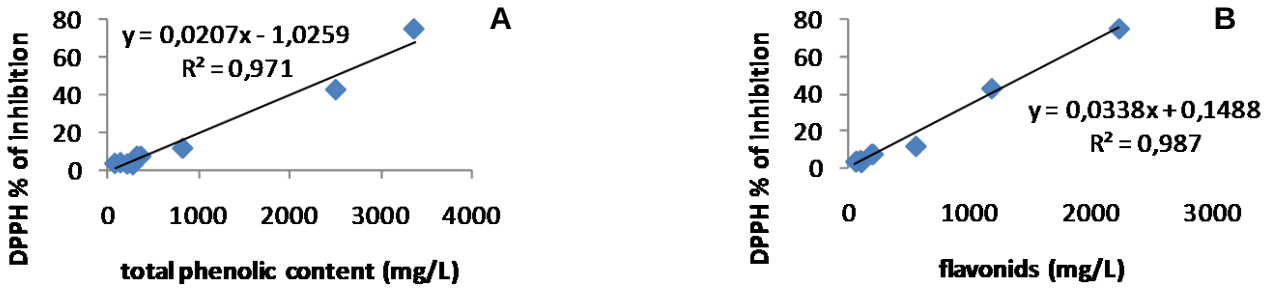

Figure 3: Correlation of DPPH antioxidant activity with total phenolic content (A) and flavonoids content (B).

CONCLUSION

The analyzed traditionally prepared beverages showed strong antioxidant capacity which was even more pronounced than in the commercial juice. The PVPP bound phenolics were predominant in commercial blackberry juice and homemade pomegranate juice, which also showed the highest antioxidative activity in both DPPH and FRAP assays. Health promotion of potential benefits of such homemade products should be enhanced.

REFERENCES

Polimeni, L., Del Ben, M., Baratta, F., Perri, L., Albanese, F., Pastori, D., Violi, F., Angelico, F. (2015). Oxidative stress: New insights on the association of non-alcoholic fatty liver disease and atherosclerosis. World Journal of Hepatology, 7 (10), 1325-36.

Cobb, C. A., Cole, M. P. (2015). Oxidative and nitrative stress in neurodegeneration. Neurobiology of Disease, doi: 10.1016/j.nbd.2015.04.020.

Pisoschi, A. M., Pop, A. (2015). The role of antioxidants in the chemistry of oxidative stress: A review. European journal of medicinal chemistry, 97, 55-74.

Lobo, V., Patil, A., Phatak, A., Chandra, N. (2010). Free radicals, antioxidants and functional foods: Impact on human health. Pharmacognosy Reviews, 4(8),118-126.

Huang, D., Ou, B., Prior, R.L. (2005). The Chemistry behind Antioxidant Capacity Assay. Journal of Agricultural and Food Chemistry, 53, 1849-1850.

Gorjanović, S. Ž., Alvarez-Suarez, J. M., Novaković, M. M., Pastor, F. T., Pezo, L., Battino, M., Sužnjević, D. Ž. (2013). Comparative analysis of antioxidant activity of honey of different floral sources using recently developed polarographic and various spectrophotometric assays. Journal of Food Composition and Analysis, 30 (1), 13–18.

Yen, G. C., Duh, P.D. (1994). Scavenging effect of methanolic extracts of peanut hulls on free-radical and active oxygen species. Journal of Agricultural and Food Chemistry, 42 (3), 629-632.

Benzie, I. F. F., Strain, J. J. (1996). The ferric reducing ability of plasma (FRAP) as a measure of "antioxidant power": The FRAP Assay. Analytical Biochemistry, 239 (1), 70-76.

Singleton V. L., Orthofer R., Lamuela-Ravento R.M. (1999). Analysis of total phenols and other oxidation substrates and antioxidants by means of Folin-Ciocalteu reagent. Methods in Enzymology, 299 (1), 152-178.

Makkar, H. P. S., Blummel, M., Borowy, N. K., Becker, K. (1993). Gravimetric determination of tannins and their correlations with chemical and protein precipitation methods. Journal of the Science of Food and Agriculture, 61 (2), 161–165.

Sun, B. S., Leandro, M. C., Ricardo-da-Silva, J. M., Spranger, M. I. (1998). Separation of grape and wine proanthocyanidins according to their degree of polymerisation. Journal of Agricultural and Food Chemistry, 46,1390-1396

Summary/Sažetak

Cilj rada je bio odrediti antioksidativni kapacitet nekih tradicionalnih bezalkoholnih napitaka u BiH. Testirano je osam uzoraka pripremljenih prema tradicionalnoj recepturi primjenom DPPH i FRAP eseja. Sadržaj ukupnih fenola je određen primjenom Folin-Ciocalteau metode, a antocijanidini su određeni vanillin-HCl metodom. Sadržaj ukupnih fenola je bio u rasponu od 74.31 mg TAE/L (sok od zove s limunom) do 3365.35 mg TAE/L (sok od nara). Sadržaj antocijanidina je bio u rasponu od 125.27 mg/L katehina (sok od zove) do 1899.08 mg/L katehina (sok od kupine). Najveću aktivnost u DPPH testu pokazao je sok od nara (%inhibicije = 75.29). Antioksidativni kapacitet utvrđen DPPH testom pokazao je pozitivnu korelaciju sa sadržajem ukupnih, kao i PVPP vezanih fenola. Rezultati FRAP testa pokazali su jači antioksidativni kapacitet za većinu ispitivanih uzoraka u odnosu na standard askorbinske kiseline. Analizirani tradicionalni napici pokazali su antioksidativni kapacitet koji je bio čak i veći nego u komercijalnim napicima.

Glasnik hemičara i tehnologa Bosne i Hercegovine

Bulletin of the Chemists and Technologists of Bosnia and Herzegovina

2015

45

13-18

Print ISSN: 0367-4444
Online ISSN: 2232-7266

UDC: _____

Original Scientific Article

Impact analysis of Brijesnica landfill site on the water system in the Majevica canal

Avdić, N.[a], Goletić, Š.[b], Šerifović E.[c], Nuhanović M[a].

[a]University of Sarajevo, Faculty of Science, Department of Chemistry, Zmaja od Bosne 33-35, 71000 Sarajevo, B&H
[b]University of Zenica, Faculty of Mechanical Engineering, Fakultetska 1, 72000 Zenica, B&H
[c]C.I.B.O.S.d.o.o, Sarajevo, 71000 Sarajevo, B&H

Article info
Received: 07/12/2015
Accepted: 09/12/2015

Keywords:
Ground water
Hydrochemical water type
Durov and Piper diagrams

***Corresponding author:**
E-mail: navdic@pmf.unsa.ba
Phone: + 387-33-279-862

Abstract: The work presents the results of an investigation on an interaction between Brijesnica landfill site and ground and surface waters in the landfill site zone. Landfill site Brijesnica is located between the 44 °N Latitude and 19 °E Longitude touching the flat Semberija region and a slightly hilly area under Mt. Majevica. The seepage of the leachate water from the landfill into the ground and surface waters and their characterization was examined on a range of samples of ground and surface waters in the landfill zone. The dominating type of ground and surface water during the examination was Ca-HCO_3, Mg-HCO_3 and Ca-Mg-HCO_3 with Ca-HCO_3-NH_3 being recorded at the periphery of the landfill site. A somewhat larger amount of ammonium has been recorded at the periphery of the landfill site and in the ground and surface waters in comparison with other samples. Microbiological contamination was noted alongside the landfill site and in the ground and surface waters.

INTRODUCTION

The examined area is located between the 44 °N Latitude and 19 °E Longitude touching the flat Semberija region and a slightly hilly area under Mt. Majevica. It is situated at the southwest brims of Semberija where this flat land begins to turn into a slightly undulated hilly area starting from the hill Obriježˇ (Šerifović, Goletić and Avdić, 2015). The location of the landfill site Brijesnica borders with the perimeter canal on the north-east side and the perimeter drainage canal from the south-west for draining the atmospheric water. The location stretching out at 950 x 250 m extends in the northwest – southeast direction while the surrounding area is scarcely populated. The landfill site "Brijesnica" is situated at the northwest side of the location in subject (Šerifović, 2014). The total area of the location with the projected construction site for a waste management centre (sanitary landfill site) amounts to approximately 250.000 m^2. As for the topography, the location can be characterized as a plain with elevations between 90.00 to 97.00 m. The terrain slightly drops from the south and southeast towards the north and northeast in the direction of the Majevica perimeter canal. The anticipated area for the sanitary landfill site is to be located on the north and north-eastern part of the location. In terms of geomorphology, the area is located in the border zone of the fluvial terraces of Drina and Sava.

River Brijesnica is located one kilometre northwest of the location while the Majevica canal makes up the northeast border of the location. Watercourse Dašnica is 2 km away from the subject location. In hydrological terms, the terrain generally represents a double-layer medium where the upper, immediate roof (silty-clay

sediments) presents a relative hydrogeological barrier while the lower gravelly layer represents a relative hydrogeological accumulator – ground water reservoir. The natural construction of the terrain holds a unique aquifer with a free layer of water (Šerifović,, 2014).
This aquifer is in a direct hydraulic connection with rivers Sava and Drina and we can say that that it represents an integral part of a unique aquifer formed at an alluvial plane of the mentioned rivers. Therefore, the oscillations in water levels of these rivers are reflected on the levels of ground waters. The oscillations of ground water levels in the study zone are largely influenced by the water level of rivers Drina and Sava. Furthermore, as we can see on the geotechnical cross-section of the terrain, with the digging of the Majevica canal in the zone downstream from the geotechnical cross-section 5-5' (Figure 1), a connection between the ground and surface waters was made and thus the aquifer recharge is also performed through the Majevica canal. At the time of high ground water levels, the water level of the Majevica canal practically represents the level of ground waters.
Based on the analysis and results of ground water level measurements, it was established that the measured levels are mostly found in the formations of clay sediments. In view of the fact that the terrain construction implies that the main aquifer is a series of gravel that lies in the clay slope, we can note that the aquifer is mostly under certain pressure, up to several meters of the water column (Nakić, Prce and Posavec, 2007).
.

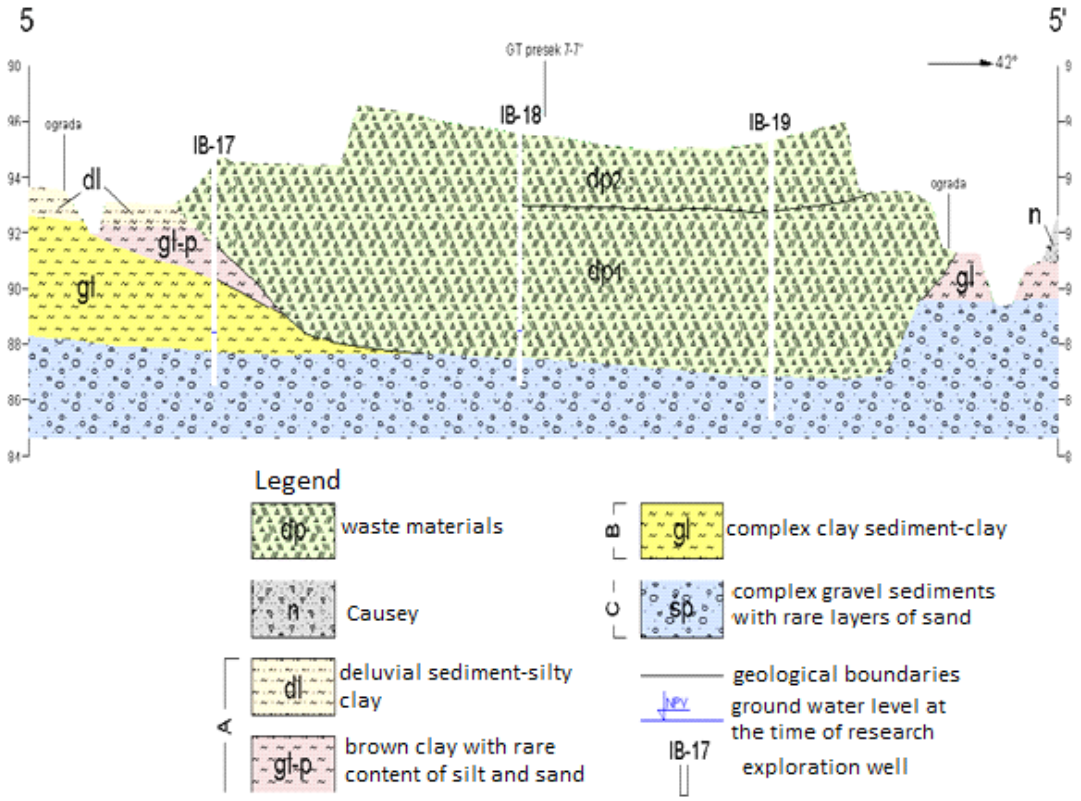

Figure 1. Geotechnical section terrain landfills (Hidrozavod, 2007)

EXPERIMENTAL

Ground water sampling

Research drilling was conducted with the general aim of establishing the lithological composition and soil structure and the level of ground waters at the research area and to take representative samples of soil for laboratory and geomechanical analysis as well as samples of ground and surface waters for establishing the chemical composition and the level of contamination.
For the purpose of periodical monitoring, data collection, composition and flow of ground waters, physical and chemical composition of the water systems during a longer period of time which would be used for project development of "Brijesnica" landfill site, 16 piezometric constructions were installed. The piezometers were made of PVC pipes, 50 mm in diameter with a 2.0 m metal part at the end.
The sampling and analysis of ground and surface waters in the subject zone was conducted in accordance with the standard regulations and norms which included: BAS ISO 5667-11; BAS ISO 5667-14; BAS ISO 5667-3.
After the installation of piezometric constructions into the drills, monitoring of ground water levels in these constructions was conducted. The piezometers were marked as engineering piezometric drills IpB-1 to IpB-16. Recording of the water levels was carried out with the help of electric gauges constructed on a principle of electrical circuit being generated after the electrode is immerged into water. All the observations of ground

water levels in a piezometer were conducted during rainy periods (October-December 2007). The engineering-geological map, Figure 2, presents the ground and surface water flow at the "Brijesnica" landfill site and the location of all piezometric drills in the whole study area (Šerifović, Goletić and Avdić, 2015). The samples were also taken from the perimeter canal upstream Mku and downstream Mkn in relation to the landfill.

The ground water course (Figure 2) is generally from the southeast towards the northwest towards the lowest recipient – river Sava as shown on Figure 2. The most prominent level of bacteriological contamination was registered at the current landfill site "Brijesnica." A high level of microbial contamination was also present in the ground and surface water samples (Figure 2). The microbial contamination was most noticeable in the Majevica zone canal because of its direct connection with the contaminated leachate water.

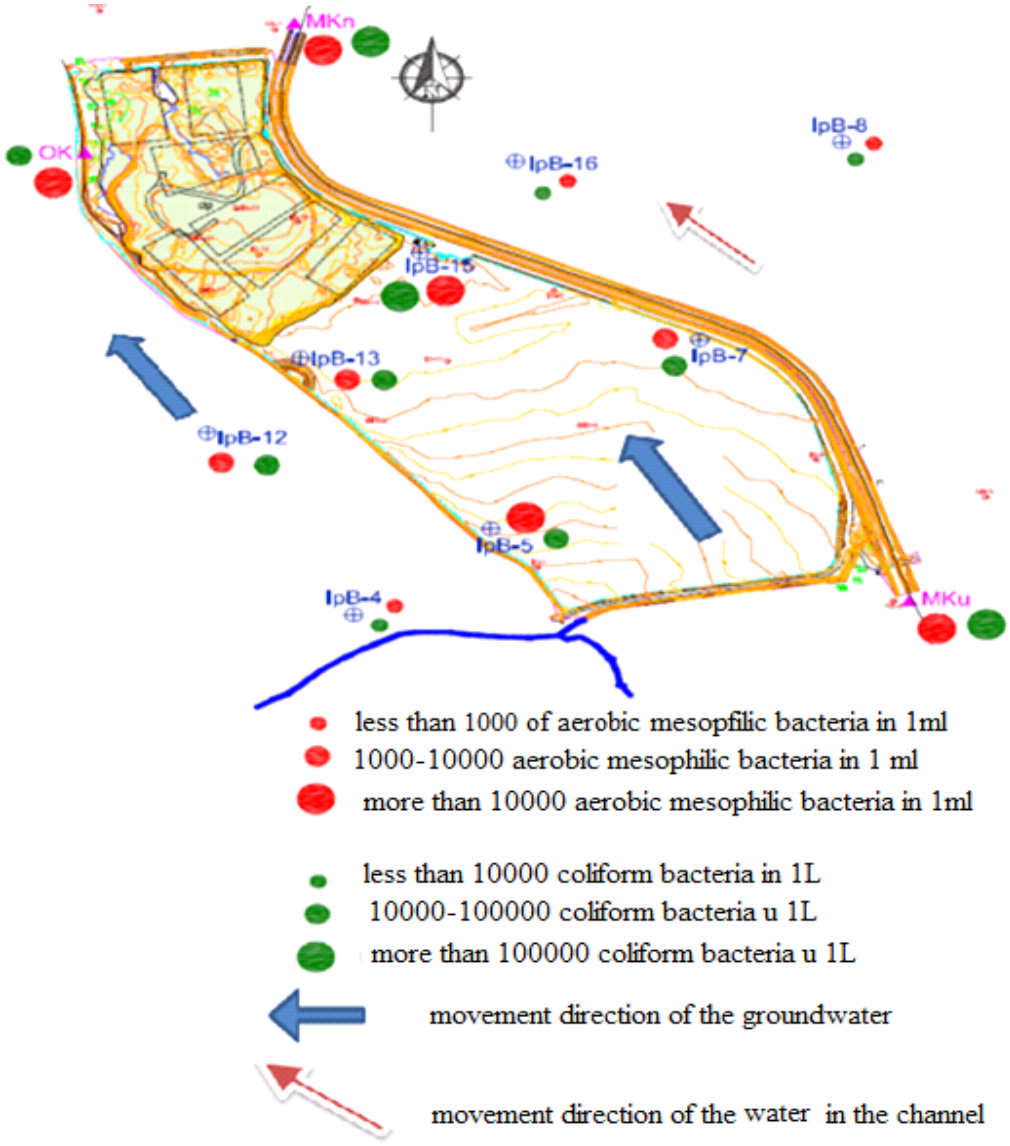

Figure 2. Groundwater flow and microbial contamination (Hidrozavod, 2007)

RESULTS AND DISCUSSION

The chemical composition of the ground water is the result of the interaction between the ground water and solid materials and gases during the hydrological cycle. The type and concentration of ions in the ground waters varies in relation to the physical and chemical processes which the water was exposed to (Nakić, Prce and Posavec, 2007). The changes in the quality of ground waters usually occur due to natural or anthropogenic influence with the latter undermining the water system balance. Every measurable chemical indicator in the ground water that can be linked to a certain process may be deemed as a hydro-chemical tracer for the process in matter (Nakić, Prce and Posavec, 2007).

Table 1. Chemical analysis of water outside the landfill zone measured in piezometers IpB-4 IpB-5 IpB-7 IpB-8, IpB-12, IpB-16

Average	Total dry residue	EC µS/cm	pH	Anions meq/L			Cations meq/L					KPK mg O_2/L
				Na^+	K^+	Mg^{2+}	Ca^{2+}	HCO_3^-	NH_4^*	SO_4^{2-}	Cl^-	NO_3^-	
Average	471	653.5	7.42	0.55	0.07	2.12	4.62	6.63	0.10	0.49	0.50	0.21	3.63
Min.	433	591.8	7.05	0.44	0.04	1.65	2.60	6.30	0	0.33	0.45	0	1.30
Max.	555	686.1	7.69	0.73	0.15	3.56	6.35	7.40	0.27	0.84	0.52	0.30	12.47

Table 2. Physical and chemical analysis of water around Brijesnica landfill site, MkN; Mku – water samples from the Majevica canal taken downstream and upstream from the Brijesnica landfill respectively, IpB-13; IpB-15 water samples from piezometers before the Brijesnica landfill site

Parameter		Mkn			Mku			Piezometers	
		Average	Min.	Max.	Average	Min.	Max.	IpB-13	IpB-15
Total dry residue mg/L		296	204	363	275	225	316	493	406
EC µS/cm		600	290	861	475	271	791	649.4	600.1
pH		8.09	7.14	8.70	7.78	6.80	8.70	7.22	7.67
Anions meq/L	Na^+	1.08	0.29	1.53	1.08	0.33	1.56	0.56	0.30
	K^+	0.45	0.18	0.64	0.40	0.44	0.78	0.05	0.05
	Mg^{2+}	0.89	0.71	1.15	1.07	0.63	1.90	2.99	3.04
	Ca^{2+}	2.41	1.28	3.32	2.20	1.44	2.81	4.14	3.37
	HCO_3^-	3.20	1.05	4.67	2.78	1.10	3.85	7.40	6.50
	NH_4^+	0.12	0.06	0.18	0.14	0.07	0.18	0	0
Cations meq/L	SO_4^-	0.84	0.48	1.10	0.76	0.20	1.12	0.33	0.41
	Cl^-	0.88	0.41	1.23	0.80	0.38	1.17	0.49	0.48
	NO_3^-	0.67	0.51	1.07	0.76	0.54	0.79	0.25	0.20
KPK mg O_2/L		38.91	19.93	57.80	37.80	19.32	55.10	1.25	1.62

Electrical conductivity and pH

The electrical conductivity (EC) of samples outside the landfill zone (Table 1) ranges between 653.5 µS/cm to 686.1 µs/cm with an average value of 591.8 µS/cm. The other samples were closer to the mean rather than the minimum or maximum values. This information indicates that part of the watercourse has not been subjected to changes regarding the salinity. Table 2 presents electrical conductivity values of the perimeter canal before Mku and after Mkn landfill as well as the electrical conductivity values of samples from piezometers IpB-13 and IpB-15 that are located in the immediate vicinity of the landfill zone. The average electrical conductivity value of the samples from Mkn landfill amounted to 600 µs/cm while the maximum and minimum values were noted at 861 µs/cm and 290 µs/cm respectively. The average, maximum and minimum EC values of samples from the Mku were 475 µs/cm, 791 µs/cm, 271 µs/cm respectively and were somewhat lower after the landfill, which clearly indicates to the presence of landfill leachate water in the perimeter canal. The EC values in the samples from piezometers IpB-13 and IpB-15 were close to the mean values of other samples. In view of the fact that the impact of ground waters of the Sava and Drina river basin is great and that there is a large number of agricultural holdings without adequate treatment of waste waters which are usually disposed in septic tanks and end up in the ground watercourses in the densely populated area around the landfill, it is clear that they have an important influence on their quality. However, the results indicate to the fact that the aquifer has been subjected to either a natural or anthropogenic process of salinity.

All pH values in the samples are above neutral and are slightly alkaline which reflects the basic nature of ground water. The surface waters in the perimeter canal before and after the landfill site do not have prominent differences in the pH values and are somewhat higher than the pH values of ground waters which indicates that in addition to possible effects of leachate water from the landfill there is also the environmental impact of the area through which the water flows. Moreover, we cannot say that any change to the above parameter correlates with the content of sodium and potassium in the samples.

Classification of water at the research area

The chemical composition of ground water primarily depends on geology and geochemical processes undergoing in the ground water system (Kazemi and Azam, 2012).

By analysing the physical and chemical data, we established that piezometer IpB-12 located behind the outskirts of the landfill site has registered a type of ground water containing a larger amount of ammoinium ion (NH_4^+) in comparison with other measuring sites. The significant presence of ammonium ions in the ground water in the immediate vicinity of the landfill site outskirts indicates to the development of a geochemical zone with methane (CH_4) (Nakić, Prce and Posavec, 2007; Appelo and Postma, 1994) and an ammoinium ion (NH_4^+) under the landfill site. The piezometers located directly at the outskirts of the landfill site registered ground waters of the following composition Ca-HCO3-NH4 i Ca-HCO3-Cl-NH4. Other nitrogen compounds nitrates and nitrites are present in lower concentrations

with a higher concentration of nitrates being only registered at a perimeter canal downstream.

The chemical consumption of oxygen in all samples is very low and ranges between 1.30 to 2.84 mgO_2/L with the exception of piezometer IpB-12 where the value was 12.47 mgO_2/L which indicates to a low content of organic material in the ground waters. On the contrary, the water from the perimeter canal both upstream and downstream from the landfill has a significantly larger content of organic material which is indicated by the consumption of oxygen that ranges between 19.32 to 57.80 mgO_2/L.

The results of the chemical analysis and characterization of ground waters from the research area can easily be illustrated on a Piper diagram (Kumar, 2013). Figures 3 and 4 show such diagrams including the zones that present the chemical composition of waters characteristic for ground waters and penetration of leachate water into the water system.

From the Piper diagram shown in Figure 4 and Table 1 we can note that the ground water at the landfill site at the time of low water levels was mostly of the Ca-Mg-HCO_3 type. The predominant cation is Ca^{2+} with an approximate share of 70% and Mg^{2+} with a share of 30%. The predominant anion is HCO_3^- with a presence of more than 80% while SO_4^{2-} and Cl^- together participate with less than 20% in the overall composition of ground water. At the time of high waters, the dominating type of ground waters is Ca-Mg-HCO_3. This only differs at piezometers IpB-7 and IpB-6 where the ground water type is Ca-Na-Mg-HCO_3 and a somewhat higher content of Mg in comparison with other samples.

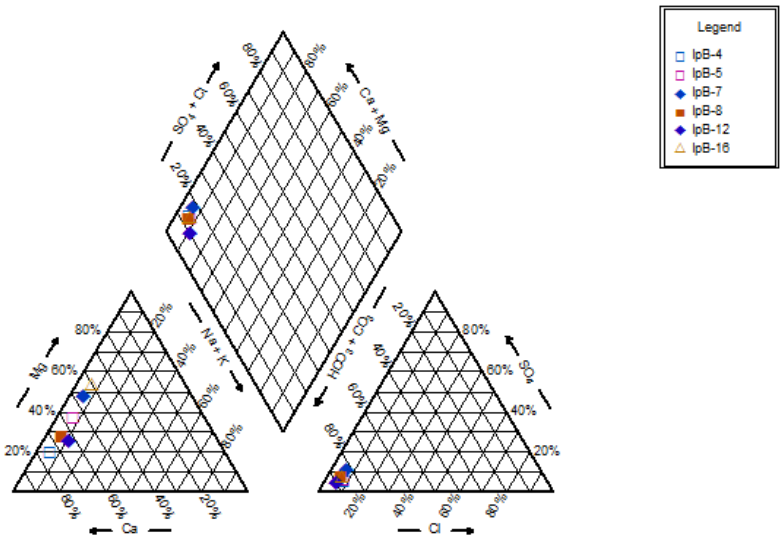

Figure 3. Piper diagram of analysed ground water samples in piezometers IpB-4, IpB-5, IpB-7, IpB-12, IpB-16

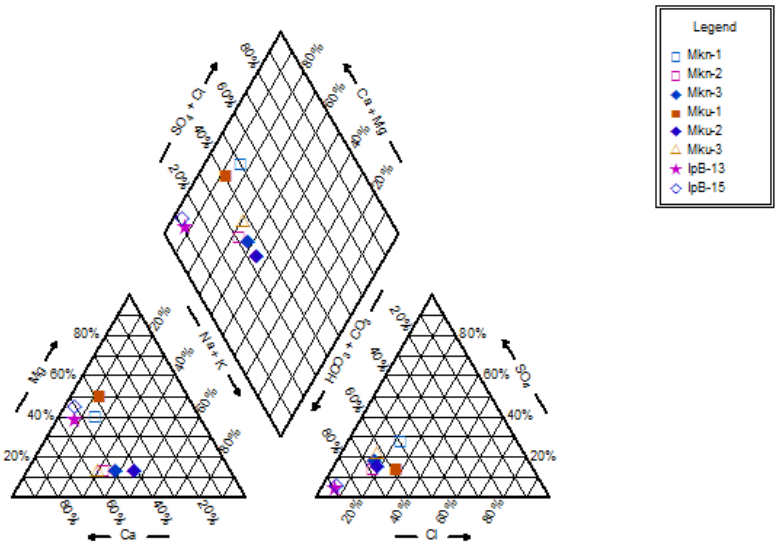

Figure 4. Piper diagram of the ionic composition of ground and surface waters around the "Brijesnica" landfill site as indicated in Table 2

Furthermore, the microbial contamination is highest around the landfill zone itself which conditioned by the direct contact with leachate waters being produced in the body of the landfill site "Brijesnica." The microbial pollution in the surface waters and analysed piezometric samples found downstream and in the vicinity of the landfill site indicate to the penetration of leachate waters into the watercourse and the effect of the landfill onto the water system (Figure 4).

From table 2 and Piper diagram in Figure 4 we can note the effect of the landfill onto the water system, the increased content of Na^+, K^+ , Cl^- and NH_4^+ ions with concurrent decrease in the content of Ca^{2+} and Mg^{2+} in comparison with other samples. This variation has been recorded on the Piper diagram (Figure 4) where the water type was shifted towards the Ca-Mg-Na-HCO_3 plot. A slight rise in the pH value of the analysed samples is also clearly evident.

CONCLUSION

The results of the physical and chemical analysis indicate that all water samples are naturally slightly alkaline. The influence of water systems of rivers Sava and Drina onto the quality of the ground water in the landfill zone is very prominent notably at the time of high water levels.

The types of ground and surface waters are defined on the grounds of physical and chemical analysis and the Piper diagram. Most of the water samples are of the Ca-HCO_3 type followed by $MgHCO_3$ and Ca-$MgHCO_3$ types. The effect of the landfill site has been noted downstream in the watercourse and in the water system in the landfill zone through an increased presence of Na^+, Cl^- i NH_4^+ ions in comparison with the upstream samples

REFERENCE

Appelo, C.A.J., Postma, D. (1994). *Geochemistry, groundwater and pollution*. Balkema, Rotterdam.

Hidrozavod, dtd. (2007). Glavni projekat sanitarne deponije Brijesnica u Bijeljini, Novi Sad.

Kazemi G. A., Azam M. Significance of Hydrogeochemical Analysis in the Management of Groundwater Resources: A Case Study in Northeastern Iran**,** *Hydrogeology – A Global Perspective*, (p.p. 141-158), In Tech.

Kumar, P.J.S. (2013). Interpretation of groundwater chemistry using piper and chadhas diagrams: a comparative study from perambalur taluk, *Elixir Geoscience 54*, 12208-12211.

Nakić,S., Prce, M., Posavec, K. (2007). *Uticaj odlagališta Jakuševac-Prudenc na kakvoću podzemne vode.* Rudarsko-geološko-naftni zbornik, Zagreb.

Šerifović, E., Goletić, Š., Avdić, N. (2015). Characterization of ground and surface waters at the landfill site "Brijesnica, *The 5th International Conference on Environmental and Material Flow Management* "EMFM 2015", 05-07 November 2015, Zenica, B&H,

Šerifović, E.(2014). Istraživanje uticaja odlagališta otpada "Brijesnica" na vodeni sistem u zoni majevičkog kanala, magistarski rad, Univerzitet u Zenici.

Summary/Sažetak

U radu su prikazani rezultatai istraživanja interakcijskih djelovanja između odlagališta Brijesnica te podzemnih i površinskih voda u zoni odlagališta. Odlagalište Brijesnica locirano je između Lantitude 44 °N i Longitude 19 °E, a na dodiru ravne Semberije i blagog podbrđa Majevice. Prodor procjedne vode odlagališta u podzemne i površinske vode i njihova karakterizacija ispitana je na nizu uzoraka podzemnih i površinskih voda u zoni odlagališta. Dominantan tip podzemne i površinske vode tokom trajanja ispitivanja bio je Ca-HCO_3, Mg-HCO_3 i Ca-Mg-HCO_3 te uz rub odlagališta Ca-HCO_3-NH_3. Uz rub odlagališta i u podzemnim i površinskim vodama pojavljuje se nešto veći sadržaj amonijaka nego u ostalim uzorcima. Mikrobiološko onečišćenje uočeno je uz deponiju i u podzemnim i u površinskim vodama.

Glasnik hemičara i tehnologa Bosne i Hercegovine

Bulletin of the Chemists and Technologists of Bosnia and Herzegovina

2015

45

19-22

Print ISSN: 0367-4444
Online ISSN: 2232-7266

UDC: _____

Original Scientific Paper

Solid state synthesis and characterization of $LiFePO_4$/C as cathode material for Li-ion batteries

Karaman, N., Aliefendić, M., Pljuco, S., Kozlica, Dž., Nalić, N., Korać, F., Gutić, S. *

University of Sarajevo, Faculty of Science, Department of Chemistry, Zmaja od Bosne 33-35, 71000 Sarajevo, B&H

Article info
Received: 23/11/2015
Accepted: 12/122015

Keywords:
Lithium - ion batteries
Lithium iron phosphate
Solid state reaction
Olivine structure

***Corresponding author:**
E-mail:
karaman_nejra@hotmail.com

Abstract: Lithium transition metal phosphates have been recognized as potential positive electrodes for use in large scale production of lithium ion batteries, specially due to high thermal and chemical stability. Amongst all positive electrode materials, such as $Li_3V_2(PO_4)_3$, $LiMnPO_4$ $LiVPO_4F$, the olivine $LiFePO_4$ has the most promising characteristics. The $LiFePO_4$/C composite was synthesized by solid state reaction using LiOH as source of lithium ion, stearic acid which acts as reductive agent and carbon source and $FePO_4$ precursor prepared from $FeSO_4 \times 7H_2O$ and $NH_4H_2PO_4$. The starting materials were mixed in stoichiometric ratio and heated at 700°C under N_2 flow to form the composite $LiFePO_4$/C. Properties of synthesized material were analyzed by Raman spectroscopy, cyclic voltammetry (CV) and electrochemical impedance spectroscopy (EIS). Raman spectral analysis indicated some amorphous sp^3 bonded carbon, sp^2 graphite like phase and presence of carbides. Cyclic voltammograms confirmed good reversibility of intercalation and deintercalation of lithium ions from structure. Impedance response of the cells consisted of a depressed semicircle in the high frequency region, which is attributed to the charge-transfer process and sloping line in low frequency region which corresponds to the Warburg impedance.

INTRODUCTION

In the past few decades, over-consumption of fossil fuels led to serious environmental issues and depletion of their reserves. High demand for replacement of these sources of energy with renewable ones, has directed researchers toward lithium ion batteries. Outstanding performance of lithium ion batteries makes them attractive for wide range of applications, such as portable electronic devices, electric vehicles and hybrid electric vehicles.

Active material for positive electrode is one of the most important parts of the battery, which mostly determines its cost and performance. Many cathode materials have been subjects of studies over years and they include different classes of crystal structures: layered ($LiCoO_2$), spinel ($LiMn_2O_4$) and olivine ($LiFePO_4$) frameworks (Julien et al., 2014). However, iron-based compounds containing phosphate anion have been under intense research since 1997, when Goodenough and co-workers proposed $LiFePO_4$ as the most promising candidate for cathode material in lithium ion battery (Padhi et al., 1997).

The discharge reaction for $LiFePO_4$ includes intercalation of lithium ion along with an equivalent number of electrons into the electrode material:

$$FePO_4 + Li^+ + e^- \rightarrow LiFePO_4$$

Olivine structured $LiFePO_4$ has significant advantages, such as high theoretical capacity (170 $mAhg^{-1}$), low cost, nontoxicity, long cycle life and superior thermal and chemical stability. In the case of overoxidation (overcharge), phosphate group stabilizes the structure and material does not release oxygen (Kurzweil and Brandt 2009), which makes it safer than commercial, oxide based materials. Nevertheless, $LiFePO_4$ suffers from low electronic conductivity ($<10^{-9}$ Scm^{-1}) and low diffusion coefficient of lithium ion, which is close to $D = 10^{-14}$ cm^2s^{-1} (Julien et al., 2014).

Coating $LiFePO_4$ particles with carbon results in better electrochemical performance. This is usually achieved by adding carbon source during calcination in inert atmosphere. The presence of carbon may also limit particle growth, which ensures short lithium ion diffusion paths within positive electrode. Carbon source acts also as reducing agent and suppresses formation of Fe^{3+} impurities (Wang et al., 2012). Recently, several studies have shown that doping with supervalent metal ions can stabilize the crystal structure, improve electronic conductivity and reduce internal impedance of the cell, due to the enlarged lattice volume that provides more space for lithium ion transfer (Zhang et al., 2011). In order to enhance electrochemical performance of $LiFePO_4$, optimization of synthetic procedure is necessary. Several preparative methods are commonly used, such as solid state reaction, sol-gel method, coprecipitation and hydrothermal processes (Koltypin et al., 2007).

In this work, $LiFePO_4$/C cathode material was synthesized by solid-state reaction, after preparation of $FePO_4$ precursor by inorganic synthesis procedure. Stearic acid was added as carbon source as well as reducing agent. In order to control particle size, stearic acid was added during calcination at high temperature in inert atmosphere. $LiFePO_4$/C-Li half cells were fabricated in an argon-filled glove box. Properties of synthesized material were analyzed using Raman spectroscopy, cyclic voltammetry and electrochemical impedance spectrosopy.

EXPERIMENTAL

Synthesis of precursor ($FePO_4$)

$FePO_4$ precursor was prepared using low cost $FeSO_4 \times 7H_2O$ (Merck) and $NH_4H_2PO_4$ (Merck) as raw materials. Aqueous solutions of $FeSO_4 \times 7H_2O$ and $NH_4H_2PO_4$ were mixed together in stoichiometric amounts, and pH value was adjusted to 9 by adding $NH_3 \times H_2O$. In order to obtain $Fe_3(PO_4)_2 \times 8H_2O$ precipitate, mixture was stirred for 30 minutes at room temperature. The precipitate was dissolved in H_3PO_4 (Merck, p.a.) and H_2O_2 (Sigma-Aldrich, p.a.) is added as oxidizing agent, as well as $NH_3 \times H_2O$ for adjustment of pH value to 9. The mixture was stirred for 6 hours at 90°C and bright yellow precipitate of $FePO_4 \times 2H_2O$ is obtained. Afterwards, $FePO_4 \times 2H_2O$ was dried at 120°C for 5 hours, followed by drying at 500°C for 6 hours and final precursor $FePO_4$ was formed.

Preparation of $LiFePO_4$/C

Composite material was prepared by solid state reaction. Stearic acid was dissolved in isopropanol (Carlo Erba) to form transparent solution and added to LiOH (Sigma-Aldrich) powder. The mixture was stirred and homogenised in mortar. The precursor, $FePO_4$, was added to previous mixture along with 100 mL of isopropanol. The molar ratio of $FePO_4$ and LiOH was 1:1, but excessive amount of LiOH was added to compensate the loss of Li during calcination. Isopropanol was removed from mixture by heating it up to 50°C for 72 hours, under continuous stirring at moderate speed. The obtained paste was dried at 70°C for 6 hours. Carbon coating of $LiFePO_4$ material was carried out in the tube furnace at 700°C under nitrogen flow for 6 hours. The obtained composite, $LiFePO_4$/C was cooled down to room temperature, under inert atmosphere.

Electrochemical measurements

Electrochemical characterization was conducted using PAR263A potentiostat/galvanostat, connected to PowerCV software. All electrochemical measurements were carried out at room temperature.

The working electrode was prepared by mixing the active material with graphite and poly(vinylidene fluoride) in a weight ratio of 80:10:10 dissolved in an appropriate amount of dimethylformamide (DMF) to make slurry, using ultrasound treatment. The slurry was coated on aluminum foil current collector using automatic film-coating equipment, with controlled thickness of 300 μm and dried at 180°C for 3 hours. Afterwards, the electrode was cut into round samples of required size.

Metallic lithium foil was used as reference and counter electrode. The electrolyte was composed of 1 $moldm^{-3}$ $LiPF_6$ in a 1:1 solvent mixture of propylene carbonate (PC) and dimethyl carbonate (DMC). Commercial three-electrode Gamry cell was assembled in an argon-filled dry glove box, followed by electrochemical testing outside the glove box.

Cyclic voltammetry was measured at scan rates of 0.1 and 1 mVs^{-1} between 2.7 and 4.2 V. Electrochemical impedance spectroscopy was performed by applying a 10 mV amplitude signal in the frequency range of 10^5-10^{-2} Hz.

RESULTS AND DISCUSSION

Figure 1 shows a cyclic voltammogram of $LiFePO_4$/C measured at room temperature, at scan rate of 0.1 mVs^{-1}. As shown in figure 1, oxidation and reduction peaks appear at 3.64 and 3.15 V vs. Li/Li^+. These redox reaction peaks correspond to the insertion (discharge reaction) and extraction (charge reaction) of lithium ion from $LiFePO_4$. The ratio between anodic and cathodic peak currents is close to 1, implying good reversibility of lithium intercalation into and deintercalation from $LiFePO_4$/C.

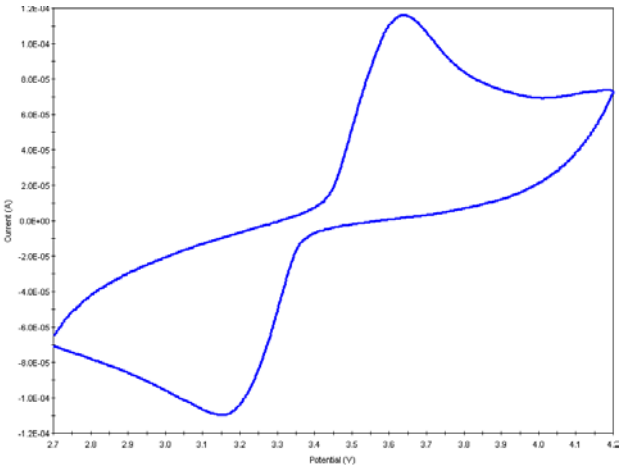

Figure 1. Cyclic voltammogram for $LiFePO_4$/C at scan rate of 0.1 mVs^{-1}

Figure 2 shows the effect of the potential scanning rate on the cyclic voltammograms, measured at 0.1 and 1 mVs^{-1}. The shapes of anodic and cathodic peaks were almost symmetrical in both cases. The anodic peak shifts to higher potential and the cathodic peak shifts to lower potential, which indicates increased kinetic polarization and increased internal resistance.

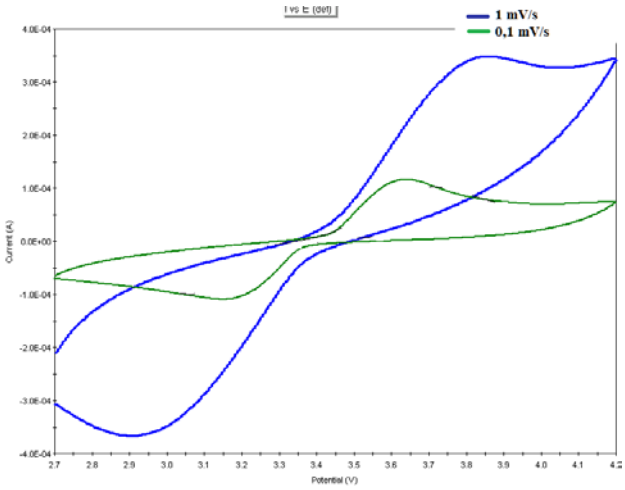

Figure 2. Cyclic voltammogram for $LiFePO_4/C$ at scan rates of 0.1 mVs^{-1} and 1 mVs^{-1}

Figure 3 shows Nyquist diagram obtained by electrochemical impedance spectroscopy, at 2.7 and 4.0 V. Both spectra have a depressed semicircle in high frequency region which corresponds to the charge transfer resistance (R_{CT}) and an inclined line in low frequency region which represents Warburg impedance or lithium ion diffusion resistance. As seen from the spectrum, the high frequency impedance of $LiFePO_4/C$ electrode is lower as Li deintercalation proceeds. At potential of 4.0 V high frequency impedance is about 663 Ω, whilst high frequency impedance at 2.7 V is about 905 Ω.

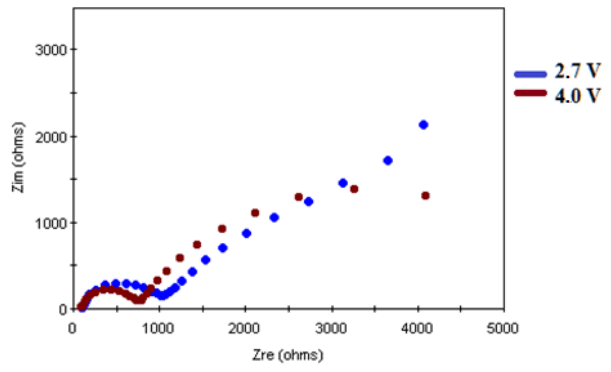

Figure 3. Nyquist diagram at 2.7 V and 4.0 V

Two intense broad bands in Raman spectrum at 1395 and 1590 cm^{-1} can be assigned to the D and G bands of carbon in the $LiFePO_4/C$ composite, respectively. Raman modes in the range of 900 to 1150 cm^{-1} are due to the stretching mode of PO_4^{3-} unit and involve symmetric and asymmetric of P-O bonds. Raman modes observed around 200 cm^{-1} indicate presence of iron carbide, Fe_3C (Kumar et al., 2009). Iron carbide was formed during calcination at high temperatures, and affects the performance of cathode.

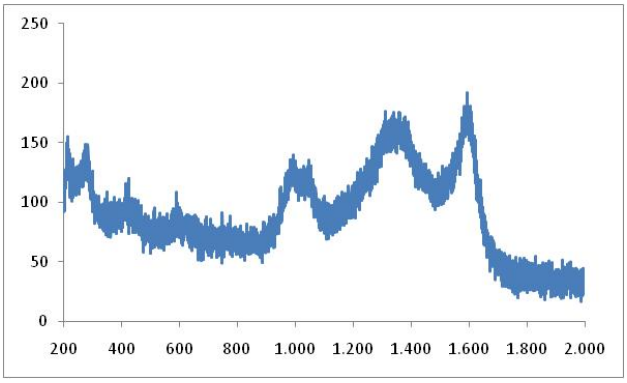

Figure 4. Raman spectrum

CV peaks are significantly broader than ideal intercalation/deintercalation peaks, which suggests existence of some difficulties in charge transport. Broadened peaks are present due to the low kinetics mechanism of lithium extraction and insertion in $LiFePO_4$ crystal structure. Possible cause can be presence of some impurities, particularly iron carbide (Koltypin et al., 2007). Hysteresis in CV peaks increased as scan rate increased, which might be due to an increase in the internal impedance of cell during charge/discharge cycling (Jin et al., 2008).

As seen from figure 3, high frequency response of impedance spectroscopy is higher than expected for $LiFePO_4/C$. Possible explanation is weak distribution of carbon on the surface of $LiFePO_4$ particles. Another reason might be the quality of graphite used for preparation of slurry, with particles size of less than 20 μm. Deppresed semicircles observed in high frequency region are not complete, which is a strong indication for the slow kinetics of electrode, due to impeded charge transfer (Koltypin et al., 2007). Another explanation for high impedance could be due to the $LiPF_6$ electrolyte used during electrochemical measurements. Trace HF, which is always present in $LiPF_6$, can lead to formation of surface LiF films. These films are resistive to Li-ion migration and their presence probably increases the charge transfer resistance of positive electrode (Koltypin et al., 2007).

CONCLUSION

$LiFePO_4/C$ particles have been successfully synthesized by solid state reaction, using $FePO_4$ precursor prepared by inorganic synthesis. Stearic acid was used as carbon source, and Raman spectrum showed presence of amorphous and graphitic carbon. Calcination at temperature around 700°C led to formation of iron carbide, which significantly deteriorates electrochemical performance. The ratio of anodic and cathodic currents, which is close to 1, indicated good reversibility of lithiation and delithiation processes. Electrochemical measurements indicated slow lithium ion diffusion, which can be observed from broadened CV peaks and incomplete high frequency semicircles.

REFERENCES

Jin, B., Gu, H.B., Zhang, W., Park, K.H., Sun, G. (2008). Effect of different carbon conductive additives on electrochemical properties of $LiFePO_4$-C/Li batteries. *Journal of Solid State Electrochemistry*, 12(12), 1549-1554.

Julien, C.M., Mauger, A., Zaghib, K., Groult, H. (2014). Comparative Issues of Cathode Materials for Li-Ion Batteries. *Inorganics*, 2(1), 132-154.

Koltypin, M., Aurbach, D., Nazar, L., Ellis, B. (2007). More on the performance of $LiFePO_4$ electrodes – The effect of synthesis route, solution composition, aging, and temperature. *Journal of Power Sources*, 174(2), 1241-1250.

Kumar, A., Thomas, R., Karan, N.K., Saavedra- Arias, J.J., Singh, M.K., Majumder, S.B., Tomar, M.S., Katiyar, R.S. (2009). Structural and Electrochemical Characterization of Pure $LiFePO_4$ and Nanocomposite C-$LiFePO_4$ Cathodes for Lithium Ion Rechargeable Batteries. *Journal of Nanotechnology*, 1-10.

Kurzweil, P., Brandt, K. (2009). Secondary batteries – Lithium rechargeable systems. *Encyclopedia of Electrochemical Power Sources*, 1-26.

Padhi, A.K., Nanjundaswamy, K.S., Goodenough, J.B. (1997). Phospho-olivines as positive-electrode materials for rechargeable lithium batteries. *Journal of the Electrochemical Society*, 144(4), 1188–1194.

Wang, W.L., Jin, E.M., Gu, H.B. (2012). Electrochemical Performance of Lithium Iron Phosphate by Adding Graphite Nanofiber for Lithium Ion Batteries. *Transactions on Electrical and Electronic Materials*, 13(3), 121-124.

Zhang, L.L., Liang, G., Ignatov, A., Croft, M.C., Xiong, X.Q., Hung, I.M., Huang, Y.H., Hu, X.L., Zhang, W.X., Peng, Y.L. (2011). Effect of Vanadium Incorporation on Electrochemical Performance of $LiFePO_4$ for Lithium-Ion Batteries. *The Journal of Physical Chemistry*, 115(27), 13520-13527.

Summary/Sažetak

Zahvaljujući visokoj termičkoj i hemijskoj stabilnosti, katodni materijali na bazi fosfata prepoznati su kao potencijalne pozitivne elektrode za masovnu proizvodnju Li-jonskih baterija. Od svih katodnih materijala na bazi fosfata, kao što su $Li_3V_2(PO_4)_3$, $LiMnPO_4$, $LiVPO_4F$, olivinski $LiFePO_4$ pokazuje obećavajuće performanse. Kompozit $LiFePO_4$/C sintetiziran je pomoću reakcije u čvrstoj fazi. Kao polazni spojevi korišteni su LiOH kao izvor litijumovog jona, stearinska kiselina koja se koristi kao reducirajući agens i izvor ugljika, te $FePO_4$ prekursor pripremljen iz $FeSO_4 \times 7H_2O$ i $NH_4H_2PO_4$. Reaktanti su pomiješani u stehiometrijskom odnosu i zagrijani na 700°C u atmosferi azota, pri čemu se dobije $LiFePO_4$/C. Karakteristike sintetiziranog materijala analizirane su Raman spektroskopijom, cikličnom voltametrijom i elektrohemijskom impedansnom spektroskopijom. Raman spektar pokazao je prisustvo amorfnog sp^3 vezanog ugljika, sp^2 vezanog grafita i karbida. Cikličnom voltametrijom potvrđena je dobra reverzibilnost procesa interkalacije i deinterkalacije litijumovog jona iz strukture. Impedansni spektar sastoji se od polukruga u visoko-frekventnom području, što se pripisuje procesima prenosa naboja, te pravolinijski tok pod približno 45° u odnosu na realnu osu što odgovara difuziono kontroliranim procesima, odnosno Warburgovoj impedansi.

Glasnik hemičara i tehnologa Bosne i Hercegovine

Bulletin of the Chemists and Technologists of Bosnia and Herzegovina

2015

45

23-30

Print ISSN: 0367-4444
Online ISSN: 2232-7266

UDC: _____

Original Scientific Paper

Chemical composition and antioxidant activity of three Lamiaceae species from Bosnia and Herzegovina

Odak, I., Talić, S.*, Martinović Bevanda, A.

Department of Chemistry, Faculty of Science and Education, University of Mostar, Matice hrvatske bb, 88 000 Mostar, Bosnia and Herzegovina

Article info
Received: 01/09/2015
Accepted: 11/12/2015

Keywords:
Essential oil
Salvia officinalis
Rosmarinus officinalis
Lavandula angustifolia
Antioxidant activity

***Corresponding author:**
E-mail: stanislavatalic@gmail.com
Phone: 00387 36 445 480
Fax: 00387 36 355 458

Abstract: The components of essential oils of rosemary, sage and lavender were investigated by GC-MS and assayed for their antioxidant activities. The plants were collected after the end of the vegetative cycle. The principal components of sage essential oil were 1,8-cineole (28.03%), α-thujone (11.98%), veridiflorol (11.17%), and α-humulene (11.0%). Rosemary essential oil was mainly composed of α-pinene (14.02%), camphor (13.62%), 1,8-cineole (13.02%), borneol (12.45%), and berbenone (10.04%). Predominant compounds in lavender essential oil were 1,8-cineole (40.68%) and camphor (29.82%). Antioxidant activity was examined by two different methods: the 2,2'-diphenyl-1-picrylhydrazyl (DPPH) radical scavenging method and determination of ferric reducing antioxidant power (FRAP). The results indicate that the tested essential oils have low antioxidant activity compared to synthetic antioxidant butylated hydroxytoluene (BHT). In relation to the other oils investigated, rosemary essential oil showed the highest antioxidant activity by both methods.

INTRODUCTION

Production and usage of the essential oils is the part of tradition, cultural and historical heritage of Bosnia and Herzegovina (B&H). Many plants, such as chamomile, sage and immortelle are already recognized at global market due to its unique composition and organic farming. B&H is a leading medicinal and aromatic plant exporting country in the region and has a high potential for development of the products based on geographical origin and organic farming.

Various beneficial properties of essential oils have been recognized since ancient times. Nowadays essential oils found application in pharmaceutical, cosmetics, sanitary and food industries owing to their odour and biological effects such as antiseptic, antibacterial, antioxidant activity etc. (Bakkali *et al.*, 2008). In B&H, there are 30 medical species of the family Lamiaceae. Although entire flora of B&H is dominated by species of family Asteraceae (Redžić, 2007), in medicinal flora the most abundant are species of family Lamiaceae (13%), with usage of its ground herbal organs, leaves and flowers. These are mostly ingredients for preparation of different kind of tea infusion which is common for treatment of respiratory system illnesses, stomach discomfort and nervous tension.

As a part of our research on plants from southern part of B&H, we carried out analysis of chemical composition and antioxidant activity of essential oils from three Lamiaceae species which are widely used in folk medicine, cosmetics, phytopharmacy, and the flavouring of food products. Essential oils of sage (*Salvia officinalis* L.), lavender (*Lavandula angustifolia* L.) and rosemary (*Rosmarinus officinalis* L.) were analyzed. Samples were collected in October, in order to examine yield and antioxidant activity of essential oils in non-vegetative cycle.

EXPERIMENTAL

Plant material

Sage (*Salvia officinalis* L.), rosemary (*Rosmarinus officinalis* L.) and lavender (*Lavandula angustifolia* L.) were collected near the city Mostar, central Herzegovina (43°20’30”N; 017°48’47”E), in October 2014. The

species were identified at the Department of Biology, Faculty of Science and Education, University of Mostar. The plant material was air-dried for 20 days and stored at ambient temperature (25±2°C) without exposure to direct sunlight.

Isolation of the essential oils

The air-dried samples of each plant were submitted to hydro-distillation for 1.5 hour using Clevenger type apparatus according to European Pharmacopeia. The collected *n*-pentane extracts were dried over anhydrous sodium sulphate and stored in sealed vials at -15°C until analysis. The essential oil yields were determined by the gravimetric method.

Gas Chromatography-Mass Spectrometry

Analysis of the oils were carried out using Shimadzu GC-MS QP2010 system equipped with an AOC-20i autosampler, using two fused silica capillary columns with different polarity. The non-polar column was Inert Cap (30 m × 0.25 mm × 0.25 μm) and the polar column was Rtx-Wax (30 m × 0.25 mm × 0.25 μm). Solutions of 2 μL of essential oil in pentane were injected in splitless mode at 250°C. Helium was the carrier gas. The operating conditions for non-polar column were as follows: flow rate of carrier gas: 1.15 mL min^{-1}; oven temperature program: 70°C (1.5 min), 70-120°C (5°C min^{-1}), 120-240°C (4°C min^{-1}), 240°C (2 min). For polar column operating conditions were as follows: flow rate of carrier gas: 1.21 mL min^{-1}; oven temperature program: 60°C (2 min), 60-240°C (3°C min^{-1}), 240°C (10 min). MS conditions: ionization voltage: 70 eV, ion source temperature: 250°C, mass range: m/z 40-400.

Identification

Identification of oil components was based on retention indices on a polar and non-polar column relative to a homologous series of *n*-alkanes (C_8-C_{40}) as well as on comparison of their mass spectra with the NIST and Wiley spectra library. Relative percentages of components were calculated based on GC peak areas without using correction factors.

Determination of antioxidant capacity of essential oils

Free Radical Scavenging Capacity Using the Stable Radical (DPPH)

Antioxidant activity of the essential oils were measured in terms of hydrogen donating or radical scavenging ability, using the stable radical, 2,2'-diphenyl-1-picrylhydrazyl (DPPH). In the DPPH assay, the ability of essential oils of interest to act as donors of hydrogen atoms or electrons in transformation of DPPH· into its reduced form DPPH-H was investigated (Brand-Williams *et al.*, 1995; Jukić *et al.*, 2006). The 50 μL methanolic solution of the essentials oils (concentrations of stock solutions were 5, 10, 15, 20, 30, 40 and 50 g L^{-1}) was placed in a cuvette, and 1 mL of 6 × 10^{-5} M methanolic solution of DPPH was added. The reaction progress absorbance of the mixture is monitored at 517 nm for 1 hour using an UV-Vis (double-beam) Shimadzu spectrophotometer. Synthetic antioxidant butylated hydroxytoluene (BHT) was used as a positive control (concentrations of methanolic stock solutions were 0.1, 0.5, 0.7, 1.0, 1.5, 2.0, 10.0 and 20.0 g L^{-1}). Methanol was used to zero the spectrophotometer. The absorbance of DPPH radical without antioxidant was measured daily. All determinations were performed in triplicate. Inhibition of DPPH expressed in percentage was calculated according to equation (1), were $A_{C(0)}$ is the absorbance of the control at t=0 min, and $A_{A(t)}$ is the absorbance of the antioxidant at t=1 h.

$$\text{Inhibition (\%)} = \frac{A_{c(o)} - A_{A(t)}}{A_{c(0)}} x100 \quad (1)$$

Determination of FRAP- Ferric Reducing/Antioxidant Power

The total antioxidant potential of essential oils and BHT were determined using the ferric reducing ability of plasma (FRAP) assay of Benzie and Strain (1996) as a measure of antioxidant power. The FRAP assay measures the change in absorbance at 593 nm owing to the formation of a blue colour Fe^{2+} tripyridyltriazine compound from the colourless oxidized Fe^{3+} form by the action of electron donating antioxidants (Politeo *et al.*, 2007; Tomaino *et al.*, 2005). The FRAP reagent was prepared by mixing 10 parts of acetate buffer (300 mmol L^{-1}, pH 3.6) with 1 part of TPTZ (2,4,6-tripyridil-*s*-triazine, 10 mmol L^{-1} in 40 mmol L^{-1} hydrochloric acid) and with 1 volume of ferric chloride (20 mmol L^{-1}). All solutions were used on the day of preparation. A linear calibration graph for $FeSO_4 \times 7H_2O$ in the concentration range over 0.1-5.0 mmol L^{-1} was prepared. The corresponding regression calibration equation was: A=0.6152c+0.0606, were A is absorbance at 593 nm, c is concentration of $FeSO_4 \times 7H_2O$ in mmol L^{-1}, (R^2 = 0.9998). The procedure for preparation of calibration graph was as follows. The reaction mixture was consisted of 150 μL of deionized water, 1.5 mL of FRAP reagent and 50 μL solution of $FeSO_4 \times 7H_2O$ at different concentrations given above. The FRAP reagent (1.5 mL) was warmed to 37°C and a reagent blank reading was taken at 593 nm. The same procedure was used for spectrophotometric measurements with solutions of essentials oils. Instead of 50 μL of solution of Fe^{2+}, a 50 μL methanolic solution of the essential oil was added in reaction mixture in concentration range over 5-50 g L^{-1}. All reaction mixtures were incubated at 37°C throughout the monitoring period. The change in absorbance between the final reading (4-min reading) and blank reading was selected for the calculation of FRAP values. The butylated hydroxytoluene (BHT) was used as a positive control (concentrations of methanolic stock solutions were 0.1-20.0 g L^{-1}). In the FRAP assay, the antioxidant efficiency of the antioxidant tested was calculated with reference to the reaction signal given by a Fe^{2+} solution of known concentration. All determinations were performed in triplicate.

RESULTS AND DISCUSSION

The yields of essential oils obtained by hydro-distillation were 2.1% for sage, 1.1% for rosemary, and 1.1% for lavender. The chemical composition is presented in Table 1 according to the retention indices of compounds on a non-polar column. All oil extracts are characterized by a high concentration of monoterpenes (sage 65.5%, rosemary 88% and lavender 90.4%), including mostly oxygenated monoterpenes (Table 1). Concerning the content of sesquiterpenes, rosemary and lavender have similarly low content (5-8%) while sage oil contain total of 30.9% of sesquiterpenes.

Table 1: Chemical composition (%) of essential oils from Lamiaceae species

Name	K_i[a]	K_i[b]	*S. officinalis*	*R. officinalis*	*L. angustifolia*
α-Pinene	935	1095	4.1	14.0	2.5
Sabinene	974	1133	-	-	0.3
β-Pinene	978	1127	2.4	0.6	2.7
β-Myrcene	986	1166	0.6	1.4	-
δ–3-Carene	1009	1160	-	1.0	3.3
(*E*)-3-Caren-2-ol	1024	1508	-	0.4	0.2
Limonen	1025	1197	-	1.6	-
Cymol	1025	1261	0.3	-	-
1,8-Cineole	1033	1203	28.0	13.0	40.7
γ-Terpinene	1056	1244	0.2	0.4	0.2
Sabinene hydrate	1068	1454	0.1	0.1	0.1
α-Terpinolene	1085	1275	tr	0.9	0.6
Linalool	1100	1542	0.7	6.7	0.4
α-Thujone	1109	1408	12.0	-	-
β-Thujone	1119	1426	8.5	-	-
Chrysantenone	1126	1486	-	0.2	-
allo-Ocimene	1126	1365	-	-	0.3
cis-Verbenol	1144	1663	-	0.5	-
Camphor	1150	1495	3.3	13.6	29.8
3-Pinanone	1160	1522	0.1	-	-
Pinocarvone	1163	1637	-	0.7	-
Borneol	1174	1685	4.0	12.5	5.2
4-Terpineol	1180	1587	0.4	1.3	0.8
p-Cymen-8-ol	1186	1827	-	-	0.7
α-Terpineol	1195	1657	0.6	2.6	2.0
Berbenone	1207	1677	-	10.0	0.1
trans-Carveol	1217	1848	tr	0.1	tr
Myrtenal	1219	1602	-	-	0.2
β-Citronelol	1225	1758	-	0.3	-
cis-Myrtanol	1241	1848	-	0.8	-
Carvone	1242	1706	-	-	0.4
Geraniol	1249	1819	-	2.9	-
β-Citral	1267	1712	-	0.2	-
(+)-Isopiperitone	1268	1807	-	0.5	-
m-Thymol	1278	2192	tr	tr	-
Bornyl acetate	1283	1566	0.2	2.9	tr
Carvacrol	1296	2151	tr	tr	-
α-Terpinelyl acetate	1331	-	-	tr	-
Piperitenone	1336	1848	-	0.1	-
Eugenol	1349	2139	-	0.1	-
1-Acetomethyl-3-isopropenyl-2-methyl-cyclopentane	1361	2028	-	0.1	-
α-Ylangene	1368	1471	tr	-	-
Copene	1375	1480	0.2	0.2	tr
2-Ethylidene-6-methyl-3,5-heptadienal	1392	2028	-	1.1	-
Methyl eugenol	1397	1994	-	0.7	-
α-Gurjunene	1406	1517	-	-	0.3
trans-Caryophyllene	1419	1579	2.1	1.3	1.1

Cumarine	1430	2389	-	-	tr
α-Guaiene	1439	1671	0.2	-	-
Neryl acetone	1446	1840	tr	0.3	-
α-Humulene	1456	1650	11.0	0.2	tr
Aromadendrene	1460	1625	0.6	-	tr
γ-Muurolene	1473	1672	0.3	0.2	-
Alloaromadendrene	1487	1626	0.5	-	-
Ledene	1490	1679	1.2	-	-
α-Selinene	1494	1702	tr	tr	-
α-Amorphene	1496	1707	tr	tr	-
β-Bisabolene	1506	1714	-	0.1	-
γ-Cadinene	1511	1740	0.1	0.2	1.0
δ-Cadinene	1516	1741	0.3	0.3	0.7
Nerolidol D	1522	1912	-	-	0.3
Germacrene-D-4-ol	1574	2034	-	-	0.1
Caryophyllene oxide	1580	1966	0.1	1.0	1.0
Viridiflorol	1596	2061	11.2	-	-
β-Selinene	1598	1981	0.3	-	-
Ledol	1603	1999	0.1	-	tr
Humulene oxide	1608	2003	1.0	0.1	-
Cubenol	1612	2032	-	-	0.2
δ-Cadinol	1625	2161	-	tr	-
Aromadendrene oxide 1	1631	2254	1.2	-	-
Aromadendrene epoxide	1634	2266	-	0.2	0.1
tau-Cadinol	1639	2148	tr	0.3	0.1
Bicyclo[4.4.0]dec-1-ene, 2-isopropyl-5-methyl-9-methylene	1640	2147	-	-	2.4
α-Cadinol	1653	2203	0.2	0.7	0.4
Andrographolide	1667	-	tr	0.1	tr
Aromadendrene oxide 2	1678	2365	0.1	-	-
3-Methyl-5-propyl-4-butylidene-cyclohex-2-ene-1-one	1681	-	-	-	tr
α-Bisabolol	1683	2195	-	0.2	-
6-Isopropenyl-4,8a-dimethyldecahydro-1-naphthalenol	1691	-	-	-	0.1
Bifromene	1925	2338	0.1	-	-
Manool	2042	-	2.3	-	-
Monoterpene Hydrocarbons			7.6	19.9	9.9
Oxygenated Monoterpenes			57.7	68.0	80.6
Sesquiterpene Hydrocarbons			16.8	2.5	5.5
Oxygenated Sesquiterpenes			13.9	2.5	2.3
Diterpene Hydrocarbons			0.1	-	-
Oxigenated diterpenes			2.3	0.1	-
Others			0.2	3.7	-
Total			98.6	96.7	98.3

Note: A = Kovats index on apolar column Inert Cap; B = Kovats index on polar column Rtx-Wax; Percentage and order of elution are given on the apolar column; tr = trace < 0,1%

Forty-six components were indentified in the sage oil, representing 98.6% of the total oil. The major compound is 1,8-cineole with 28.0%, followed by α-thujone (12.0%), viridiflorol (11.2%) and α-humulene (11.0%). Other compounds present in noticeable amounts were β-thujone (8.5%), α-pinene (4.1%), borneol (4.0%), camphor (3.3%), β-pinene (2.4%), manool (2.3%) and *trans*-caryophyllene (2.1%). Analysed oil showed surprisingly high concentration of 1,8-cineole and low content of camphor with respect to the previously investigated samples from Herzegovina (Marić *et al.*, 2006). This variability might be attributed to different

developmental stages, type of soil and exposure to light. In order to obtain the same chemical composition, essential oils should be extracted under the same conditions from the same organ of the plant which has been growing on the same soil, under the same climate and picked in the same season (Bakkali *et al.*, 2008).

The predominant components in rosemary oil are α-pinene (14.0%), camphor (13.6%), 1,8-cineole (13.0%), borneol (12.5%) and berbenone (10.0%). Other main

components included linalool (6.7%), α-terpineol (2.6%) and geraniol (2.9%). In rosemary extract 52 components were determined representing 96.7% of the essential oil. Lakušić *et al.* (2012) found that essential oils of rosemary from Balkan Peninsula can be classified in two major types: 1,8-cineol and camphor-type, and two intermediate types: camphor/1,8-cineole/borneol type and 1,8-cineole/camphor type. Analysed sample belongs to intermediate type which contains approximately equal amounts of camphor, 1,8-cineol and borneol. Among Balkan Peninsula this chemotype of rosemary is distributed along south Adriatic coast (Albania) and Italian Adriatic coast (Pescara) (Arnold *et al.*, 1997).

Total of 41 compounds were identified in the oil from lavender, corresponding to 98.3% of the components in oil. Two main components are 1,8-cineole (40.7%) and camphor (29.8%), followed by borneol (5.2%), β-pinene (2.7%), α-pinene (2.5%), 2-isopropyl-5-methyl-9-methylenebicyclo[4.4.0]dec-1-ene (2.4%) and α-terpineol (2.0%). High concentration of 1,8-cineole in lavender is typical for old leaves, collected from August till June (Lakušić *et al.*, 2014).

There are 22 compounds that occur in all three oils. 1,8-Cineole is the main component of sage and lavender, but it is also one of major compound in rosemary. The main component in rosemary is α-pinene which is also present in other two oils in appreciable amounts. However, some of the components present in one of the oil as one of the major compounds were absent in the other oils. For example, significant constituents from sage oil like α-thujone, β-thujone, viridiflorol and manool were absent in rosemary and lavender oils.

The oils were evaluated for antioxidant activity using two different methods. Like in numerous studies, 2,2'-diphenyl-1-picrylhydrazyl radical scavenging method (DPPH) and ferric reducing antioxidant power (FRAP) can be cited as relatively simple methods that can be used to measure the antioxidant potential of essential oils (Pajero *et al.*, 2003; Politeo *et al.*, 2011; Tomaino *et al.*, 2005). The DPPH method is sensitive and requires little sample material. The FRAP method is fast, easy to handle, with highly reproducible results. The antioxidant activity of the tested essential oils of rosemary, sage and lavender has been evaluated as a series of mass concentrations of essential oils (5-50 g L^{-1}). Concentrations of essential oils for both antioxidant methods are given as the concentrations of stock solutions.

All examined essential oils were able to reduce the stable, purple-coloured radical DPPH into yellow-coloured DPPH–H, without reaching 50% of DPPH radical inhibition (Figure 1). Rosemary essential oil showed the greatest inhibition of DPPH radicals by 33.7% at a concentration of 50 g L^{-1}, then lavender with 13.3% inhibition at a concentration of 20 g L^{-1} and sage with 9.2% of inhibition at a concentration of 50 g L^{-1}. According to this method, all examined oils had a low antioxidant activity compared to synthetic antioxidant butylated hydroxytoluene (BHT) (IC_{50} = 1.5 g L^{-1}) (Figure 2).

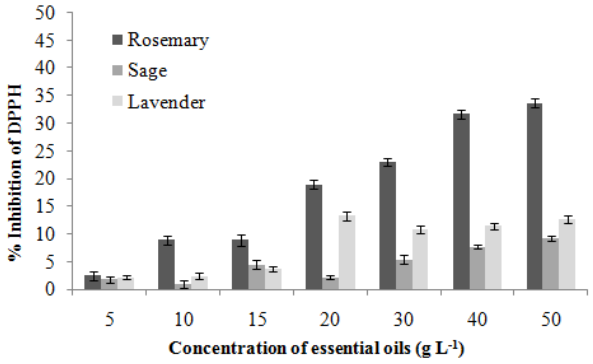

Figure 1. The inhibition percent of the DPPH radical in the presence of different concentrations of essential oils of rosemary, sage and lavender.

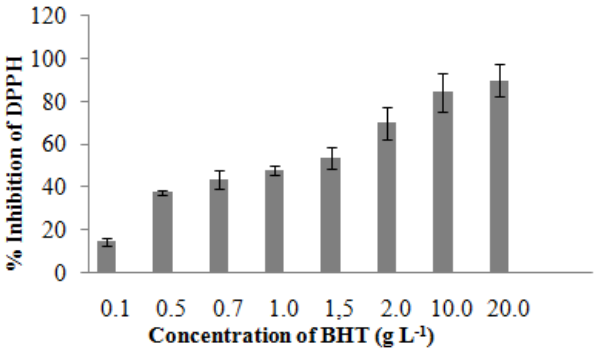

Figure 2. The inhibition percent of the DPPH radical in the presence of different concentrations of BHT.

The reducing power of the essential oils and BHT were determined by FRAP assay (Figure 3 and Figure 4). FRAP assay is based on redox-colorimetric reaction of the reduction of colourless Fe^{3+} compounds into blue colored Fe^{2+} tripiridyltriazine in the presence of the antioxidants (Politeo *et al.*, 2011). As in the previous method, the essential oil of rosemary showed the greatest reducing power. The essential oil of rosemary at the concentration of 30 g L^{-1} is equivalent to 1.6 mmol L^{-1} Fe^{2+} then sage at 20 g L^{-1} is equivalent to 0.9 mmol L^{-1} Fe^{2+} and lavender at 30 g L^{-1} is equivalent to 0.6 mmol L^{-1} Fe^{2+} in reducing power. The concentration of 2 g L^{-1} of synthetic antioxidant BHT is equivalent to 2.6 mmol L^{-1} Fe^{2+} in reducing power. High concentrations of all tested samples showed decrease in antioxidant activity.

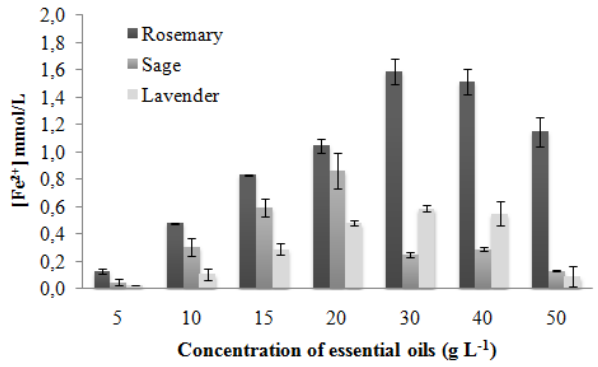

Figure 3. The antioxidant capacity in the presence different concentrations of essential oils of rosemary, sage and lavender measured by the FRAP assay.

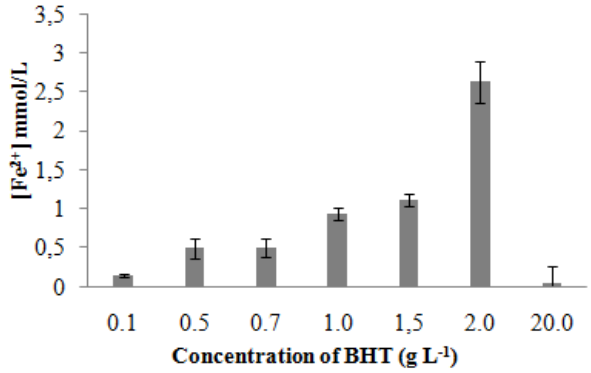

Figure 4. The antioxidant capacity in the presence different concentrations of BHT measured by the FRAP assay.

The results obtained from both methods show that the essential oils of rosemary, sage and lavender have low to moderate antioxidant activity. The major compound present in analyzed oils, 1,8-cineole, was previously tested and showed weak antioxidant activity using FRAP assay and almost none inhibition of DPPH radical (Zengin & Baysal, 2014). Low values of antioxidant activity obtained by both methods could be consequence of high content of other compounds such as camphor, borneol, β-pinene and α-pinene, none of which exhibited antioxidant activity (Tepe *et al.*, 2005). The lowest antioxidant activity is recorded for lavender oil where 1,8-cineole, camphor and α-pinene represent more than 75% of the total content. Somewhat greater antioxidant ability of rosemary oil could be attributed to other compounds present or to synergy effect between oil components. Dawidowicz and Olszowy (2014) showed that camphor, one of the main components in essential oil of sage (*Salvia hispanica*), has lower antioxidant ability than the essential oil. This finding suggests that antioxidant properties of sage oil are significantly affected not only by main components but also by other components. Earlier studies on 1,8-cineole/camphor/α-pinene type of rosemary oil (Rašković *et al.*, 2014) revealed notably stronger radical scavenging activity then it is found in our sample. Antioxidant properties are influenced by several factors, including the species, part of the plant, season of harvesting, geographical origin and extraction method, which also influence the chemical composition of plant essential oils (Teixeira *et al.*, 2013). Therefore, all effects of Lamiaceae essential oils should be carefully examined, considering the chemical composition of the investigated oil.

CONCLUSION

These results showed that studied oils consisted of various components among which most of them were present in all three species in different relative proportion. Nevertheless, some constituents were found only in one of the oils. The results obtained from both antioxidant methods showed low activity of sage and lavender and moderate activity for rosemary essential oil. It is difficult to make a direct relation among bioactivity and composition in such complex mixture like rosemary oil, but it can be suggested that synergism among components may increase antioxidant activity. Season of harvesting (October, non-flowering period) influences the chemical composition of essential oils (Teixeira *et al.*, 2013) and thereby affects the antioxidant activity. Although plants collected in October gave good yields on essential oil distillation, it was found that this chemical composition of all three species has low antioxidant activity.

ACKNOWLEDGEMENT

This work was supported by grant from the Federal Ministry of Education and Science, Bosnia and Herzegovina (Grant No.1000039). The authors thank Dr. Sc. A. Lasić for her help in plant identification.

REFERENCES

Arnold, N., Valentini G., Bellomaria, B., Hocine, L. (1997). Comparative study of the essential oils from *Rosmarinus eriocalyx* Jordan & Fourr. from Algeria and *R. officinalis* L. from other countries. *Journal of Essential Oil Research*, *9*(2), 167-175.

Bakkali, F., Averbeck, S., Averbeck, D., Idaomar, M. (2008). Biological effect of essential oils – A review. *Food and Chemical Toxicology*, *46*(2), 446-475.

Benzie, I. F. F. & Strain, J. J. (1996). The Ferric Reducing Ability of Plasma (FRAP) as a Measure of 'Antioxidant Power': The FRAP Assay. *Analytical Biochemistry*, *239*(1),70–76.

Brand-Williams, W., Cuvelier, M. E., Berset, C. (1995).Use of a free radical method to evaluate antioxidant activity. *LWT - Food Science and Technology*, *28*(1), 25-30.

Dawidowicz, A. L., Olszowy M. (2014). Does antioxidant properties of the main component of essential oil reflect its antioxidant properties? The comparison of antioxidant properties of essential oils and their main components. *Natural Product Research*, *28*(22), 1952-1963.

Jukić, M., Politeo, O., Miloš, M. (2006). Chemical Composition and Antioxidant Effect of Free Volatile Aglycones from Nutmeg (*Myristica fragrans* Houtt.) Compared to Its Essential Oil. *Croatica Chemica Acta*, 79 (2) 209-214.

Lakušić, D.V., Ristić, M.S., Slavkovska, V.N., Šinžar-Sekulić, J.B., Lakušić, B.S. (2012). Environment-related variations of the composition of the essential oils of rosemary (*Rosmarinus officinalis* L.) in the Balkan peninsula. *Chemistry and Biodiversity*, *9*(7), 1286-1302.

Lakušić, B. S., Lakušić, D. V. Ristić, M.S., Marčetić, M., Slavkovska, V. N. (2014) Seasonal Variations in the Composition of the Essential Oils of *Lavandula angustifolia* (Lamiaceae). *Natural Product Communication*, *9*(6), 859-862.

Marić, S., Maksimović, M., Miloš, M. (2006). The impact of the locality altitudes and stages of development on the volatile constituents of *Salvia officinalis* L. from Bosnia and Herzegovina. *Journal of Essential Oil Research*, *18*(2), 178-180.

Rašković, A., Milanović, I., Pavlović, N., Ćebović, T., Vukmirović,S., Mikov, M. (2014). Antioxidant

activity of rosemary (*Rosmarinus officinalis* L.) essential oil and its hepatoprotective potential. *Complementary and Alternative Medicine*, 14:225.

Redžić, S.S. (2007). The ecological aspect of ethnobotany and ethnopharmacology of population in Bosnia and Herzegovina. *Collegium Antropologicum*, *31*(3), 869-890.

Pajero, I., Viladomat, F., Bastida, J., Rosas-Romero, A., Saavedra, G.,. Murcia, M. A, Jimenez, A. M., Codina, C. (2003). Investigation of Bolivian plant extracts for their radical scavenging activity and antioxidant activity. *Life Sciences*, *73*(13), 1667–1681.

Politeo, O., Jukić, M., Miloš, M. (2007). Chemical composition and antioxidant capacity of free volatile aglycones from basil (*Ocimum basilicum* L.) compared with its essential oil. *Food Chemistry*, *101*(1), 379-385.

Politeo, O., Botica, I., Bilusić, T., Jukić, M., Carev, I., Burcul, F., Miloš, M. (2011). Chemical composition and evaluation of acetylcholinesterase inhibition and antioxidant activity of essential oil from Dalmatian endemic species *Pinus nigra* Arnold ssp. *dalmatica* (Vis.) Franco. *Journal of Medicinal Plants Research*, *5*(30)**,** 6590-6596.

Teixeira, B., Marquesa, A., Ramosa C.,Nengc, N.R., Nogueirac, J.M.F., Saraivab, J.A., Nunesa, M.L. (2013). Chemical composition and antibacterial and antioxidant properties of commercial essential oils. *Industrial Crops and Products*, 43, 587– 595.

Tepe, B., Sokmen, M., Akpulat, H.A., Daferera, D. Polissiou, M., Sokmen, A. (2005). Antioxidative activity of the essential oils of *Thymus sipyleus* subsp. *sipyleus* var. *sipyleus* and *Thymus sipyleus* subsp. *sipyleus* var. *rosulans*. *Journal of Food Engineering*, *66*(4), 447–454.

Tomaino, A., Cimino, F., Zimbalatti, V., Venuti, V., Sulfaro, V., De Pasquale, A., Saija, A. (2005). Influence of heating on antioxidant activity and the chemical composition of some spice essential oils. *Food Chemistry*, *89*(4), 549–554.

Zengin, H., Baysal, A.H. (2014). Antibacterial and antioxidant activity of essential oil terpenes against pathogenic and spoilage-forming bacteria and cell structure-activity relationships evaluated by SEM microscopy *Molecules*, *19*(11), 17773-17798.

Summary/Sažetak

Ispitivane su komponente eteričnih ulja ružmarina, kadulje i lavande GC-MS-om kao i njihova antioksidacijska aktivnost. Ulja su destilirana u listopadu, nakon vegetativnog ciklusa biljke, kako bi se ispitala antioksidacijska aktivnost u ovom periodu. Glavne komponente eteričnog ulja kadulje su 1,8-cineol (28.03%), *a*-tujon (11.98%), veridiflorol (11.17%) i *a*-humulen (11.0%). Ružmarinovo eterično ulje čine najvećim dijelom *a*-pinen (14.02%), kamfor (13.62%), 1,8-cineol (13.02%), borneol (12.45%) i berbenon (10.04%). Glavni spojevi eteričnog ulja lavande su 1,8-cineol (40.68%) i kamfor (29.82%). Antioksidacijska aktivnost je ispitivana koristeći dvije metode: 2,2'-difenil-1-pikrilhidrazil (DPPH) metodu vezanja radikala i FRAP metoda određivanja antioksidacijskog kapaciteta. Rezultati pokazuju da analizirana eterična ulja kadulje i lavande imaju slabu antioksidacijsku aktivnost u usporedbi sa sintetskim antioksidansom butiliranim hidroksitoluenom (BHT), dok ružmarinovo eterično ulje ima umjerenu aktivnost.

Glasnik hemičara i tehnologa Bosne i Hercegovine

Bulletin of the Chemists and Technologists of Bosnia and Herzegovina

2015

45

31-34

Print ISSN: 0367-4444
Online ISSN: 2232-7266

UDC: _____

Original Scientific Paper

Determination of gross alpha and beta activity and uranium isotope content in commercially available, bottled, natural spring waters

Nuhanović, M.*, Mulić, M., Mujezinović, A., Grgić, Ž., Bajić, .I

University of Sarajevo, Faculty of Science, Department of Chemistry, Zmaja od Bosne 33-35, 71000 Sarajevo,B&H

Article info
Received: 23/10/2015
Accepted: 09/12/2015

Keywords:
Uranium Isotopes
Activity
Anion Exchange Resin
Source Preparation
Electro Deposition
Co-Precipitation
Alpha Spectrometry
Gross Alpha-Beta Activity

***Corresponding author:**
E-mail: mirza.nuhanovic@yahoo.com
Tel: +387/33/279-865

Abstract: Determination of content (active concentration) of radio-nuclides has recently become an indispensable part of the study dealing with the protection of the environment. Uranium concentration levels in aquatic environment are of great importance for environmental and safety assessment and for the protection of public health. Achieving this purpose, monitoring program for this radio-nuclide, radium and thorium, as well as gross alpha and beta activities, seems necessary and it is applied in many countries. This study determined the activity concentration of uranium isotopes in 10 samples of drinking water, natural spring and mineral water (bottled, commercially available water). Also, gross alpha and beta activity has been determined for all samples. Activity concentration of uranium isotopes was measured with alpha-spectrometry, while gross alpha-beta activity was measured by low level gas-flow proportional alpha-beta counter. Results of the research show that the concentration of isotopic uranium activities in the tested samples of drinking water varies from 10-8 to 10-2 Bq/L, while gross alpha-beta activity is between 10-3 and 10-1 Bq/g. The results show that the analyzed brands of spring, commercially available bottled waters meet the defined criteria of radiological safety.

INTRODUCTION

Throughout the world, tap water is being replaced by commercially available natural spring and mineral waters used in households and industry, as well as in the production of various soft drinks. This increased consumption and the fact that exposure to natural radiation sources contributes more than 98% of the total irradiation of population call for determination of total effective dose received from consumption of these products and for determination of contributions of particular natural radio-nuclides to the total effective dose. A major contribution comes from uranium and thorium series radio-nuclides in the following order:

^{210}Po > ^{228}Ra > ^{210}Pb > ^{226}Ra > ^{234}U > ^{238}U > ^{224}Ra > ^{235}U.

Radiological control of water is necessary due to its importance for human life and the need for minimum exposure to radiation. Therefore, maximum permissible concentration limits of radio-nuclide activity in drinking water have been prescribed by the World Health Organization (Mačefat *et al*., 2011).
Water plays a big and diverse role in the world. Processed or not, water is used in industry and commercial sector, for irrigation, sanitation and primarily for supplying the population with drinking water and water for household needs.

Uranium is a naturally occurring radioactive element, widely distributed in nature, consists of the isotopes ^{234}U, ^{235}U and^{238}U,with a mass ratio of 0.0054 : 0.711 : 99.2836%.

All of these three nuclides are alpha emitters, which have a particular biological effectiveness (Pimpl *et al.*,1992). Natural uranium can be detected in low concentrations in almost all materials from the environment. Long half-lives of uranium and transuranic isotopes make these elements long-term hazardous. Considering toxicity and radio-toxicity of uranium (Becker *et al*., 1997), its determination at trace and ultra-trace levels with high accuracy is very important. The average concentration of uranium in the Earth's crust is 3 mg/kg (Bleise *et al.*, 2003). Uranium concentration in ground and surface waters is three orders of magnitude lower, approximately 1 mg/L, although it can range from 0.001 to 1000 mg/L (Osmond *et al.,* 1983). Uranium isotopes and its decay series radio-nuclides, enter the human body mainly through food and drinking water (Bansal *et al.*, 1992). Water comes into contact with several minerals under the earth's surface, and uranium is transferred to water by its leaching action. Also, human activity, such as the use of depleted uranium ammunition, which is the case in some areas in BiH, inappropriately stored radioactive waste and other activities, can affect the radio-nuclide content in drinking water. $^{234}U/^{238}U$ activity ratio in natural water is an important indicator of the origin of the uranium in the studied sample. Typically, the $^{234}U/^{238}U$ activity ratio in natural water varies from 1 to 2, but it can range up to 30 in extreme cases (Osmond *et al.,* 1983). Commonly observed fractionation and disequilibrium between ^{234}U and ^{238}U in water is a result of nuclear recoil effects (Fleischer and Raabe, 1978; Osmond *et al.*, 1983) and extensive rock/water interactions.

The aim of this study is to determine uranium isotopes activity concentration, $^{234}U/^{238}U$ activity ratio in the spring waters (bottled, non-mineral and mineral, and crude spring water), and gross alpha beta activity of the supra samples. According to the available literature, drinking water quality monitoring in BiH mainly comes down to chemical and microbiological analyses. Given the use of depleted uranium ammunition in the war in the 90 s and a highly varied geo-structure of soil, among many other parameters (microbiological, chemical), radium and uranium isotopes have to be regularly monitored in drinking waters (Vasile *et al.,* 2008) (Council Directive 98/83/EC,1998). We analyzed ten bottled samples of drinking water, the most commonly used on the BiH market, in order to obtain some detailed information about content of uranium, and gross alpha beta activity in spring drinking water.

EXPERIMENTAL

This study analyzed mineral and natural commercially available spring waters, ten randomly selected brands of well-known producers, in order to determine uranium isotopes and gross alpha-beta activity.

Gross alpha-beta activity was determined by standard methods from ISO 9696 or ISO 9697.

1 mL of concentrated H_2SO_4 was added to each 1 L sample aliquot. The aliquots were then evaporated to dryness. The obtained dry residue was transferred to pre-weighed crucibles. These samples were calcinated in the calcinator at the temperature of 350°C. The calcinated residue was homogenized and 100 mg was transferred to a 5-cm-diameter planchet for measurement. Gross alpha-beta activity was measured by the gas-flow proportional counter MPC-9604, Protean Instruments Corporation, for 84600 seconds. Efficiency for gross alpha activity was 7.6% and 38.6% for gross beta activity.

Activity concentration of uranium isotopes was determined by alpha spectrometry. Approximately 1 L of each water sample was taken and the liquid was weighed in glasses of known mass.

Each sample was acidified with 1 mL concentrated HNO_3 and known mass of U-232 tracer was added. Uranium was precipitated with $CaCl_2$ and $(NH_4)_2HPO_4$ according to the Eichrom procedure (Eichrom Technologies Inc., 2001).

Several mL of $NH_{3(aq)}$ were then added to each sample and heated for 20 minutes until deposition formed, which was obvious from the white turbidity of the sample. The liquid above the deposition was decanted, and several mL of 8 mol/L HCl were added to the deposition to dissolve it. Uranium was separated from interfering elements by passing it through an anion exchange column, DOWEX 1x8, Cl^- form, 100-200. After thorium isotopes were removed with 45 mL 8 mol/L HCl, uranium was eluted with 15 mL 0.5 mol/L HCl. The samples were prepared for measurement by electro-deposition and were measured for 2 hours at 1.2 A amperage according to HASL-300 procedure (DOE EML, 1997). The measurement was performed by alpha spectrometer Alpha Analyst, Canberra, equipped with silicon detector (PIPS) with 450 mm^2 active surface. Sample counting time was 172800 s, and the chemical yield was 15-96%. Lower limit of detection was 0.717-3.69 mBq/L ^{238}U, 0.0897-0.222 mBq/L ^{235}U, and 0.269-5.45 mBq/L for ^{234}U. The results are reported with combined standard uncertainty with coverage factor 1.

RESULTS AND DISCUSSION

The tested samples of the above mentioned water were analyzed for gross alpha and beta activity, including an isotopic analysis of uranium. Results of the analyses of tested samples are shown in Tables 1, 2, 3, 4, 5 and 6.

Table 1. Gross alpha and beta activity of analyzed samples of mineral commercially available water

Water samples	Gross alpha activity (Bq/g)	Gross beta activity (Bq/g)
1	0.019	0.00318
2	0.00115	0.177
3	0.0112	0.0584
4	0.034	0.0123
5	0.00439	0.105

Table 2. Gross alpha and beta activity of analyzed samples of mineral commercially available natural spring water

Water samples	Gross alpha activity (Bq/g)	Gross beta activity (Bq/g)
1	0.0190	0.0266
2	0.0389	0.0626
3	0.00240	0.0364
4	0.0241	0.0423
5	0.038	0.0772

According to the Rulebook on Sanitary Quality of Drinking Water (Official Gazette of BIH, No.40/10) and recommendations of the World Health Organization *(WHO*, 2011), permissible level of gross α-activity is 0.5 Bq/g, and permissible level of gross β-activity is 1 Bq/g. Order of magnitude of the results of all processed samples is between 10^{-2} and 10^{-4} Bq/g, which shows that the gross alpha and beta activity of all ten analyzed samples does not exceed the permissible level of activity.

The highest gross alpha activity was registered in sample No. 4, while the lowest alpha activity was registered in sample No. 2. The highest gross beta activity was registered in sample No. 2, while the lowest activity was registered in sample No.1

Table 3. Results of uranium radioisotopes activity concentration obtained through Alpha-spectrometric analysis of commercially available mineral spring water samples

Water samples	A(^{238}U) (Bq/L)	A(^{235}U) (Bq/L)	A(^{234}U) (Bq/L)	Activity ratio ^{234}U/^{238}U
1	$6.07\cdot10^{-3}$	$4.78\cdot10^{-4}$	$4.04\cdot10^{-2}$	6.6557
2	$1.08\cdot10^{-3}$	$5.40\cdot10^{-5}$	$7.07\cdot10^{-3}$	6.5463
3	$2.80\cdot10^{-3}$	$2.77\cdot10^{-5}$	3.6310^{-3}	1.2964
4	$2.21\cdot10^{-3}$	$1.03\cdot10^{-4}$	$2.00\cdot10^{-3}$	0.9049
5	$4.14\cdot10^{-4}$	$3.45\cdot10^{-5}$	$1.73\cdot10^{-4}$	0.4179

Table 4. Results of uranium radioisotopes activity concentration obtained through Alpha-spectrometric analysis of commercially available natural spring water samples

Water samples	A(^{238}U) (Bq/L)	A(^{235}U) (Bq/L)	A(^{234}U) (Bq/L)	Activity ratio ^{234}U/^{238}U
1	$3.27\cdot10^{-7}$	$1.87\cdot10^{-7}$	$2.86\cdot10^{-6}$	0.8746
2	$1.17\cdot10^{-6}$	$2.97\cdot10^{-8}$	$1.31\cdot10^{-6}$	1.1197
3	$1.72\cdot10^{-5}$	$6.72\cdot10^{-7}$	$2.54\cdot10^{-5}$	1.4767
4	$2.14\cdot10^{-6}$	$2.93\cdot10^{-8}$	$6.55\cdot10^{-6}$	3.0607
5	$1.17\cdot10^{-7}$	$3.38\cdot10^{-8}$	$6.82\cdot10^{-7}$	5.8291

According to the World Health Organization (WHO), (Water Sanitation Health, Chapter 9), permissible level of activity concentration (content) of uranium isotopes is as follows: For ^{238}U 10 Bq/kg, for ^{235}U 1 Bq/kg and for ^{234}U 1 Bq/kg.

Therefore, all ten analyzed samples of known brands of commercially available mineral and natural spring water contain a permissible concentration of uranium isotopes, within the limits prescribed by the World Health Organization.

The analysis of commercially available mineral waters shows the highest concentration of uranium isotopes in sample No. 1, while the lowest concentration was registered in sample No. 3. The analysis of commercially available natural spring waters shows the highest concentration of uranium isotopes in sample No. 3, while the lowest concentration was registered in sample No. 5.

^{234}U/^{238}U ratio in natural waters is within the limit of 0.5-1.2. Activity ratio in this study varies between 0.4179-6.6557. ^{234}U/^{238}U activity ratio value larger than 2 indicates a more intensive solid to liquid phase transition than normal and/or transition to liquid phase in slow moving waters, while the value lower than 1 indicates less intensive dissolution or contact with fast moving waters (Vidic, 2010).

Table 5. Results for dry residue and conductivity of commercially available mineral water samples

Water samples	V (mL of sample)	m (g) dry residue before drying)	m (g) dry residue after drying, 350°C)	Conductivity (μS/cm)
1	1000	2.859	2.5029	1300
2	1000	2.755	2.1471	1840
3	1000	1.5568	0.8829	1260
4	1000	2.3028	1.6966	2570
5	1000	2.901	1.7948	2130

Table 6. Results for dry residue and conductivity of commercially available natural spring water samples

Water samples	V (mL of sample)	m (g) dry residue before drying)	m (g) dry residue after drying, 350°C)	Conductivity (μS/cm)
1	1000	0.3916	0.3000	412
2	1000	0.4621	0.4100	462
3	1000	0.4682	0.3600	434
4	1000	0.4862	0.3800	611
5	1000	0.5999	0.5800	471

The analyzed waters have relatively high values for dry residue and specific conductivity which indicates that they are very hard waters with high ion content, which was expected since we are talking about mineral waters. Lack of correlation is usually connected with different origin and different chemical composition of waters.

CONCLUSIONS

After described processing and preparation of samples, the obtained data were calculated and concentration values of all three uranium isotopes present in the samples were obtained, as well as gross alpha-beta activity. According to the Rulebook on Sanitary Quality of Drinking Water (Official Gazette of BIH, No. 40/10) and recommendations of the World Health Organization (WHO, 2011), permissible level of gross α-activity is 0.5 Bq/g, and permissible level of gross β-activity is 1 Bq/g. Order of magnitude of the results of all processed samples is between 10^{-3} and 10^{-1} Bq/g, which shows that the gross alpha and beta activity of all five analyzed samples does not exceed the permissible level of activity. According to the World Health Organization (WHO), (Water Sanitation Health, Chapter 9), permissible level of activity concentration (content) of uranium isotopes is as follows: 10 Bq/kg for ^{38}U, 1 Bq/kg for ^{235}U and 1 Bq/kg for ^{234}U. All ten analyzed samples contain a permissible concentration of uranium isotopes and are very well-correlated with the quantity of total water mineralization. The analysis showed that the water samples are fully radiologically safe and not harmful to human health and environment.

REFERENCES

Bansal, K.C., Viret, J.F., Haley, J., Khan, B.M., Schantz, R., Bogorad, L. (1992). Transient expression from cab-ml and rbcS-m3 promoter sequences is different in mesophyll and bundle sheath cells in maize leaves. *Proceding of the National Academy of Sciences*. 89(8), 3654-3658.

Becker, G.S., and Mulligan, C.B. (1997). The endogenous determination of time preference. *The Quarterly Journal of Economics*, 729-758.

Bleise, A., Danesi, P.R., Burkart, W. (2003). Properties, use and health effects of depleted uranium (DU): a general overview, *Journal of Environmental Radioactivity*, 64(2),93-112.

DOE EML Procedures Manual HASL-300, (1997). 1(28).

Eichrom Technologies Inc. (2001). Analytical Procedures-Uranium and Thorium in Water-ACW03 Version 1.7.

EU (1998). Council Directive 98/83/EC of 3 November 1998 on The Water Intended for Human Consumption. European Uninion *Official Journal L* 330 (05/12/98).

Fleischer, R.L., Raabe, O.G. (1978). Recoiling alpha-emitting nuclei. Mechanisms for uranium-series disequilibrium. *Geochimica et Cosmochimica Acta*, 42(7), 973-978.

ISO 9696 (2007). Water quality - Measurement of gross alpha activity in non-saline water Thick source method. International Standardization Organization, Geneva, Switzerland.

ISO 9697 (2008). Water quality - Measurement of gross beta activity in non-saline water - Thick source method. International Standardization Organization, Geneva, Switzerland.

Mačefat, M., Krmpotić, M., Barišić, D. (2011). Determination of natural alpha emitting radio-nuclides in bottled drinking and mineral water. In *Eight symposium of the Croatian Radiation Protection Association with international participation*, Croatian Scientific Bibliography and Ministry of Science, Education and Sports -Svibor.

Osmond, J.K., Cowart, J.B., Ivanovich, M. (1983). Uranium isotopic disequilibrium in ground water as an indicator of anomalies. *The International Journal of Applied Radiation and Isotopes*, 34(1), 283-308.

Pimpl, M., Yoo, B., Yordanova, I. (1992). Optimization of a radioanalytical procedure for the determination of uranium isotopes in environmental samples. *Journal of radioanalytical and nuclear chemistry*, 161(2), 437-441.

Rulebook on Sanitary Quality of Drinking Water (*Official Gazette of BIH, No.40/10*). Public Health Institute.

Vasile, M., Altzitzoglou, T., Benedik, L., Spasova, Y., Wätjen, U. (2008). Radiochemical separation and determination of 228Ra in mineral waters by low-level liquid scintillation counting. *LSC*, 375-380.

Vidic, A. (2010). *Radiohemijska separacija i alfaspektrometrijsko određivanje uranovih izotopa u rejonu TRZ Hadžići,* Magistarski rad, Prirodno-matematički fakultet, Univerzitet u Tuzli.

World Health Organization (WHO). (2008). Guidelines for drinking-water quality, 1st Ed.

World Health Organization (WHO). (2011). Guidelines for drinking-water quality, 4st Ed.

Summary/Sažetak

Određivanje sadržaja (aktivne koncentracije ili koncentracije aktivnosti) radionuklida u posljednje vrijeme postaje neizostavni dio studija koje se bave zaštitom okoliša. Sadržaj urana u vodenom okruženju je od velike važnosti za okoliš i sigurnosne procjene istog, a u svrhu zaštite zdravlja. Shodno navedenom, praćenje sadržaja ovog radionuklida, radija, torija, kao i ukupne alfa i beta aktivnosti u okolišu, se nameće kao neophodno i primjenjuje se u mnogim zemljama u svijetu. U ovom radu određena je koncentracija aktivnosti uranovih izotopa u deset uzoraka vode za piće, prirodne izvorske i mineralne vode (flaširane, komercijalno dostupne vode). Također, za sve navedene uzorke vode određena je ukupna alfa i beta aktivnost. Koncentracija aktivnosti uranovih izotopa mjerena je alfa-spektrometrijski, a ukupna alfa-beta aktivnost je mjerena na niskofonskom, gas-proporcionalnom alfa-beta brojaču. Rezultati istraživanja su pokazali da se koncentracija aktivnosti uranovih izotopa ispitivanih uzoraka vode za piće kreće od 10^{-8} do 10^{-2} Bq/L, a ukupna alfa-beta aktivnost od 10^{-3} do 10^{-1} Bq/g. Dobijeni rezultati su pokazali da su analizirani brendovi izvorskih, komercijalno dostupnih, flaširanih voda, radiološki ispravni.

Glasnik hemičara i tehnologa Bosne i Hercegovine

Bulletin of the Chemists and Technologists of Bosnia and Herzegovina

2015

45

35-38

Print ISSN: 0367-4444
Online ISSN: 2232-7266

UDC: _____

Original Scientific Article

Graphite, Graphite Oxide, Graphene Oxide, and Reduced Graphene Oxide as Active Materials for Electrochemical Double Layer Capacitors: A comparative Study

Kozlica Dž*, Korać F., Gutić S.

Department of Chemistry, Faculty of Science, University of Sarajevo, Zmaja od Bosne 35, 71 000 Sarajevo, Bosnia and Herzegovina

Article info
Received: 21/11/2015
Accepted: 14/12/2015

Keywords:
Graphene oxide
Reduced graphene oxide
Aqueous solution
Supercapacitors

***Corresponding author:**
E-mail:strider_shire@hotmail.com

Abstract: In this paper report we compare the properties and the performance of four different carbonaceous materials, namely graphite, graphite oxide, graphene oxide and reduced graphene oxide, as active materials for electrochemical double layer capacitors (EDLCs). Compared to ordinary graphite, and graphite oxide, rGO have superior capacitive behavior and power output in EDLCs due to their unique nanoporous structure, porosity and enormous BET surface area close to 1200 m^2g^{-1}. The electrochemical properties of these carbonaceous materials were determined by cyclic voltammetry. The result of this investigations indicate reduced graphene oxide as a very promissing candidate for the realization of high performance EDLCs, able to display high energy and high power. In the potential range of (0 to -0.8) V, rGO has the specific capacitance of 85.9 Fg^{-1} in 1 $molL^{-1}$ $LiNO_3$ solution using three-electrode system. A further analysis of the electrochemical behavior in different electrolytic aqueous media showed that in Li^+ solution rGO have the highest capacitance, as we compare to Na^+ and K^+ solutions.

INTRODUCTION

Electrochemical capacitors (or supercapacitors) are very attractive power sources for portable electronic systems and automotive applications due to their high specific power and very long durability (Conway, 1999; Kotz and Carlen, 2000; Frackowiak and Beguin, 2001). Electric double layer capacitors (EDLCs) are advantageous over modern secondary batteries in power capability and long cycle life. There are two energy storage mechanisms for supercapacitors: double-layer capacitance and pseudocapacitance. Although the energy densities of devices based on pseudocapacitance are greater than those on double-layer capacitance, the phase changes in the pseudocapacitance materials limit their lifetime and power density due to the faradaic reaction. As we know, carbon materials, commonly corresponding to double-layer capacitance, are the most ideal materials for supercapacitors (Pandolfo and Hollenkamp, 2006; Simon and Gogotsi, 2008).

The performance of porous carbons as EDLCs is strongly dependent on a number of factors which include carbon material properties (such as porosity, surface chemistry and electrical conductivity), preparation method of the electrode and electrolyte characteristics (such as ions dimensions, dielectric constant, etc.). A unit cell od EDLC works on the principle of double-layer capacitance at the electrode/electrolyte interface where electric charges are accumulated on the elecrode surfaces and ions of opposite charge are arranged in the electrolyte side. Since this phenomenon is controlled by

the surface area of the interface, activated carbons are the most widely used electrode materials for EDLSs. Considering that only charging of the double-layer is involed, it should be expected that higher the specific surface area of the carbonaceous material, higher the capacitance (Castello *et al*., 2003; Shi, 1996).

Altough a high specific surface area is regarded as a primarly requirement for carbon electrodes to be used in EDLCs, some other aspects of the surface physicochemical properties can be critical for the electrochemical performance. Beside the pore size distribution, the electric conductivity of the carbon material is a key parameter. and there is a possibility that heteroatoms as oxygen or nitrogen can induce pseudo-capacitance effects. The foreign atoms in the graphene layers modify also their electron donor/acceptor character, and are consequently expected to affect the charging of the electrical double layer (Qu and Shi, 1998; Martinez *et al.*, 2005).

Graphene based materials have shown immense theoretical and practical advantages among carbonaceous materials, such as a high surface area, excellent conductivity and capacitance, and relatively low production costs (mass production) (Brownson and Banks, 2010).

Graphene is two-dimensional one atom-thick planar sheet of sp^2 bonded carbon atom, which is considered as the fundamental foundation for all fullerene allotropic dimensionalities. Chemically, graphene oxide is similar, if not identical, to graphite oxide, but structurally it is very different. Rather than retaining a stacked structure, the material is exfoliated into monolayers or a few stacked layers, and graphene oxide contains a range of reactive oxygen functional groups (Dreyer *et al.*, 2010).

It is graphene oxide that is the product obtained by Hummers method, and hence it is graphene oxide that undergoes the reduction to graphene, or more precisely GO is reduced to r-GO.

The present work is focused on an advanced understanding of the electrochemical behavior of different carbonaceous materials as candidate for electrode material for supercapacitors in aqueous media.

EXPERIMENTAL

Preparation of working electrode and electrochemical characterization

The composite carbon electrodes used in this paper were prepared by mixing the pure carbon material with poly (vinyliden fluoride) binder, 5% nafion solution and of a conductive additive carbon. The ration of carbon material to other ingredients is 9:1. The suspension was made in water-alcohol mixture.

Electrochemical measurements were carried out in three-electrode setup with PAR 263A Potentiostat/Galvanostat workstation operating at room temperature. The working electrode was glassycarbon which consists of added composite carbon materials as active material. Before CV measurements, suspension is put under vacuum treatment to remove an excess oxygen from the solution and its fine suspendedusing ultrasound treatment. Ag /AgCl electrode and Pt wire served as reference electrode and counter electrode, respectively. 1M LiCl, NaCl, and KCl aqueous solution was used as electrolyte. The cyclic voltammetry (CV) curves were acquired at scan rates of 50, 100, 200 and 500 mV s^{-1} in potential window (-1 to 0.8 V).

RESULTS AND DISCUSSION

In first series of experiments, cyclic voltammetry at various scan rates were carries out for EDLCs with graphite and graphite oxide as active materials using 1M Li^+, Na^+ and K^+ aqueous electrolytes. Figure 1 shows the results of these CV measurements exemplary for a different scan rates of 50, 100, 200 and 500 mVs^{-1} in potential window (-1 to 0.8 V). At the low voltage sweep rate of 50 mVs^{-1}, graphite and graphite oxide roughly maintains the rectangular shape indicative of an acceptable capacitive behavior. However, the voltammograms become distorted dramatically with the increase of voltage sweep rate, which indicates that graphite and graphite oxide are not suitable for quick charge-discharge operations. In positive potential window there is a significant influence of the pseudocapacitnace for both graphite and its oxide form.

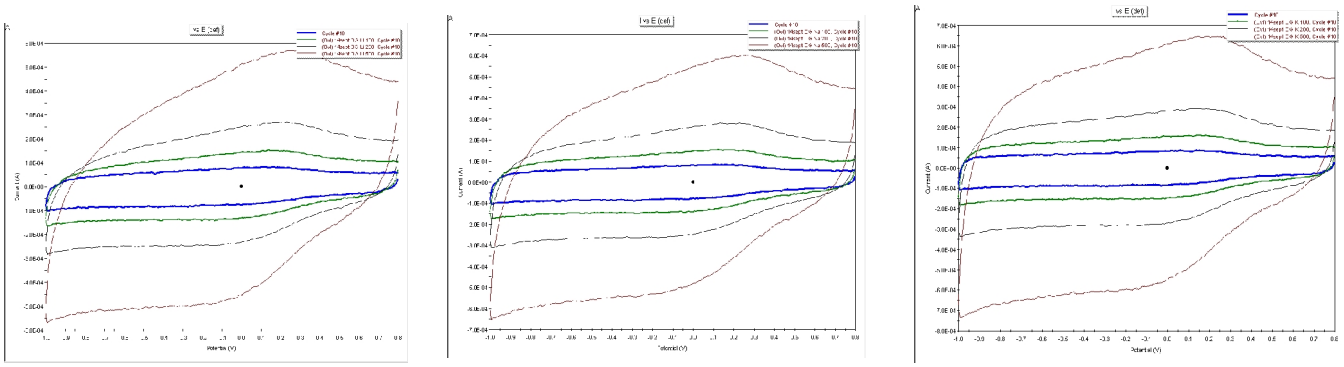

Figure 1. Different sweep rates (50 - smallest rectangular, 100, 200, 500 mV/s – biggest rectangular) of cyclic voltammetry for graphite oxide in 1M Li^+, Na^+ and K^+ aqueous electrolyte. Voltammogram for graphite material is very similar to its oxide form.

The voltammograms of graphene oxide with voltage sweep rates from 50 mV/s to 500 mV/s are presented in Fig. 2.

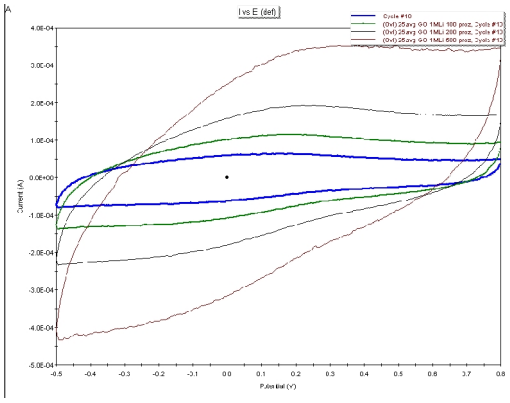

Figure 2. Different sweep rates (50-smallest rectangular to 500-biggest rectangular) mV/s of cyclic voltammetry for graphene oxide (GO) in1M $Li^{+,}$ Na^{+} and K^{+} aqueous electrolyte.

As in case for graphite materials, voltrammogram for graphene oxide become distorted dramatically with increase of voltage sweep rate, which indicates that graphene oxide is not suitable for quick charge-discharge operations. The rectangular shape of voltammogram of GO is less distorted with increase voltage sweep rate than that of graphite and graphite oxide, which means that GO possesses better capacitive behavior than GO.

From the electrochemical point of view, the three-electrode cyclic voltammograms of GO (Fig. 2) and rGO (Fig. 3) are very comparable. Since the functional groups on graphene cannot undergo redox reactions thoroughly during the fast charge/discharge process and the fact that GO contains more functional groups, more significant double-layer capacitance drop can be observed at higher scan rates compared to that of r-GO. However, the presence of additional pseudocapacitance from GO still contributes to the higher total specific capacitance (tab 1).

The voltammogram of r-GO (Fig. 3) maintain good box-like shape at all voltage sweep rates from 50 mV/s to 500 mV/s, which indicates the excellent capacitive behavior even in quick charge-discharge operations. Generally, the better accessibility of the ions to the electrochemically active surface, the better capacitive at high voltage sweep rate.

The total specific capacitance in LiCl (85.90 Fg^{-1}) is a little bit higher than that in NaCl (77.70 Fg^{-1}), revealing that the reversible adsorption of Li^{+} can gain access to almost all available pores or voids of the r-GO electrode, leading to a higher occupancy and, thereby, a higher $C_{S,T,M}$ value.

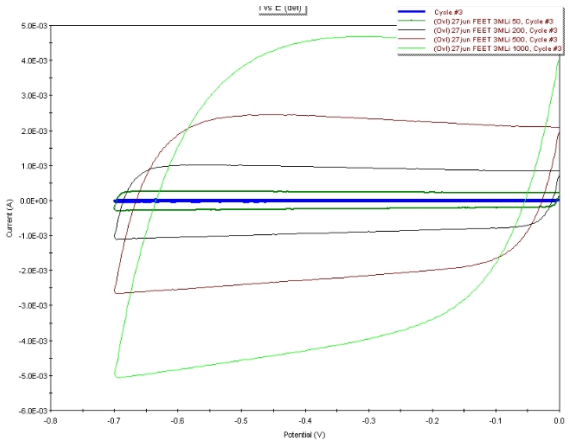

Figure 3. Different sweep rates (50-smallest rectangular to 500-biggest rectangular) mV/s of cyclic voltammetry for graphene oxide (GO) 1M $Li^{+,}$ Na^{+} and K^{+} aqueous electrolytes.

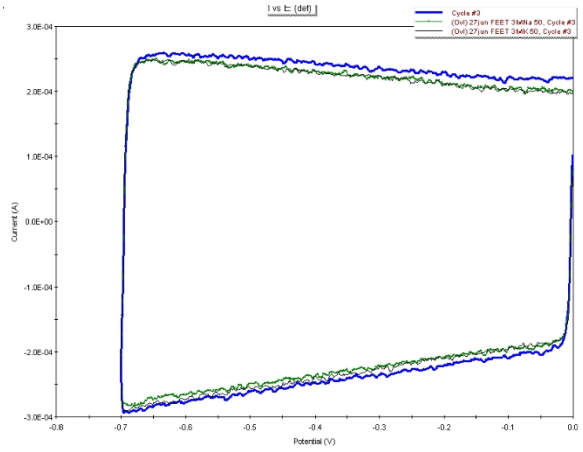

Figure 4. Shows the voltammogram of r-GO at sweep rate of 100 mV/s which compares rectangulars in Li^{+}, Na^{+} and K^{+} aqueous electrolyte.

Table 1. Summary of maximum total capacitance ($C_{S,T,M}$), double-layes capacitance (C_{dl}), and pseudocapacitance (C_p) for graphite, graphite oxide, GO and r-GO in Li^{+} aqueous electrolyte

Sample	$C_{S,T,M}$ (Fg^{-1})	C_{dl} (Fg^{-1})	C_p (Fg^{-1})	$C_p/C_{S,T,M}$
Graphite	17.04	5.12	11.92	69.91
Graphite oxide	17.35	4.71	12.64	72.86
Graphene oxide (GO)	87.62	13.51	74.10	84.57
Reduced graphene oxide (r-GO)	85.90	65.56	20.34	23.68

The total specific capacitance in LiCl (85.90 Fg^{-1}) is a little bit higher than that in NaCl (77.70 Fg^{-1}), revealing that the reversible adsorption of Li^+ can gain access to almost all available pores or voids of the r-GO electrode, leading to a higher occupancy and, thereby, a higher $C_{S,T,M}$ value. There may be an explanation for that on the basis of the different ionic sizes. First, the sizes of Li^+ and Na^+ ions are 0.74 and 1.02 Å, respectively. In an aqueous electrolyte, each ion is assumed to attract four water molecules on the outer shell, and the radii of hydrated cations for Li^+ and Na^+ are estimated to be 3.49 and 3.77 Å, respectively. This is based on the fact that one water molecule has an average diameter of 2.75 Å. Thus, the area occupied by the hydration molecules, S_o, can be determined by

$$S_o = \frac{C_s N \Delta V \sigma}{F} \quad (1)$$

where N is Avogadro's number, σ is the cross-sectional area of hydration molecule, and F is the Faraday constant.Higher value for Li^+ demonstrates that r-GO plane provides a higher surfaceaccessibility for the Li ions than the Na ions in aqueous electrolyte. The n_s value is a crucial factor in evaluating the electrochemical charge density on the r-GO sheets. The n_s values for both Li^+ and Na^+ are 1.21 and 0.68, respectively. This finding reflects that the Li-containing molecules tend to stack dual layers, whereas Na^+ hydration molecules favor monolayer adsorption on the partially oxidized graphene planes. Voltammogram is often used to calculate the specific capacitance value of the electrode materials. Capacitance value expressed in Farads (F) is given by the following formula:

$$C = \frac{I}{m\left(\frac{dV}{dt}\right)} \quad (2)$$

where I is the applied current, m is the mass of active electode material, and dV/dt is the slope of the discharge curve. The obtained capacitance values of all investigated materials are listed in table 1. The GO shows the highest total specific capacitance but r-GO shows the highest double-layer specific capacitance which is of great importance due to fast charge-discharge processes in supercapacitors. Generally the higher the specific surface area of carbon, the higher the ability for charges accumulation. At slow sweep rate, the ions have enough time to diffuse into the micro and mesopore surface of GO, while at high voltage sweep rate the ions can only penetrate into some external large pores, which explain why the total capacitance of GO changes so much with the variation of voltage sweep rate compared to r-GO.

CONCLUSION

In this work we presented a comparison of different active materials, namely graphite, graphite oxide, graphene oxide and reduced graphene oxide for EDLCs. Electrochemical studies show the superior electrochemical performances for GO, and especially for r-GO. Cyclic voltammograms show that r-GO possesses the highest capacitance at slow sweep rate, such as 50 mV/s and it seems to be a promising alternative to other active materials. This material also shows the best performance in terms of energy and power. The worst capacitive behavior of graphite and graphite oxide is believed to be due to both its disordered pore structure, and small available surface area. These results indicate that r-GO active material may find applications in diverse fields, such as negative electrode for supercapacitors, flexible batteries, seawater desalination, and biomedical applications.

REFERENCES

Bleda-Martinez, M. J., Macia-Agullo, J. A., Lozano-Castello, D., Morallon, E., Cazorla-Amoros, D., Linares-Solano, A. (2005). Role of surface chemistry on electric double layer capacitance of carbon materials. *Carbon 43*, 2677–2684.

Conway, B. E. (1999) *Electrochemical supercapacitors scientific fundamentals and technological applications.* New York, Kluwer Academic/ Plenum.

Brownson D. A. C., Banks C. E. (2010). Graphene electrochemistry: an overview of potential applications. *Analyst 135*, 2768-2778.

Dreyer, D. R., Park, S., Bielawski, C. W., & Ruoff, R. S. (2010). The chemistry of graphene oxide. *Chemical Society Reviews 39(1)*, 228-240.

Frackowiak, E., Beguin, F. (2001). Carbon materials for the electrochemical storage of energy in capacitors. *Carbon 39*, 937–950.

Kotz, R., Carlen, M. (2000). Principles and applications of electrochemical capacitors. *Electrochim Acta 45*, 2483–2498.

Lozano-Castello, D., Cazorla-Amoros, D., Linares-Solano, A., Shiraishi, S., Kurihara, H., Oya, A. (2003) Influence of pore structure and surface chemistry on electric double layer capacitance in nonaqueous electrolyte. *Carbon 41(3),* 1765–75.

Pandolfo, A. G., Hollenkamp, A. F. (2006) Carbon properties and their role in supercapacitors. *J Power Sources157(1)*,11–27.

Shi, H. (1996) Activated carbons and double layer capacitance. *Electrochim Acta 41(10),* 1633–1639.

Simon, P, Gogotsi, Y. (2008) Materials for electrochemical capacitors. *Nat Mater 7(11),* 845–854.

Qu, D., Shi, H. (1998) Studies of activated carbons used in double layer capacitors. *J Power Sources 74*, 99–107.

Summary / Sažetak

Superkondendenzatori su uređaji za pohranu energije koji posjeduju veliku gustinu energije. Zasnivaju se na upotrebi karbonskih materijala. U ovom članku je napravljeno poređenje između raznih vrsta karbonskih materijala i to grafita, grafena kao i njihovih oksidovanih oblika. Vršena su elektrohemijska mjerenja, a najbolje se pokazao redukovani grafen oksid čiji je voltamogram na cikličnoj voltametriji pokazivao oblik pravougaonika, što je indikacija da se radi o kapacitivnim strujama. Izmjerena vrijednost njegovog kapaciteta je 85.9 Fg^{-1} u vodenoj sredini serije elektrolita alklanih metala u radnom prozoru potencijala od 0 do -0.8V.

Glasnik hemičara i tehnologa Bosne i Hercegovine

Bulletin of the Chemists and Technologists of Bosnia and Herzegovina

2015

45

39-42

Print ISSN: 0367-4444
Online ISSN: 2232-7266

UDC: _____

Original Scientific Paper

Determination of metal contents in various chocolate samples

Alagić, N., Huremović, J.

Faculty of Science, Department of Chemistry, Zmaja od Bosne 33-35, Sarajevo, Bosnia and Herzegovina

Article info
Received: 09/12/2015
Accepted: 17/12/2015

Keywords:
Metals
Chocolate
Wet digestion
F-AAS

***Corresponding author:**
E-mail: nermala.al@gmail.com
Phone: 00-387-64-4219201

Abstract: Seven metals (Mn, Cu, Zn, Cd, Cr, Fe, and Pb) were determined in 17 different samples of chocolate and commonly consumed cocoa products using atomic absorption spectrometry, flame technique (F-AAS). Samples were prepared by wet digestion with concentrated nitric acid. Concentrations of metals (Mn, Fe, Cu and Zn), with exception of Cr, Pb and Cd, were found to be the highest in cocoa powder and black chocolate with a high content of cocoa. Concentrations of Cu, Cd and Pb were found to be below permissible levels prescribed by national Regulation of maximum permitted quantities of certain contaminants in food B&H in all samples.

INTRODUCTION

Chocolate is one of the most commonly consumed dessert worldwide made of cocoa as the main raw material.
The term ‘cocoa’ is a corruption of the word ‘cacao’ that is taken directly from Mayan and Aztec languages. Chocolate is derived from cocoa beans, central to the fruit of cocoa tree, *Theobroma cacao*, which is indigenous to South America and believed to have originated from the Amazon and Orinoco valleys (Afoakwa, 2010).
Chocolate is a food obtained by mixing sugar with two products derived from the industrial processing of cocoa beans (cocoa butter and paste), and for some types of chocolate, by adding milk or other ingredients. As it is mainly composed of cocoa butter and sugar, chocolate has been classified as a sweet snack, a dessert or, depending on the sophistication of the processing methods or the genetic origin of the cocoa, as a luxury or gourmet food. Nevertheless, the health benefits of chocolate have been demonstrated by a number of studies which have shown that apart from its nutritional value, the bio-active components it contains can act to prevent some pathologies (Sira, 2015). Chocolate is composed of solid particles, whose normal solid concentration is about 60 to 70% sugar, cocoa and milk.
Beside these main solid constituents, other ingredients like hydrogenated vegetable oil, salts, buffering agents, permitted emulsifier and cocoa butter could be source of metals (Ciurea and Lipka, 1992; Rehman and Husnain, 2012).
Farming of cocoa and it's treatment with pesticides and fungicides can affect composition of chocolate products and their metal contamination as cocoa is the main raw material. The metal content of chocolate products can be also affected with industrial processes and metals which are used for making vessels and containers to be used in production process of making chocolate products.
Some trace metals aren't toxic and are even essential if their intake is below permissible levels prescribed by national and international legislations, but could be toxic in higher concentrations. Essential trace metals are important for the various biochemical functions and are playing crucial role in metabolic processes as parts of many enzymes. From 7 metals which were determined in this research (Zn, Cr, Mn, Fe, Cu, Cd and Pb), with exception of Cd and Pb, all the others are in a cathegory of essential elements.

The aim of this work was the assessment of metal contents in some samples of cocoa powder, chocolate for cooking, milk chocolate, black chocolate with various content of cocoa and white chocolate using wet digestion and flame atomic absorption spectrometry method.

EXPERIMENTAL

Sampling

Samples were randomly collected as they were available in the markets of the city of Sarajevo in the period from the first of January to the first of February, 2015. Samples were taken according to the content of cocoa. The following samples were taken: 3 samples of cocoa powder, 3 samples of chocolate for cooking, 3 samples of milk chocolate, 5 samples of black chocolate with various content of cocoa and 3 samples of white chocolate.

Sample Preparation Procedure

Samples were crumbled and prepared by wet digestion where weighed mass of around 2.0000 g (± 0.01 mg) (Mettler Toledo, New Classic MF-TYPE) was heated with concentrated nitric acid for 30 minutes at temperatures 70-80 °C. The solution was filtered (blue filtered paper), then the clear solution was transferred in volumetric flask (50 mL) and diluted to mark with distilled water. Digestion of each sample was done in triplicate.

Determination of the metals

The metal (Mn, Cu, Zn, Cd, Cr, Fe, and Pb) content was determined by atomic absorption spectrometry (SpectraAA-10, Varian), flame technique (FAAS). The concentrated nitric acid (Panreac, Spain) was of analytical grade. Glassware was properly cleaned. Standard solutions (Merck; Germany, CertiPUR 1000 ppm) of Mn, Cu, Zn, Cd, Cr, Fe, and Pb were used in preparing subsequent calibration curves after serial dilutions. The sample analyses were done in triplicate. The obtained metal contents were interpreted on the basis of the limit values specified by the Regulation of maximum permitted quantities of certain contaminants in food B&H (Sl. glasnik BiH, br. 68/14).

RESULTS AND DISCUSSION

The metal (Mn, Cu, Zn, Cd, Cr, Fe, and Pb) contents after wet digestion determined by atomic absorption spectrometry, flame technique (FAAS) are shown in Table 1 and Table 2. Results are shown as c (μg/g) ± SD (the average metal concentration of three parallels ± standard deviation).

Table 1 and Table 2 are showing the average concentrations of metals in the aforementioned categories of samples with their respective ingredients.

Table 1: Concentrations of Mn, Cu, Zn, Cd, Cr, Fe, and Pb in analyzed chocolate samples of different types

Sample	c(μg/g) ± SD		
	Mn	Cu	Zn
	Cocoa powder		
K1	11.5±1.06	32.37±1.58	80.02±2.76
K2	45.87±1.25	30.87±0.88	77.78±1.50
K3	36.75±0.50	38.17±0.29	36.38±1.59
	Chocolate for cooking		
JIK1	7.08±0.38	1.25±0.00	12.38±0.18
JIK2	10.42±0.95	9.42±0.63	10.88±0.53
JIK3	7.00±0.25	6.75±0.00	6.25±0.71
	Milk chocolate		
M1	3.13±0.18	2.75±0.00	9.88±0.18
M2	2.75±0.25	2.75±0.00	10.17±0.76
M3	3.08±0.13	3.38±0.18	4.38±0.18
	black chocolate with various content of cocoa		
32%K	2.33±0.29	2.63±0.17	4.5±0.35
52%K	9.83±0.38	7.58±0.38	18.58±0.38
65%K	13.67±0.63	11.42±0.63	27.50±1.14
75%K1	17.5±1.14	14.83±0.76	13.88±1.94
75%K2	22.17±0.38	16.38±0.53	38.13±0.73
	White chocolate		
B1	0.67±0.29	0.63±0.18	7.08±0.88
B2	ND	0.92±0.14	2.00±0.00
B3	0.33±0.14	0.75±0.25	2.25±0.00

ND*- non detected

Table 2: Concentrations of, Cd, Cr, Fe, and Pb in analyzed chocolate samples of different types

Sample	c(μg/g) ± SD			
	Cd	Cr	Fe	Pb
	Cocoa powder			
K1	ND	5.37±0.61	144.36±0.92	4.87±0.11
K2	0.50±0.00	1.41±0.04	86.79±0.02	2.60±0.00
K3	ND	ND	57.07±0.35	4.38±0.36
	Chocolate for cooking			
JIK1	ND	4.90±2.39	21.10±0.82	0.94±0.22
JIK2	ND	ND	39.16±3.05	1.13±0.05
JIK3	ND	ND	38.56±0.81	1.62±0.73
	Milk chocolate			
M1	ND	3.85±0.48	19.29±1.13	ND
M2	ND	2.75±0.01	18.64±0.21	ND
M3	0.25±0.00	ND	20.44±0.32	2.45±0.62
	black chocolate with various content of cocoa			
32%K	ND	ND	8.00±1.64	ND
52%K	ND	ND	20.42±1.42	ND
65%K	ND	ND	38.65±0.89	ND
75%K1	ND	0.3±0.07	74.85±1.00	ND
75%K2	0.50±0.00	ND	65.85±0.00	ND
	White chocolate			
B1	ND	5.05±0.57	3.59±0.88	1.52±0.42
B2	ND	1.94±0.29	8.28±1.42	ND
B3	0.50±0.00	1.31±0.47	14.37±0.00	0.67±0.04

ND*- non detected

The lowest concentration of Mn was observed in a white chocolate sample marked with B2, which concentration was ND (non detected). The highest concentration of Mn (45.87 μg/g) was detected in a cocoa powder marked with K2. As can be seen on the Figure 1, the concentration of

Mn grows with the higher cocoa contents in samples. In national Regulation values of permissible levels of Mn for chocolate and chocolate products aren't given. Similar analysis was made in Serbia on white and milk chocolate samples, where concentration of Mn was in a range of 0.07 – 2.98 μg/g and 1.44 – 15.26 μg/g, respectively (Cvetković, 2013). Concentration of Mn in chocolate samples published in some other countries in the world: Brazil (43.1 – 52.2 mg/kg), Pakistan (1.4 – 8.1 mg/kg) (Rehman and Husnain, 2012).

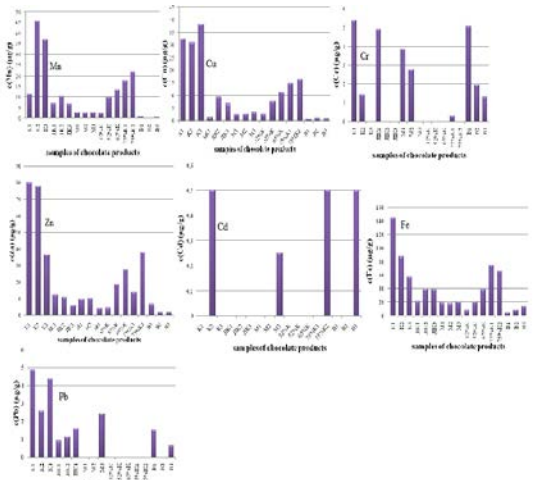

Figure 1: The metal (Mn, Cu, Zn, Cd, Cr, Fe, and Pb) contents in chocolate samples

The concentration of Cu was found to be the lowest in a white chocolate sample marked with B1, which concentration was 0.63 μg/g, whereas concentration in a cocoa powder sample marked with K3 was found to be the highest with value of 38.17 μg/g. All of the concentrations of Cu which were determined are below permissible levels (chocolate and chocolate products – 15 mg/kg, sugar-free chocolate – 30 mg/kg, and cocoa powder – 50 mg/kg) prescribed by national Regulation (Sl. glasnik BiH, br. 68/14) in all samples. According to the research made in Serbia, content of Cu in white chocolate and milk chocolate samples was in a range of ND (non detected) – 1.37 μg/g and 1.64 – 14.23 μg/g, respectively (Cvetković, 2013). Concentration of Cu in chocolate samples published in some other countries in the world: Turkey (5.7 – 10.6 mg/kg), Brazil (26.6 – 31.2 mg/kg), Malaysia (2.9 – 6.3 mg/kg), Pakistan (1.4 – 4.4 mg/kg) (Rehman and Husnain, 2012).

The content of Zn was in a range of 2.00 – 80.02 μg/g, where the lowest concentration was found in a white chocolate sample marked with B2, and the highest concentration was found in cocoa powder sample marked with K1. For Zn similar as for the other two mentioned metals (Mn and Cu), trend of growing concentration by growth of the cocoa content in the samples was found. In national Regulation values of permissible levels of Zn for chocolate and chocolate products aren't given. According to research made in Serbia content of Zn in white chocolate and milk chocolate samples was in a range of ND – 10.17 μg/g and 4.76 – 21.4 μg/g, respectively (Cvetković, 2013). Concentration of Zn in chocolate samples published in some other countries in the world: Turkey (12.1 – 16.7 mg/kg), Brazil (7.5 – 23.3 mg/kg), Pakistan (3.2 – 29.3 mg/kg) (Rehman and Husnain, 2012).

The concentration of Cd was determined in 4 samples, whereas in all the other samples concentration of Cd was not detected. Cadmium was detected in the following samples: K2 (0.5 μg/g), M3 (0.25 μg/g), 75% K2 (0.5 μg/g) and B3 (0.5 μg/g). All of the concentrations of Cd which were determined are below permissible levels (for the food supplements 1.00 mg/kg) prescribed by national Regulation (Sl. glasnik BiH, br. 68/14) in all samples.

The content of Cr was in a range of ND – 5.37 μg/g, where concentration of Cr for 8 samples was not detected, whereas the highest concentration belongs to cocoa powder sample marked with K. In national Regulation values of permissible levels of Cr for chocolate and chocolate products aren't given. According to the research made in Serbia, content of Cr in white chocolate and milk chocolate samples was in a range of 0.12 – 0.38 μg/g and ND – 0.38 μg/g, respectively (Cvetković, 2013).

Iron was present in all samples of chocolate products, with higher values of concentrations detected in cocoa powder and black chocolate with various content of cocoa. Similar as for some of the other mentioned metals (Mn, Cu, Zn) trend of growing of the concentration by growth of the content of cocoa in samples of different types was found. The content of Fe was in a range of 3.59 – 144.36 μg/g, where the lowest concentration was found in white chocolate sample marked with B1, and the highest concentration was found in cocoa powder sample marked with K1. In national Regulation values of permissible levels of Fe for chocolate and chocolate products aren't given, with exception of cocoa butter – 2.00 mg/kg. According to the research made in Serbia, content of Fe in white chocolate and milk chocolate samples was in a range of 1.19 – 6.39 μg/g and 5.90 – 37.90 μg/g, respectively (Cvetković, 2013). Concentration of Fe in chocolate samples published in some other countries in the world: Turkey (2.5 – 3.7 mg/kg), Brazil (1.2 – 140.8 mg/kg), Pakistan (3.2 – 59.6 mg/kg) (Rehman and Husnain, 2012).

The content of Pb in 8 samples was not detected. The highest content of Pb was determined in cocoa powder samples, whereas content of Pb in all samples of black chocolate with various content of cocoa were not detected. The concentration of Pb was in a range of ND – 4.87 μg/g, where the highest concentration belongs to cocoa powder sample marked with K1. All of the concentrations of Pb which were determined are below permissible levels (for the food supplements 3.00 mg/kg) prescribed by national Regulation (Sl. glasnik BiH, br. 68/14) in all samples. According to the research made in Serbia, content of Pb was detected in one white chocolate sample with concentration of 0.41 μg/g, and in milk chocolate samples content of Pb was in a range of ND – 0.78 μg/g and μg/g (Cvetković, 2013). Concentration of Pb in chocolate samples published in some other countries in the world: Turkey (30 – 40 μg/kg), India (49 – 8040 μg/kg), USA (11.9 – 69.8 μg/kg), Malaysia (1100 – 1940 μg/kg), Pakistan (28.6 – 1400 μg/kg) (Rehman and Husnain, 2012).

CONCLUSIONS

Trend of growing of the concentration by the growth of the content of cocoa in samples of different types was found for the most of determined metals, with exception of Cr, Pb and Cd. It can be concluded that the concentrations of metals (Mn, Fe, Cu and Zn), with exception of Cr, Pb and Cd, were found to be the highest in cocoa powder and black chocolate with a high content of cocoa. Toxic heavy metals such as Pb and Cd were found to be below permissible levels prescribed by Regulation of maximum permitted quantities of certain contaminants in food B&H (Sl. glasnik BiH, br. 68/14) in all samples. The metal contents of determined metals in this research which are considered as essential, the most abundant is Fe followed by the Zn, Mn and Cu, whereas the concentration of Cr in some samples was not detected. It can be concluded that all the concentrations of the metals which were determined in this research were found to be below permissible levels prescribed by national Regulation of maximum permitted quantities of certain contaminants in food B&H (Sl. glasnik BiH, br. 68/14) in all samples.

REFERENCES

Afoakwa, E. (2010). *Chocolate Science and Technology*. 1ed., Oxford,Wiley-Blackwell Publishing Inc.

Ciurea, I.C. & Lipka, Y.F. (1992). Occurrence of cadmium in cocoa and coffee. Mitteilungen aus dem Gebiete der Lebensmittelunterssuchung Hygiene, 83(2), 197-203.

Cvetković, S. (2013). *Sadržaj makro i mikroelemenata u mlečnoj i beloj čokoladi*, Master rad, Niš, Univerzitet u Nišu, Prirodno-matematički fakultet.

Pravilnik o maksimalno dozvoljenim količinama za određene kontaminante u hrani, (2014). „Službeni glasnik BiH“, br. 68 /14.

Rehman, S., & Husnain, S.M. (2012). Assessment of trace metal contents in chocolate samples by Atomic Absorption Spectrometry. *Journal of Trace Element Analysis*, 1(1), 1-11.

Sira, E.P. (2015). *Chocolate Cocoa Byproducts Technology, Rheology, Styling, and Nutrition*. Nova Science Publishers Inc.

Summary/Sažetak

Sedam metala (Mn, Cu, Zn, Cd, Cr, Fe, i Pb) su određeni u 17 različitih uzoraka čokolade i najčešće konzumiranih kakao proizvoda korištenjem atomske apsorpcione spektrometrije, plamena tehnika (F-AAS). Uzorci su pripremljeni primjenom mokre digestije sa koncentrovanom nitratnom kiselinom. Može se zaključiti da su koncentracije metala (Mn, Fe, Cu i Zn), izuzev Cr, Pb i Cd, bile najveće u uzorcima kakao praha i uzoraka crne čokolade sa različitim sadržajem kakaoa. Koncentracije Cu, Cd i Pb su u svim uzorcima bile ispod maksimalno dozvoljenih vrijednosti propisanih od strane državnog Pravilnika (Pravilnik o maksimalno dozvoljenim količinama za određene kontaminante u hrani, (Sl. glasnik BiH, br. 68/14)).

Glasnik hemičara i tehnologa Bosne i Hercegovine

Bulletin of the Chemists and Technologists of Bosnia and Herzegovina

2015

45

Print ISSN: 0367-4444
Online ISSN: 2232-7266

UDC: _____

Original Scientific Paper

43-50

Application of Web-based Learning Material for Teaching States of Matter in 8th Grade Primary School Chemistry – A Pilot Study Results

Nuić, I.[a], Glažar, S.A.[b]

[a]*University of Sarajevo, Faculty of Science, Zmaja od Bosne 33-35, Sarajevo, Bosnia and Herzegovina*
[b]*University of Ljubljana, Faculty of Education, Kardeljevaploščad 16, Ljubljana, Slovenia*

Article info
Received: 22/06/2015
Accepted: 16/12/2015

Keywords:
Web-based Learning Material
Misconceptions
States of Matter
Primary School Chemistry

***Corresponding author:**
E-mail: ividovic@pmf.unsa.ba
Phone: +387-33-279-879

Abstract: This paper presents results of a pilot study that investigated the progression in primary school students' conceptions of the structure and states of matter while learning with a new instructional approach dealing with these concepts. The study begun in May and was continued in September 2013. In the first part of the study we included 108 7th grade students (aged 12-13) from two primary schools, and in the second part we continued the study with 57 8th grade students (aged 13-14) from one school. Web-based learning material was applied as instructional tool during teaching of Structure of matter and States of matter, containing both macro and sub-micro level of representation. Students were asked to fulfill tests of knowledge dealing with macroscopic and submicroscopic level of representation. Results showed better understanding of structure and states of matter but also some persistent misconceptions that could be addressed in the following period.

INTRODUCTION

One of the fundamental concepts in science is structure of matter. The proper understanding of this concept is crucial for learning other scientific concepts. However, students tend to develop their understanding of science concepts in accordance with formal teaching as well as their everyday experience. Therefore, students could have conceptions that do not agree with scientific laws and theories, and teaching itself can be one cause for them (Osborne and Cosgrove, 1983). They can be caused by teachers who use inadequate instructional methods (Johnson, 1998), by some representations of particulate nature of matter in existing textbooks (Andersson, 1990).Also, teachers without sound scientific background can introduce misconceptions to their students (Del Pozo, 2001; Kokkotas, Vlachos and Koulaidis, 1998).

Determination of misconceptions in chemistry education is not new in scientific research. They are of particular interest for researchers in science education because they influence learning of new scientific knowledge (Özmen, 2004). Ausubel (1961) states that students' cognitive structure of knowledge impacts on interpretation of new knowledge. When students are exposed to new information, the misconceptions that are already incorporated in their cognitive structure affect the integration of new knowledge. This causes weak or wrong understanding of new concepts (Azizoğlu, Alkan and Geban, 2006). In case the misconceptions were acquired before teaching, teachers need to recognize them and consider them when teaching (Barke, Hazari and Yitbarek, 2009).

Misconceptions formed in school are primarily caused by inadequate curricula, teaching materials and textbooks (Barke, Hazari and Yitbarek, 2009).
Johnstone (1982) introduced three levels of representation in science: macroscopic (phenomenological, observable phenomena), submicroscopic (atomic, ionic, molecular), and symbolic (symbols, formulae, equations). Teaching strategies in chemistry should lead towards understanding of chemical concepts on all three levels (Johnstone, 1993). Scientists describe matter on macroscopic and on submicroscopic level, and students need to learn the relationship between levels (Johnstone, 1993; Stieff, Ryu and Yip, 2013).
Research has shown that students have problems in understanding the meaning of these three levels and they do not connect their observations on macro level with explanations on submicro level and writing on symbolic level, which leads to making ideas on their own, mostly the wrong ones (Barke, Hazari and Yitbarek, 2009). Jumping from macroscopic to symbolic level without considering submicroscopic can cause students to simply memorize formulae and equations. This makes chemistry "dry, lifeless and hard to understand" (Barke, Harsch and Schmid, 2012). Understanding processes on the level of atoms, ions and molecules is crucial for explaining concepts described or observed at macro level (Gabel, 1994; Papageorgiou and Johnson, 2005). Complete understanding of chemical concepts is acquired only when all three conceptual levels are interchanging in student's memory (Devetak, Vogrinc and Glažar, 2009, Chittleborough, 2014).
When teaching chemical concepts in primary school, teachers still mainly address and describe macroscopic level instead of linking macroscopic to submicroscopic (Gilbert and Treagust, 2009). In order for students to understand specific concepts (e.g. differences on structure and states of matter), teacher should switch from macroscopic to the submicroscopic level, which sometimes can be a significant challenge for students to understand (Stieff, Ryu and Yip, 2013).
One of the teaching strategies that showed good results in teaching science is e-learning. It is defined as instruction delivered on a digital device such as a computer or a mobile device that is intended to support learning (Clark and Mayer, 2011.). E-learning tools have profoundly transformed pedagogical approaches. A variety of media elements can be used in e-learning: (text, audio, still and motion visuals (Clark and Mayer, 2011.). The impact of e-learning on students' achievement is complex and depends also on other factors, but studies showed that students learn best with e-learning when interactively engaged in the content. Use of technology can motivate students; it significantly improves their performance, and shifts a teacher-centered to a more learner-centered classroom environment (Olson, Codde, deMaagd*et al*., 2011).
According to curricula for nine-year long primary school education in Federation of Bosnia and Herzegovina, students start to learn some fundamental scientific phenomena within subject "My environment" (1st to 4th grade), "Nature" (5th grade) and later on in "Biology" (6th to 9th grade), "Physics" (7th to 9th grade) and "Chemistry" (8th and 9th grade). Within "Physics" in 7th grade students learn some concepts relevant for this study: structure of matter and states of matter (SSM) on submicroscopic level (particulate nature of matter). Within "Chemistry" in 8th grade, students expand their knowledge about SSM. All concepts are taught on macroscopic and submicroscopic, without symbolic level.

RESEARCH METHODOLOGY

The aim of the first part of this study is to get insight into the most common misconceptions regarding structure and states of matter at the end of 7thgrade of primary school. The aim of the second part is to explore the potential application of a web-based learning material (WBLM) designed for teaching Structure and States of matter at the beginning of 8thgrade of primary school in order to address detected misconceptions.

Participants

Participants in this study were primary school students, aged 12-13 (7th grade) and 13-14 (8th grade) years. Data were collected using tests of knowledge (TK) during May (TK 7th grade), September (TK 8th grade-1) and December (TK 8th grade-2) 2013; they were confidential and given on voluntary basis. In the first part of the study we have included 108 students from two primary schools in Sarajevo. The second part of the study we have continued with students from this group who attended one primary school (n=67, aged 13-14 years).

Research instruments

Test of knowledge 7th grade (TK 7th grade) designed for the purpose of this study was used in the first part of the study. It contained 9 objective items (multiple-choice, true-false, matching and

completion), regarding macroscopic and/or submicroscopic level of representation of states of matter, mostly taught within Physics in 7th grade but also known from everyday experience.

E-unit – web-based learning material (WBLM) was used as an instructional tool when teaching Structure and States of matter (SSM) within Chemistry in the 8th grade. This e-unit contained 7 sections composed of text, pictures, videos and tasks for checking students' attention and knowledge at the end of each section. It was designed for the purpose of this study, using eXecute (a tool for design and development of electronic textbooks) and delivered to students using PCs in IT classroom.

Test of knowledge 8th grade (TK 8th grade) designed for the purpose of this study was used to establish the effects of a web-based learning material (WBLM) on understanding concepts of representation of states of matter. TK 8th grade contained 10 items of similar type as in knowledge test TK 7th grade.

Research design

Structure of matter and states of matter (SSM) are taught in primary school within Physics at the end of the 7th grade. Therefore, test of knowledge TK 7thgrade was conducted in May 2013 in two primary schools, just before the summer break.

At the beginning of 8th grade when, according to Curricula, SSM are taught again within Chemistry, we have applied e-unit as instructional tool to teach this content. In order to do so, we have combined classes of Chemistry and Informatics (IT). Teaching SSM lasted for three teaching hours: introduction to WBLM, learning SSM, and working on tasks, accompanied by filling questionnaires (results not presented in this paper). Students were working in pairs in six separate groups, due to the number of available PCs. Teachers' role was to explain details about the way that students need to learn and to assist students during learning.

One week after teaching we administered the test of knowledge TK 8th grade-1, containing concepts taught using WBLM. The same knowledge test (TK 8th grade-2) was repeated three months after teaching in order to test the retention of knowledge.

RESULTS AND DISCUSSION

Test of knowledge – TK 7th grade

TK 7th grade has been administered in two primary schools in urban region of Sarajevo in May 2013, in order to get insight into students' conceptions on states of matter on macroscopic and submicroscopic level, taught within Physics during April and May. Frequencies of correct responses are presented in Table 1.

Table 1: Frequency of correct responses: test of knowledge TK 7th grade

Item No.	1	2	3	4	5	6	7	8	9
Frequency f (%)	94.6	25.7	21.1	80.3	57.2	48.7	44.1	82.4	54.6

On TK 7th grade (Table 1) 2nd and 3rd item were most difficult ones. They both were multiple-choice items: 2nd item where students should answer what happens with water when it evaporates – only 25.7% knew that water became gaseous and went to the air; 3rd item where students should say what water is composed of and only 21.1% knew it is composed of water molecules. Molecules as particles in substances are briefly introduced within Physics (they are more thoroughly addressed within Chemistry in 8th grade) but it was expected that 7th grade students know fundamental facts about transition from liquid to gas. Other items with greater percent of correct answers were mostly about macroscopic observation from everyday life including explanation on submicroscopic level.

Most frequent 7th grade students' misconceptions are shown on Table 2:

Table 2: List of most frequent misconceptions identified in this study - TK 7th grade

7th grade	Number	%
1. We cannot obtain liquid water from water vapor since it disappeared.	31	28.7
2. We cannot obtain liquid water from water vapor since it has changed.	37	34.3
3. Bubbles formed when water is heated are made out of gaseous hydrogen and oxygen.	22	20.4
4. Bubbles formed when water is heated are made out of heat.	48	44.4
5. Evaporation can shrink water molecules.	45	41.7
6. Freezing can shrink water molecules.	19	17.6
7. If we make a leaflet of gold, its atoms become closer to each other.	22	20.4
8. If we make a leaflet of gold, its atoms become straightened.	31	28.7
9. Water is composed of hydrogen and oxygen molecules.	37	34.3
10. Water is composed of hydrogen and oxygen atoms (no chemical bond).	36	33.3
11. When spilled, water splits up to hydrogen and oxygen.	73	67.6

The most common misconceptions come from the fact that students assign macroscopic properties to submicroscopic particles (e.g. we can change the shape of atoms; water molecules shrink when water evaporates; we cannot obtain liquid water from water vapor because water is "changed"). In addition, they have misconceptions regarding the differences between chemical and physical change, concepts which are taught after Structure and states of matter.

Some phenomena about states of matter students know from everyday experience, but they are not able to explain them on submicro level. Some research already showed comparable findings (Rappoport and Ashkenazi, 2008; Treagust, Chittleborough and Mamiala, 2003;Kozma and Russell, 1997).

It was interesting to see if there was correlation between students' final marks in Physics and results of our test of knowledge TK 7th grade. Only one physics teacher was willing to provide data about final marks of his students (n=40[1]).

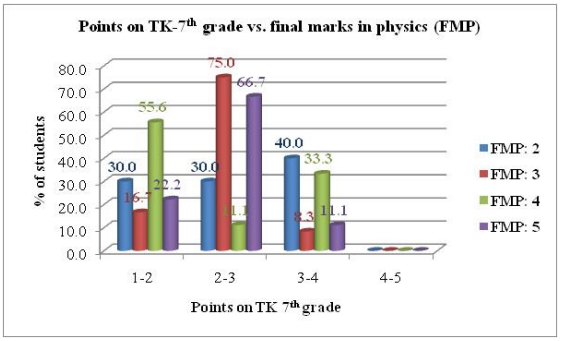

Figure 1: Comparison of results of TK 7th grade and final marks in Physics in 7th grade

Pearson correlation coefficient for these two sets of data (TK 7th grade and final marks in Physics 7th grade) shows low and insignificant correlation between students' marks and results of TK 7th grade (r = 0.0816, p>0.05), confirmed also by mean and standard deviation (Table 3)

Table 3: Descriptive statistics for TK 7th grade and FMP

	M	SD
TK 7th grade[2]	2.64	0.73
Final Marks Physics	3.43	1.11

[1] Total number of 7th grade students in this school is 41, but both physics and chemistry teacher recommended for one student to be excluded from this comparison (no data on FMP, TK 7th grade: 9.5%)

[2] Mean and standard deviation are calculated for data obtained from one school whose physics teacher provided data on final mark in physics for students who participated in this study

Test of knowledge – TK 8th grade

In order to teste-units (WBLM) and to see effects of its application, test of knowledge (TK 8th grade) was administered twice: one week after teaching Structure and States of matter using WBLM (TK 8th grade-1) and three months after teaching (TK 8th grade-2)[3].

Table 4: Frequency of correct responses: TK 8th grade

Item No.	1	2	3	4	5	6	7	8	9	10
f (%) TK 8th grade-1	59.6	35.1	42.8	9.1	72.9	51.6	25.4	50.9	36.6	33.4
f (%) TK 8th grade-2	45.6	33.3	45.7	31.5	85.1	56.1	29.8	73.7	64.9	44.2

There was a decrease in the number of correct answers for 1st and 2nd task, both regarding submicroscopic level. An increase was noted for tasks from 3rd to 10th – the highest for 9th task containing submicroscopic representations of particles in different phases.

Table 5: Descriptive statistics: TK 8th grade-1 and TK 8th grade-2

	M	SD
TK 8th grade-1	4.04	2.54
TK 8th grade-2	5.27	2.47

As shown in Table 5, overall students' achievements (mean) are higher on TK 8th grade-2, which is promising when considering retention of students' knowledge and potential teachers' actions after teaching. Pearson correlation coefficient for TK 8th grade-1 and TK 8th grade-2 shows moderate positive correlation (r = 0.619, p>0.05). A paired t-test showed statistically significant difference of a variance for these two sets of data (t (57) = -2.616.two-tail p = 0.010).

However, there were persistent misconceptions noted on both tests of knowledge in 8th grade too.

Concepts about SSM were taught more extensively within Chemistry in 8th grade than within Physics in 7th grade – therefore we could not administer same test of knowledge both in 7th and 8th grade.

Some misconceptions noted for 7th grade students persisted during 8th grade on both tests: results of TK 7th grade showed that some students believe that change in state of matter affects the size of particles (freezing (17.6%) or evaporation (41.7%) can shrink molecules (Table 2); some 8th grade students think that molecules can be increased by

[3] Data analysis showed that there were 57 (85.07%) students who were learning using WBLM and participating on both tests of knowledge (TK 8th grade-1 and TK 8th grade-2)

freezing (TK 8th grade-1: 15.8%, TK 8th grade-2: 2.1%, Table 6).

Table 6: List of most frequent misconceptions identified in this study - TK 8th grade

	TK 8th grade -1	TK 8th grade -2
	%	%
1. Water molecules will stop to move if the water freezes.	33.3	43.9
2. Water molecule can be increased by freezing.	15.8	28.1
3. When the substance is in the liquid state, its volume can easily change.	36.8	36.8
4. Particles in solids are tightly packed and do not move.	47.4	33.3
5. Particle size of the salt admits at the micro scale.	66.6	78.9
6. There are different particles in different phases of the same substance.	8.8	12.3
7. Speed of the particles of the same substance is the same in all phases.	14.0	8.8

Some incorrect answers noted on TK 7th grade did not appear in 8th grade: e.g. water disappears (28.7%) or changes (34.3%) when evaporates (Table 2) as well as answers which were somewhat expected for 7th grade students since they learn about molecules and atoms more extensively in 8th grade (in water vapor there are molecules of hydrogen and oxygen (34.3%; Table 2). Such misconceptions were not noted after teaching with WBLM.

However, we have noted misconceptions regarding the arrangement of particles in different states of matter (Table 6): particles in solids do not move (TK 8th grade-1: 47.4%; TK 8th grade-2: 33.3%), water molecules stop moving when water freezes (TK 8th grade-1: 33.3%; TK 8th grade-2: 43.9%), even though WBLM contained animations on vibration of particles in solids. The most common misconception in 8th grade is about the size of particles, which shows that students still do not perceive their size.

CONCLUSION

Results of TK 7th grade administered in May 2013 showed that most students did not differentiate macroscopic and submicroscopic level of the structure and states of matter and that they have not developed concepts of atoms and molecules. Results of both tests of knowledge in 8th grade (TK 8th grade-1 and TK 8th grade-2) showed that even though some misconceptions were noted again, e-units do have a positive impact on students' understanding of particulate nature of matter.

There is a persistent misconception noted in 7th grade and again in 8th grade before and after teaching SSM: change in state of matter affects the size of particles. This shows how much misconceptions are incorporated in students' minds.

Tests of knowledge administered both one week (TK 8th grade-1, September 2013) and three months (TK 8th grade-2, December 2013) after teaching Structure and states of matter using e-units gave positive results when considering retention of students' knowledge. There is moderate correlation but also statistically significant difference on TK 8th grade-2. Explanation for this fact can be possible teachers' intervention after teaching this content and writing test.

According to the Piaget's theory of cognitive development, students at age 11 start to develop an abstract way of thinking (Wadsworth, 2004). Learning submicro-macro thinking is abstract and thus can be difficult for students at this age (Gilbert and Treagust, 2009), which is also confirmed by results of this study. This implies that those concepts in curricula that include processes on submicro level can be too demanding for students if they are taught in a traditional way, using teacher-centered teaching.

E-units as instructional tool helped in teaching structure and states of matter mostly in representing processes on submicro level. Perhaps more extensive application of WBLM could address misconceptions that were noted and mentioned above.

ACKNOWLEDGEMENT

We would like to thank all students and their parents who voluntarily agreed to participate in this study, as well as teachers of chemistry, physics, informatics, and principals of schools where the study was conducted.

APPENDICES

Appendix I - Test of knowledge 7th grade

1. Classify these substances by their aggregate state of matter: air, water, ice, sugar, water steam, gold, milk, oxygen, oil.
   Solid:
   _____.
   Liquid:
   _____.
   Gas:
   _____.

2. You accidentally spill some water to the floor, but you do not have time to wipe it. Few hours later, the amount of spilled water decreased. What had happened to the water?

   A. The amount of water is decreased and occupies smaller area.
   B. Water turned into gas and went to the air.
   C. Water splits up to hydrogen and oxygen that went to the air.

3. What kind of particles are in the water?

   A. Water molecules.
   B. Water atoms.
   C. Atoms of hydrogen and oxygen.
   D. Molecules of hydrogen and oxygen.

4. If you take a bottle of juice from the fridge and put it on the table in warm room, on the outer side of the bottle appear drops. What are they?

   A. Juice drops from the bottle.
   B. Water drops from the water steam from air.
   C. Drops of water and juice from the bottle.
   D. Drops of water from the bottle.

5. Imagine that you have made a gold leaflet out of bit of gold. What had happened to the atoms of gold?

   A. They have not changed.
   B. Each one of them straightened.
   C. They are lighter now.
   D. They are closer to each other.

6. Which procedure can shrink water molecules?

   A. Freezing liquid water.
   B. Melting ice.
   C. Evaporation of water.
   D. They cannot shrink.

7. A pot with water is placed to hotplate. Bubbles start to form at the bottom and lift towards the water surface. What are these bubbles made of?

   A. Heat.
   B. Air.
   C. Steam.
   D. Gaseous oxygen and hydrogen.

8. Which state of matter is represented on each picture (write on the line below)?

   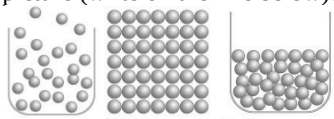

   _____ _____ _____

9. If a pot containing hot water is covered, drops start to form on the cover. Where do these drops come from?

   A. Water drops from the pot.
   B. Water drops from the steam.
   C. Water drops from the air.
   D. Drops of cold air.

   If we uncover the pot, we can observe steam. Can we obtain liquid water back from the steam?

   A. We cannot obtain liquid water since it has changed.
   B. We cannot obtain liquid water since it disappeared.
   C. We can obtain liquid water if we cool the steam.

Appendix II - Test of knowledge 8th grade

1. Which statement about water is **correct**?

   A. Water molecules will stop moving if water freezes.
   B. Water molecules will stop moving if water evaporates.
   C. Water molecules will stop moving if a glass with liquid water is not disturbed.
   D. Water molecules will not stop moving.

2. Which procedure can be used to **increase** the water molecule?

   A. Freezing.
   B. Melting.
   C. Evaporation.
   D. Condensation.
   E. None of the above.

3. Encircle the **correct** statements:

A. Liquid substance can easily change its volume.
B. The shape of liquid depends on the container.
C. Gases do not have determined shape.
D. A substance cannot change its state from solid to gas.
E. Same substance can be found in several states of matter.

4. Encircle the **correct** statements:

A. Particles in water vapor are smaller than the particles in ice.
B. Particles in liquid water are properly distributed and do not move.
C. Particles in gases are distant from each other and they move fast.
D. Particles in solids are properly distributed and do not move.
E. When water evaporates, the size of the particles does not change.

5. The arrangement of particles in water in three phases are represented on following pictures (1,2,3):

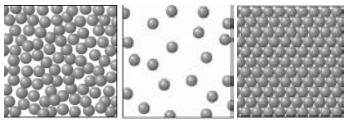

1 2 3

Arrangement in ice is represented on picture _____, in liquid water on picture _____, and in steam on picture _____.

6. Using measurement scale, fulfill the sentences.

Measurement scale:

Macro scale				Micro scale			Nano scale		
1	1	1	1	100 μm	10 μm	1 μm	100	10	1

Considering their size, sort on the measurement scale:

A. The size of a child admits to the _____ scale.
B. The size of particles in salt admits to the _____ scale.
C. The size of plant cell admits to the _____ scale.
D. The size of a pen admits to the _____ scale.
E. The size of particles in ice admits to the _____ scale.

7. Write one example of condensation from everyday life:

8. Write one example of transition between solid and liquid from everyday life:

9. Particles arrangements are represented on following pictures. For each picture write the corresponding state of matter (or states) next to the number below pictures.

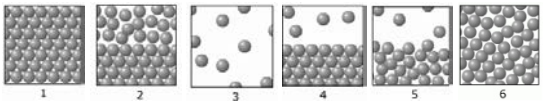

1: _____ 4: _____
2: _____ 5: _____
3: _____ 6: _____

10. Which statements are **correct** for substances in various states of matter?

A. There are different particles for the same substances in different phases.
B. Particles move freely in solids.
C. Particles in gases are more distant from each other than particles in liquids.
D. The speed of particles is the same in every phase.
E. When solid transfers to liquid, its particles move faster.

REFERENCES

Andersson, B. (1990). Pupils' conceptions of matter and its transformations. *Studies in Science Education, 18 (1),* 53–85.

Ausubel, D. P. (1961).In Defense of Verbal Learning. *Educational Theory, 11(1),* 15–25.

Azizoğlu, N., Alkan, M., Geban, Ö. (2006). Undergraduate Pre–Service Teachers' Understandings and Misconceptions of Phase Equilibrium. *Journal of Chemical Education, 83 (6),* 947–953.

Barke, H.-D., Harsch, G., Schmid, S. (2012). *Essentials of Chemical Education*. Berlin, Heidelberg: Springer-Verlag

Barke, H.-D., Hazari, A., Yitbarek, S. (2009). *Misconceptions in Chemistry: Addressing Perceptions in Chemical Education.* Berlin, Heidelberg: Springer-Verlag.

Chittleborough, G. (2014). The Development of Theoretical Frameworks for Understanding the Learning of Chemistry. In Devetak, I. and Glažar S.A. (Eds.), *Learning with Understanding in the Chemistry Classroom*, (pp. 25-40). Dordrecht, Netherlands: Springer Science+Business Media B.V.

Clark, R.C., Mayer, R.E. (2011). E-learning and the Science of Instruction: Proven Guidelines for Consumers and Designers of Multimedia Learning. (3rd Ed). Pfeiffer: San Francisco.

Del Pozo, R.M. (2001). Prospective teachers' ideas about the relationships between concepts

describing the composition of matter. *Journal of Science Education, 23 (4)*, 353–371.

Devetak, I., Vogrinc, J., Glažar, S. A. (2009). Assessing 16-Year-Old Students' Understanding of Aqueous Solution at Submicroscopic Level. *Research in Science Education, 39(2)*, 157–179.

Federalno ministarstvo obrazovanja i nauke (nd). *Okvirni nastavni plan i program za devetogodišnju osnovnu školu u Federaciji Bosne i Hercegovine.* Available at: http://www.sobih.ba/siteoo/images/stories/galerije/Zakonska_akta/okvini%20npp.pdf [07.04.2013]

Gabel, D. (1994). Improving Teaching and Learning through Chemistry Education Research: A Look to the Future. *Journal of Chemical Education, 76 (4)*, 548–554.

Gilbert, J. K., Treagust, D. (Eds.) (2009). *Multiple Representations in Chemical Education*. Dordrecht: Springer Science+Business Media B.V.

Johnson, P. (1998). Progression in children's understanding of a 'basic' particle theory: Alongitudinal study. *International Journal of Science Education, 20 (4)*, 412–493.

Johnstone, A. H. (1993). The development of chemistry teaching: A changing response tochanging demand. *Journal of Chemical Education70 (9)*, 701–705.

Johnstone, A. H. (1982). Macro- and micro-chemistry. *School Science Review64 (227)*, 377–379.

Kokkotas, P., Vlachos, I., Koulaidis, V. (1998). Teaching the topic of the particulate nature of matter in prospective teachers' training courses. *International Journal of Science Education, 20 (3)*, 291–303.

Kozma, R. B., Russell, J. (1997). Multimedia and understanding: Expert and novice responses to different representations of chemical phenomena. *Journal of Research in Science Teaching, 34(9)*, 949–968.

Olson, J., Codde, J., deMaagd, K., Tarkleson, E., Sinclair, J., Yook, S., Egidio, R. (2011).*An Analysis of e-Learning Impacts & Best Practices in Developing Countries.* Michigan State University. [Online] Available at: http://cas.msu.edu/wpcontent/uploads/2013/09/E-Learning-White-Paper_oct-2011.pdf. &Ć.03.2014]

Osborne, R. J., Cosgrove, M. M. (1983). Childrens Conceptions of the Changes of State of Water. *Journal of Research in Science Teaching, 20(9)*, 825–838.

Özmen H. (2004). Some Student Misconceptions in Chemistry: A Literature Review of Chemical Bonding. *Journal of Science Education and Technology, 13(2)*, 147–159

Papageorgiou, G., Johnson, P. (2005). Do Particle Ideas Help or Hinder Pupils' Understanding of Phenomena? *International Journal of Science Education, 27(11)*, 1299–1317.

Rappoport, L. T., Ashkenazi, G. (2008). Connecting Levels of Representation: Emergent versus submergent perspective. *International Journal of Science Education, 30(12)*, 1585–1603.

Stieff, M., Ryu, M., Yip, J. C. (2013). Speaking across levels – generating and addressing levels confusion in discourse. *Chemistry Education Research and Practice, 14 (4)*, 376-389.

Treagust, D., Chittleborough, G., Mamiala, T. (2003).The role of submicroscopic and symbolic representations in chemical explanations. *International Journal of Science Education, 25 (11)*, 1353–1368.

Wadsworth, B. J. (2004). *Piaget's Theory of Cognitive and Affective Development: Foundations of Constructivism.* Boston, MA: Pearson Education.

Summary/Sažetak

O ovom radu predstavljeni su rezultati pilot istraživanja u kojem je istraživan napredak učenika osnovne škole u razumijevanju koncepta građe tvari i agregatnih stanja tvari primjenom novog pristupa u nastavi vezanog za ove pojmove. Istraživanje je počelo u maju 2013. godine s učenicima sedmog razreda osnovne škole i nastavljeno u septembru iste godine. U prvom dijelu istraživanja sudjelovalo je 108 učenika sedmog razreda osnovne škole (uzrasta 12-13 godina) iz dviju osnovnih škola, dok je u drugom dijelu istraživanje nastavljeno s 57 učenika osmog razreda iz jedne škole. Mrežno potpomognuti materijal za učenje koji je sadržavao i makroskopske i submikroskopske prikaze primijenjen je kao nastavno sredstvo prilikom poučavanja građe tvari i agregatnih stanja tvari. Zadatak učenika je bio da urade testove znanja također bazirane na makroskopskoj i mikroskopskoj spoznajnoj razini. Rezultati su pokazali bolje razumijevanje građe tvari i agregatnih stanja tvari, ali također i postojane miskoncepcije kojima bi se trebalo posvetiti u narednom periodu.

Glasnik hemičara i tehnologa Bosne i Hercegovine

Bulletin of the Chemists and Technologists of Bosnia and Herzegovina

2015
45
51-56

Print ISSN: 0367-4444
Online ISSN: 2232-7266
UDC: _____
Original scientific article

Interpretation of results obtained from test purification of wastewater with zinc electrodes

Halilović, N.[a]*, Gutić, S.[b], Korać, F.[b], Avdić, N.[b]

[a]Tvornica ljepila, fasada, boja KOMOCHEM, Donja Zimča 68, 71300 Visoko, Bosnia and Herzegovina
[b]University of Sarajevo, Faculty of Science, Department of Chemistry, Zmaja od Bosne 33-35, 71000 Sarajevo, Bosnia and Herzegovina

Article info
Received: 03/12/2015
Accepted: 25/12/2015

Keywords:
Zinc electrodes
Wastewater
Electrochemical purification

***Corresponding author:**
E-mail: namir.halilovic@live.com
Phone: 00-387-61-495311

Abstract: Basic materials used for electrochemical purification of wastewater are iron and aluminium electrodes. In this paper, results obtained from analysis of wastewater samples before and after electrolysis with zinc electrodes are presented and compared with the results of aluminium electrodes and mixed metal oxide electrodes. In all experiments with zinc, the same materials were used as anode and cathode. After 7 min of electrolysis at only 0,018 A/dm^2, concentration of chloride in was reduced using zinc electrodes, and the efficiency of microorganisms removal is double, directly and indirectly. The effects of the main parameters in electrochemical cell with zinc electrodes – changes in the conductivity of the solution, variation of pH, turbidity of samples, removal of chloride and production of hypochlorous acid were investigated.

INTRODUCTION

Wastewater treatment is closely related to the standards and/or expectations set for the effluent quality. Wastewater treatment processes are designed to achieve improvements in the quality of the wastewater. One of the most effective ways for wastewater disinfection is by using chlorine. The disinfecting effect of free chlorine is based on the release of atomic oxygen according to (Chen, 2004):

$$HClO \rightarrow O + Cl^- + H^+ \quad (1)$$
$$ClO^- \rightarrow O + Cl^- \quad (2)$$

The wastewater used in this research contained high concentrations of chlorides. Our goal is an electrochemical production of chlorine.
First, chlorine is electrochemically produced from chloride ions dissolved in the water (Mendia, 1982):

$$2Cl^- \rightarrow Cl_2 + 2e^- \quad (3)$$

The next step is the dissolution of chlorine in the water. The maximum amount of Cl_2 (g) which can be dissolved in water at 20 ºC is about 7.1 g or 0.1 mol/kg$_{water}$ (Halilović, 2015).
Solubility of Cl_2 in water was shown in Figure 1.

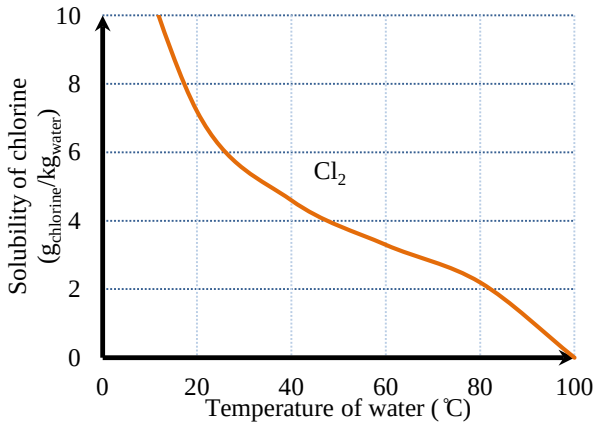

Figure 1: Solubility of Cl_2 in water, g$_{chlorine}$/kg$_{water}$

Our interest is found the best electrode material in this purpose.

Aluminum and iron metal salts are used in raw water and wastewater treatment. Both metals can form multivalent ions, Al^{3+}, Fe^{2+} and Fe^{3+}, and various hydrolysis products (Kostamo et al., 2003). Metal cations go through a series of hydrolytic reactions depending on the pH of the solution and mononuclear (Eq. 4) and polynuclear hydroxides form in the solution (Halilović, 2015).

$$Me^{3+}(aq) + nH_2O \leftrightarrow Me(OH)_n^{3-n} + nH^+(aq) \quad (4)$$

It can be concluded that iron dissolved in Fe(II) form and dissolution followed Faraday's law. This was consistent with the results of other researchers (Sasson et al., 2009; Linares-Hernández et al., 2009; Bagga et al., 2008). This result was significant because it is known that Fe(II) is a poor coagulant and should be oxidized to Fe(III) form before it can be used to remove organic matter (Bratby, 2006).

Water temperature had a significant effect on the dissolving speed of the aluminum electrodes. According to the results, the chemical dissolution of aluminium cathodes was affected by temperature. At low temperatures, chemical dissolution initiated more slowly than at higher temperatures (Vepsäläinen, 2012).
Vepsäläinen (2012) studies showed that increased removal of pollutants at high temperatures has been obtained by Yilmaz et al. (2008), and Vasudevan, et al. (2009), whereas Katal and Pahlavanzedah (2011) and El-Naas et al. (2009) reported the opposite effect in their studies.
Main reaction of electrocoagulation by aluminum anode in experiment with wastewater is (Halilović, 2015a):

$$Al^{3+} + 3OH^- \rightarrow Al(OH)_3 \quad (5)$$

Our goal is to test zinc anode-cathode material for electrochemical disinfection and removal of chloride from wastewater.
Zinc standard redox potential is $E^o(Zn^{2+}/Zn)$ = -0.762 V, which means that this material is relatively easily oxidized in aqueous solutions, that is, zinc is the reducing agent.

EXPERIMENTAL

Chemicals and instruments

Sodium thiosulfate, p.a. (Merck); potassium iodide, p.a. (Merck); starch, p.a. (Merck); hydrochloric acid, p.a. (Merck); sodium chloride, p.a. (Merck); conductivity meter (Iskra); pH meter (PHYWE); constanter (PHYWE); amperemeter (PHYWE); digital multimeter (DT9205A); magnetic stirrer (TEHTNICA ŽELEZNIKI); analytical balance (Mettler); thermometer; zinc anode and cathode and laboratory glassware were used for the experiment process.

Procedure

The effect of the main parameters in electrochemical cell with zinc electrodes - changes in the conductivity of the solution, variation of pH, turbidity of samples, removal of chloride and production of hypochlorous acid was investigated. Electrolysis duration for all experiments was 7 min. Dimension of used electrodes was 7 cm × 3 cm and the distance between the electrodes was 5 mm. The volume of the tested samples was the same, 0.4 dm^3. Experiments were carried out at 500 rpm on a magnetic stirrer. Scheme for electrolysis using zinc electrodes is given in Figure 2.

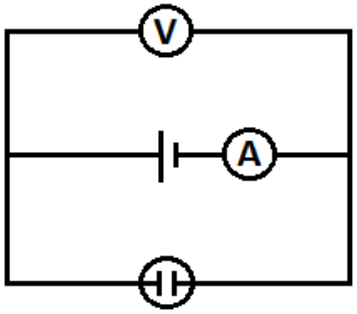

Figure 2: Scheme for electrolysis using zinc electrodes

The determination of chloride in wastewater

Determination of the chloride in the wastewater before and after electrolysis is carried out by titration method. The Mohr method uses chromate ions as an indicator in the titration of chloride ions with a silver nitrate standard solution. The reactions are:

$$Ag^+ + Cl^- \leftrightarrow AgCl_{(s)} \quad (6)$$
$$2Ag^+ + CrO_4^{2-} \leftrightarrow Ag_2CrO_{4(s)} \quad (7)$$

By knowing the stoichiometry and moles consumed at the end point, the amount of chloride in an unknown sample can be determined.

The decrease in total chloride is presented:

$$\omega(\%) = \frac{c_{Cl^-(before\ electrolysis)} c_{Cl^-(after\ electrolysis)}}{c_{Cl^-(before\ electrolysis)}} \cdot 100 \quad (8)$$

The determination of hypochlorite

Hypochlorous acid reacts with iodide when the solution is acidic:

$$HOCl_{(aq)} + HCl_{(aq)} + 3I^-(aq) \rightarrow I_3^-{}_{(aq)} + 2Cl^-_{(aq)} + H_2O_{(l)} \quad (9)$$

A dark blue complex is formed when triiodide is combined with starch.

This is useful because the result of these reactions is the formation of a dark blue complex. In the next step, the starch-triiodide product is titrated by sodium thiosulfate to form a colorless solution of iodide, dithionate, and uncomplexed starch:

$$[I_3^-][starch] + 2S_2O_3^{2-} \rightarrow 3I^- + S_4O_6^{2-} + starch \quad (10)$$

Zinc anode and cathode was used in experiment for determining hypochlorous acid as a product of electrolysis of NaCl, which concentration was 0.05 mol/dm^3 (this concentration is defined as the most common in the wastewater). The obtained results were compared with results for same wastewater reported by other (Halilović et al., 2015b) for electrochemical cell of aluminum anode and cathode and, otherwise, for anode of the mixed metal oxides (RuO_2, IrO_2) and cathode of steel.

Conductivity of the solution, pH, turbidity of samples

These parameters were determined before and after electrolysis with zinc electrodes for samples of wastewater and for samples of NaCl (c = 0.05 mol/dm^3) because of comparison.

RESULTS AND DISCUSSION

Results of chemical analysis of solution of NaCl and wastewater obtained with volumetric method are given in Tables 1. and 2.

Table 1: Results of determination of hypochlorite, pH and conductivity of NaCl with zinc electrodes.

Electrode pair (A, K)	HOCl [mol/dm^3]	ΔpH (pH_0=7,14)	Δκ (mS/cm)
Zn	$3.7 \cdot 10^{-5}$	2.04	0.08
Al*	$2.3 \cdot 10^{-5}$	1.11	0.159
MMO*	$90 \cdot 10^{-5}$	1.91	0.25

*Values reported by other (Halilović et al., 2015b). MMO – mixed metal oxide

Conductivity of NaCl (c = 0.05 mol/dm^3), which is subjected to electrolysis, before electrolysis amounted to 2.930 mScm^{-1}. Some of the reactions that take place during electrolysis of chloride are:

Anode: $2Cl^- \rightarrow Cl_2 + 2e^-$ (11)

Cathode: $2H_2O + 2e^- \rightarrow H_2 + 2OH^-$ (12)

$2NaCl + 2H_2O \rightarrow Cl_2 + H_2 + 2NaOH$ (13)

Formation of NaOH increases the pH of the solution (ΔpH in Table 1). Compared to the other electrodes mentioned in the tables 1, zinc showed the biggest change in pH. The conductivity of the solution is also increased due to an increase in the concentration of OH^- ions (Δκ in Table 1) in the order: aluminum > MMO > zinc. This sequence can be explained by Figure 3.

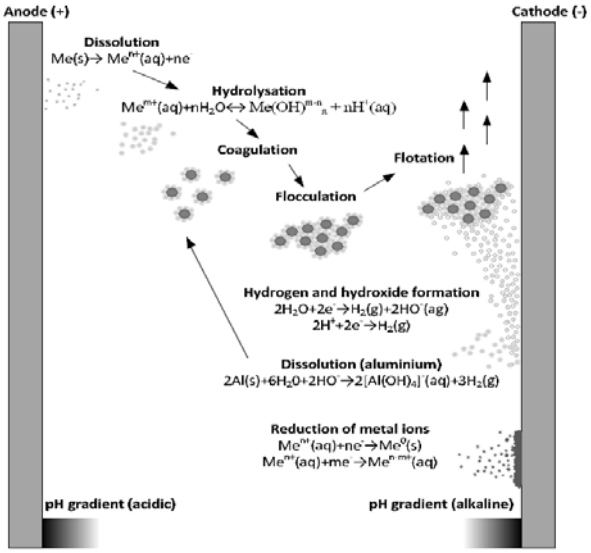

Figure 3: Schematic representation of typical reactions during the electrochemical treatment (Kraft, 2008)

MMO comes before zinc because in this experiment formed hydroxide does not react with the metal ion of MMO electrodes. Aluminum is the first in the series because of the reactions shown in Figure 3.

Electrolysis of NaCl solution with Zn electrodes is created gray-white solution in which the white precipitate was formed gradually. Aluminum gives more sludge because of properties that will be mentioned below.

The essence of the disinfectant action of chlorine, consists in oxidizing-reduction processes, which occur during the interaction of chlorine and its compounds with organic matter of microbial cells (Kraft, 2008). Because of this, we determined the amount of formation of hypochlorite (Table 1) and decrease of chloride in wastewater (Table 2).

Table 2: Results of determination of chloride before and after electrolysis of wastewater with zinc electrodes.

Electrode pair (A+K)	c(Cl^-)** [mol/dm^3]	$\omega_{\text{total removal of chloride}}$[%]
Zn	0.0141	33.18
Al*	0.0051	75.8

*Values reported by other (Halilović et al., 2015b)

** $c(Cl^-)_{\text{before electrolysis}}$ = 0,0211mol/dm^3

After 7 min of electrolysis at 0.018 A/dm^2, Cl^- was reduced in all experiments. The reasons are electrocoagulation, electroflotation and electroflocculation effects of metal ions that are released from the anode. Compared to aluminum, zinc did not show substantial removal of chloride (Table 2). Aluminum shows very good electrocoagulation effect. MMO is not tested on wastewater because of high price of material.

The presence of ZnO in the protective film on the electrode can be explained by the following equations (Antonijević et al., 2009):

$Zn^{2+} + H_2O \rightarrow ZnO + 2H^+$ (14)

$Zn + H_2O \rightarrow ZnO + 2H^+ + 2e^-$ (15)

In the NaCl solution, Cl^- react with the zinc anode according to the following reaction:

$$Zn_{(s)} + Cl_{2(g)} \rightarrow ZnCl_{2(s)} \quad (16)$$

From an aqueous solution of zinc, it crystallizes as the dihydrate, $ZnCl_2$ $2H_2O$ and it is very difficult to remove traces of water from the dihydrate. $ZnCl_2$ is used for wood preservatives.

Secondary reaction on anode, when used in the experiment a magnetic stirrer, is:

$$Zn_{(s)} + 2H_2O + 2OH^- \rightarrow Zn(OH)_4^{2-} + H_{2(g)} \quad (17)$$

However, due to the existence of the Na^+ ions in the solution, the reaction is insignificant compared to the reaction:

$$Na^+ + OH^- \rightarrow NaOH \quad (18)$$

After the electrolysis, pH of NaCl is measured, and its value was 9.18, so it is important to mention the following reaction:

$$Zn^{2+} + 2OH^- \rightarrow Zn(OH)_{2(s)} \quad (19)$$

CONCLUSIONS

The electrochemical treatment of wastewater resulted in the production of chlorine gas and hypochlorite, which is a microorganisms inactivator.

The concentration of hypochlorous acid produced by electrolysis, after dissolving chlorine, following order: MMO > Zn > Al and it increased compared to the theoretically expected. The reason is the mixing of solution, the impact of the hydroxide, the temperature and the participation of secondary reactions.

Compared to aluminum, zinc did not show substantial removal of chloride. The reason is because Al(III) shows very good electrocoagulation effect and Zn(II) is a poor coagulant.

The largest increase in conductivity mixed metal oxide electrode occurs due to the inertia of the material, and there is no dissolution of the anode. It resulting the generation of NaOH, and OH^- ions are responsible for the increased conductivity compared to Al and Zn.

Due to the large loss of zinc ions by electrolysis from the anode and the same is not reduced at the cathode due to the mixing of the solution, a zinc electrode is not applicable to the waste water purification at high current densities.

REFERENCES

Antonijević, M. M., Gardić, V., Milić, S. M., Alagić, S. Č., Stamenković, A. T., Jojić, M. (2009). Elektrohemijsko ponašanje Cu24Zn5Al legure u rastvoru boraksa u prisustvu 1-fenil-5-merkapto-tetrazola. *Zaštita materijala.* Beograd: Tehnički fakultet Bor.

Bagga, A., Chellam, S., Clifford, D.A. (2008). Evaluation of iron chemical coagulation and electrocoagulation pretreatment for surface water microfiltration. *J. Membr. Sci.* 309, 82–93.

Bratby, J. (2006). *Coagulation and flocculation in water and wastewater treatment*. 2nd ed..IWA Publishing. UK.

Chen, G. (2004). *Separation and Purification Technology*.38, 11–41.

El-Naas, M.H., Al-Zuhair, S., Al-Lobaney, A., Makhlouf, S. (2009). Assessment of electrocoagulation for the treatment of petroleum refinery wastewater, *J. Environ. Manage.* 91, 180–185.

Halilović, N., Avdić, N. (2015). *Elektrohemijsko uklanjanje hlorida i dezinfekcija otpadnih voda kožarske industrije*. Završni rad. Sarajevo: Prirodno-matematički fakultet.

Halilović, N., Gutić, S., Goletić, Š., Avdić, N. (2015a). Electrocoagulation, electroflotation and oxidation processes with aluminium anode in the treatment of wastewaters, *19h International Research/Expert Conference, Trends in the Development of Machinery and Associated Technology, TMT 2015 Proceedings*, Barcelona, Spain, 2015, 245-249.

Halilović, N., Malinović B., Gutić, S., Korać, F., Avdić, N. (2015b). Electrochemical treatment of leader industry wastewater. *5TH Symposium on electrochemistry South-East Europe*. Bulgaria. 139.

Katal, R., Pahlavanzadeh, H.(2011). Influence of different combinations of aluminum and iron electrode on electrocoagulation efficiency: Application to the treatment of paper mill wastewater. *Desalination.* 265 199–205.

Kostamo, A., Kukkonen, J.V.K. (2003). Removal of resin acids and sterols from pulp mill effluents by activated sludge treatment. *Water Res.* 37., 2813-2820.

Kraft, A. (2008). *Platinum Metals Rev.*. 52, 177–185.

Linares-Hernández, C., Barrera-Díaz, G., Roa-Morales, B., Bilyeu, F. (2009). Influence of the anodic material on electrocoagulation performance. *Chem. Eng. J*. 148, 97–105.

Mendia, L. (1982). *Wat. Sci. Tech*., 14, 331-344.

Sasson, M.B., Calmano, W., Adin, A. (2009). Iron-oxidation processes in an electroflocculation (electrocoagulation) cell.*J. Hazard. Mater.* 171, 704–709.

Vasudevan, S., Lakshmi, J., Jayaraj, J., Sozhan, G. (2009). Remediation of phosphatecontaminated water by electrocoagulation with aluminium, aluminium alloy and mild steel anodes. *J. Hazard. Mater*. 164, 1480–1486.

Yilmaz, A.E., Boncukcuoglu, R., Kocakerim, M.M., Yilmaz, M.T., Paluluoglu,C. (2008). Boron removal from geothermal waters by electrocoagulation, *J. Hazard. Mater*. 153, 146–151.

Summary/Sažetak

Osnovni materijali koji se koriste za elektrohemijsko prečišćavanje otpadne vode su željezne i aliminijske elektrode. Ovaj rad sadrži interpretaciju rezultata dobijenih analizom uzoraka otpadne vode prije i poslije elektrolize sa elektrodama od cinka i usporedbu istih sa rezultatima elektrolize otapadne vode koristeći elektrode od aluminija u prvom i elektrodu miješanih metalnih oksida u drugom slučaju. U svim eksperimentima je cink korišten kao anoda i katoda. Poslije 7 minuta elektrolize na samo 0,018 A/dm^2, koncentracija hlorida je smanjena koristeći elektrode od cinka, a efekat na uklanjane mikroorganizama je dvostruk (direktan i indirektan). Istraženi su efekti glavnih parametara u elektrohemijskoj ćeliji u kojoj su korištene elektrode od cinka – promjene u provodljivosti uzoraka, pH, promjena mutnoće uzoraka, uklanjanje hlorida i nastanak hipohloritne kiseline.

INSTRUCTIONS FOR AUTHORS

GENERAL INFORMATION

Bulletin of the Chemists and Technologists of Bosnia and Herzegovina (Glasnik hemičara i tehnologa Bosne i Hercegovine) is a semiannual international journal publishing papers from all fields of chemistry and related disciplines.

Categories of Contributions

1. *Original Scientific Papers* – (about 10 typewritten pages) report original research which has not been published previously, except in a preliminary form. The paper should contain all the necessary information to enable reproducibility of the described work.
2. *Short Communications* – (about 5 typewritten pages) describing work that may be of a preliminary nature but which merits immediate publication.
3. *Notes* – (about 3 typewritten pages) report unpublished results of short, but complete, original research or describe original laboratory techniques.
4. *Reviews* – (about 30 typewritten pages) present a concise and critical survey of a specific research area. Generally, these are prepared by the invitation of the Editor.
5. *Book and Web Site Reviews* – (about 2 typewritten pages).
6. *Extended Abstracts* – (about 2 typewritten pages) of Lectures given at international meetings.
7. *Technical Papers* – (about 10 typewritten pages) report on applications of an already described innovation. Typically, technical articles are not based on new experiments.

Reviewing the Manuscript

All contributors are evaluated according to the criteria of originality and quality of their scientific content, and only those deemed worthy will be accepted for publication. To facilitate the reviewing process, authors are encouraged to suggest three persons competent to review their manuscript. Such suggestions will be taken into consideration but not always accepted.

The Editor-In-Chief and Editors have the right to decline formal review of a manuscript when it is deemed that the manuscript is:

1. on a topic outside the scope of the Journal;
2. lacking technical merit;
3. of insufficient novelty for a wide international readership;
4. fragmentary and providing marginally incremental results; or
5. is poorly written.

Proofs

When a manuscript is ready for printing, the corresponding author will receive a PDF-formatted manuscript for proof reading, which should be returned to the journal within one week. Failure to do so will be taken as the authors are in agreement with any alteration which may have occurred during the preparation of the manuscript.

Copyright

Subscribers may reproduce tables of contents or prepare lists of articles including abstracts for internal circulation within their institutions. Permission of the Publisher is required for resale or distribution outside the institution and for all other derivative works, including compilations and translations.

Professional Ethics and Publication Policy

The journal expects the Editors, Referees and authors to adhere to the well-known standards of professional ethics. Authors are responsible for the factual accuracy of their contributions. Submission of the paper commits the author not to submit the same material elsewhere. Referees should act promptly. If certain circumstances preclude prompt attention to the manuscript at the time it is received, the non-received manuscript should be returned immediately to the Editor or the Referee should contact the Editor for possible delay of the report submission date. The Editor accepts full responsibility for his decisions on the manuscripts.

PREPARATION AND SUBMISSION OF MANUSCRIPT

Cover Letter

Manuscripts must be accompanied by a cover letter in which the type of the submitted manuscript. It should contain:

1. full name(s) of the author(s),
2. mailing address (address, phone and fax numbers, e-mail) of the author to whom correspondence should be addressed,
3. title of the paper (concise, without any abbreviations),
4. type of contribution,
5. a statement that the article is original and is currently not under consideration by any other journal or any other medium, including preprints, electronic journals and computer databases in the public domain, and
6. the names, full affiliation (department, institution, city and country), and
7. e-mail addresses of three potential Referees.

Contributors from Bosnia and Herzegovina should provide the name and full affiliation of at least one Referee from abroad.

Authors are fully encouraged to use ***Cover Letter Template*.**

Manuscript preparation

The submitted articles must be prepared with Word for Windows. Manuscripts should be typed in English (either standard British or American English, but consistent throughout) with 1.5 spacing (12 points Times New Roman; Greek letters in the character font Symbol) in A4 format leaving 2.5 cm for margins. Authors are fully encouraged to use ***Manuscript Template***.

All contributions should be written in a style that addresses a wider audience than papers in more specialized journals. Manuscripts with grammar or vocabulary deficiencies are disadvantaged during the scientific review process and, even if accepted, may be returned to the author to be rewritten in idiomatic English. The authors are requested to seek the assistance of competent English language expert, if necessary, to ensure their English is of a reasonable standard. The journal maintains its policy and takes the liberty of correcting the English of manuscripts scientifically accepted for publication.

Tables and figures and/or schemes should not be embedded in the manuscript but their position in the text indicated. In electronic version (Word.doc document) tables and figures and/or schemes should follow the text, each on a separate page. Please number all pages of the manuscript including separate lists of references, tables and figures with their captions.

IUPAC and International Union of Biochemistry and Molecular Biology recommendations for the naming of compounds should be followed.

SI units, or other permissible units, should be employed. The designation of physical quantities should be in Times New Roman font. In text, graphs, and tables, brackets should be used to separate the designation of a physical quantity from the unit. Please do not use the axes of graphs for additional explanations; these should be mentioned in the figure captions and/or the manuscript (example: "pressure at the inlet of the system, kPa" should be avoided).

Percents and *per mills*, although not being units in the same sense as the units of dimensioned quantities, can be treated as such. Unit symbols should never be modified (for instance: w/w %, vol.%, mol.%) but the quantity measured has to be named, *e.g.* mass fraction, w=95 %; amount (mole) fraction, x=20 %.

Latin words, as well as the names of species, should be in *italic*, as for example: *i.e., e.g., in vivo, ibid, Artemisia annua* L., *etc*. The branching of organic compound should also be indicated in *italic*, for example, *n*-butanol, *tert*-butanol, *etc*.

Decimal numbers must have decimal points and not commas in the text (except in the Bosnian/Croatian/Serbian abstract), tables and axis labels in graphical presentations of results. Thousands are separated, if at all, by a comma and not a point.

Structure of the Manuscript

The manuscript must contain, each on a separate page, the title page, abstract in English, (abstract in Bosnian/Croatian/Serbian), graphical abstract (optional), main text,

list of references, tables (each table separately), illustrations (each separately), and legends to illustrations (all on the same page).

1. ***Title page*** must contain: the title of the paper (bold letters), full name(s) of the author(s), full mailing addresses of all authors (italic), keywords (up to 6), the phone and fax numbers and the e-mail address of the corresponding author.
2. A one-paragraph ***abstract*** written of 150–200 words in an impersonal form indicating the aims of the work, the main results and conclusions should be given and clearly set off from the text. Domestic authors should also submit, on a separate page, a Summary/Sažetak. For authors outside Bosnia and Herzegovina, the Editorial Board will provide a Bosnian/Croatian/Serbian translation of their English abstract.
3. Authors are encouraged to submit a ***graphical abstract*** that describes the subject matter of the paper. It should contain the title of the paper, full name(s) of the author(s), and graphic that should be no larger than 11 cm wide by 5 cm tall. Authors are fully encouraged to use ***Graphical Abstract Template.***
4. ***Main text*** should have the following form:
   - ***Introduction*** should include the aim of the research and a concise description of background information and related studies directly connected to the paper.
   - ***Experimental*** section should give the purity and source of all employed materials, as well as details of the instruments used. The employed methods should be described in sufficient detail to enable experienced persons to repeat them. Standard procedures should be referenced and only modifications described in detail.
   - ***Results and Discussion*** should include concisely presented results and their significance discussed and compared to relevant literature data. The results and discussion may be combined or kept separate.
   - The inclusion of a ***Conclusion*** section, which briefly summarizes the principal conclusions, is highly recommended.
   - ***Acknowledgement*** (optional).
   - Please ensure that every ***reference*** cited in the text is also present in the reference list (and *vice versa*). Unpublished results and personal communications are not recommended in the reference list, but may be mentioned in the text. If these references are included in the reference list they should follow the standard reference style of the journal and should include a substitution of the publication date with either "Unpublished results" or "Personal communication" Citation of a reference as "in press" implies that the item has been accepted for publication. As a minimum, the full URL should be given and the date when the reference was last accessed. Any further information, if known (DOI, author names, dates, reference to a source publication, etc.), should also be given. No more than 30 references should be cited in your manuscript.

     In the text refer to the author's name (without initials) and year of publication (e.g. "Steventon, Donald and Gladden (1994) studied the effects..." or "...similar to values reported by others (Anderson, Douglas, Morrison, *et al.*, 1990)..."). Type the names of the first three authors at first citation. At subsequent citations use

first author *et al.* The list of references should be arranged alphabetically by authors' names and should be as full as possible, listing all authors, the full title of articles and journals, publisher and year.

Examples of ***reference style***:

a) Reference to a journal publication:
Warren, J. J., Tronic, T. A., Mayer, J. M. (2010). Termochemistry of proton-coupled electron transfer reagents and its implications. *Chemical Reviews*, *110 (12)*, 6961-7001.

b) Reference to a book:
Corey, E. J., Kurti, L. (2010). *Enantioselective chemical synthesis*. (1st Ed.) Direct Book Publishing, LLC.

c) Reference to a chapter in an edited book:
Moody, J. R., Beck II, C. M. (1997). Sample preparation in analytical chemistry. In Setlle, F. A. (Ed.), *Handbook of instrumental techniques for analytical chemistry*. (p.p. 55-72). Prentice Hall.

d) Reference to a proceeding:
Seliskar, C. J., Heineman, W.R., Shi, Y., Slaterbeck, A.F., Aryal, S., Ridgway, T.H., Nevin, J.H. (1997). *New spectroelectrochemical sensor*, in Proceedings of 37th Conference of Analytical Chemistry in Energy and Technology, Gatlinburg, Tenesee, USA, p.p. 8-11.

e) Patents:
Healey, P.J., Wright, S.M., Viltro, L.J., (2004). *Method and apparatus for the selection of oral care chemistry*, The Procter & Gamble Company Intellectual Property Division, (No.US 2004/0018475 A1).

f) Chemical Abstracts:
Habeger, C. F., Linhart, R. V., Adair, J. H. (1995). Adhesion to model surfaces in a flow through system. *Chemical Abstracts,* CA 124:25135.

g) Standards:
ISO 4790:1992. (2008). *Glass-to-glass sealings - Determination of stresses*.

h) Websites:
Chemical Abstract Service, www.cas.org, (18/12/2010).

- ***Tables*** are part of the text but must be given on separate pages, together with their captions. The tables should be numbered consequently in Latin numbers. Quantities should be separated from units by brackets. Footnotes to tables, in size 10 font, are to be indicated consequently (line-by-line) in superscript letters. Tables should be prepared with the aid of the Word table function, without vertical lines. Table columns must not be formatted using multiple spaces. Table rows must not be formatted using Carriage returns (enter key; ↵ key). Tables should not be incorporated as graphical objects.
- ***Figures and/or Schemes*** (in high resolution) should follow the captions, each on a separate page of the manuscript. High resolution illustrations in TIF or EPS format (JPG format is acceptable for colour and greyscale photos, only) must be uploaded as a separate archived (.zip or .rar) file.

Figures and/or Schemes should be prepared according to the artwork instructions.

- ***Mathematical and chemical equations*** must be numbered, Arabic numbers, consecutively in parenthesis at the end of the line. All equations should be embedded in the text except when they contain graphical elements (tables, figures, schemes and formulae). Complex equations (fractions, inegrals, matrix…) should be prepared with the aid of the Word Equation editor.

Artwork Instructions

Journal accepts only TIF or EPS formats, as well as JPEG format (only for colour and greyscale photographs) for electronic artwork and graphic files. MS files (Word, PowerPoint, Excel, Visio) are NOT acceptable. Generally, scanned instrument data sheets should be avoided. Authors are responsible for the quality of their submitted artwork.

Image quality: keep figures as simple as possible for clarity - avoid unnecessary complexity, colouring and excessive detail. Images should be of sufficient quality for the printed version, i.e. 300 dpi minimum.

Image size: illustrations should be submitted at its *final size* (8 cm for single column width or 17 cm for double column width) so that neither reduction nor enlargement is required.

Photographs: please provide either high quality digital images (250 dpi resolution) or original prints. Computer print-outs or photocopies will not reproduce well enough for publication. Colour photographs rarely reproduce satisfactorily in black and white.

The facility exist for color reproduction, however the inclusion of color photographs in a paper must be agreed with Editor in advance.

Reporting analytical and spectral data

The following is the recommended style for analytical and spectral data presentation:

1. ***Melting and boiling points***:
   mp 163–165°C (lit. 166°C)
   mp 180°C dec.
   bp 98°C
   Abbreviations: mp, melting point; bp, boiling point; lit., literature value; dec, decomposition.
2. ***Specific Rotation***:
   $[a]^{23}_{D}$ –222 (*c* 0.35, MeOH).
   Abbreviations: a, specific rotation; D, the sodium D line or wavelength of light used for determination; the superscript number, temperature (°C) at which the determination was made; In parentheses: *c* stands for concentration; the number following *c* is the concentration in grams per 100 mL; followed by the solvent name or formula.

3. ***NMR Spectroscopy***:
   ^{1}H NMR (500 MHz, DMSO-d_6) d 0.85 (s, 3H, CH_3), 1.28–1.65 (m, 8H, 4´CH_2), 4.36–4.55 (m, 2H, H-1 and H-2), 7.41 (d, *J* 8.2 Hz, 1H, ArH), 7.76 (dd, *J* 6.0, 8.2 Hz, 1H, H-1'), 8.09 (br s, 1H, NH).
   ^{13}C NMR (125 MHz, $CDCl_3$) d 12.0, 14.4, 23.7, 26.0, 30.2, 32.5, 40.6 (C-3), 47.4 (C-2'), 79.9, 82.1, 120.0 (C-7), 123.7 (C-5), 126.2 (C-4).
   Abbreviations: d, chemical shift in parts per million (ppm) downfield from the standard; *J*, coupling constant in hertz; multiplicities s, singlet; d, doublet; t, triplet; q, quartet; and br, broadened. Detailed peak assignments should not be made unless these are supported by definitive experiments such as isotopic labelling, DEPT, or two-dimensional NMR experiments.
4. ***IR Spectroscopy***:
   IR (KBr) n 3236, 2957, 2924, 1666, 1528, 1348, 1097, 743 cm^{-1}.
   Abbreviation: n, wavenumber of maximum absorption peaks in reciprocal centimetres.
5. ***Mass Spectrometry***:
   MS *m/z* (relative intensity): 305 (M^+H, 100), 128 (25).
   HRMS–FAB (*m/z*): $[M+H]^+$ calcd for $C_{21}H_{38}N_4O_6$, 442.2791; found, 442.2782.
   Abbreviations: *m/z*, mass-to-charge ratio; M, molecular weight of the molecule itself; M^+, molecular ion; HRMS, high-resolution mass spectrometry; FAB, fast atom bombardment.
6. ***UV–Visible Spectroscopy***:
   UV (CH_3OH) l_{max} (log e) 220 (3.10), 425 nm (3.26).
   Abbreviations: l_{max}, wavelength of maximum absorption in nanometres; e, extinction coefficient.
7. ***Quantitative analysis***:
   Anal. calcd for $C_{17}H_{24}N_2O_3$: C 67.08, H 7.95, N 9.20. Found: C 66.82, H 7.83, N 9.16. All values are given in percentages.
8. ***Enzymes and catalytic proteins relevant data:***
   Papers reporting enzymes and catalytic proteins relevant data should include the identity of the enzymes/proteins, preparation and criteria of purity, assay conditions, methodology, activity, and any other information relevant to judging the reproducibility of the results[1]. For more details check Beilstein Institut/STRENDA (standards for reporting enzymology data) commission Web site (http://www.strenda.org/documents.html).

[1] For all other data presentation not mentioned above please contact Editor for instructions.

Submission Checklist

The following list will be useful during the final checking of an article prior to sending it to the journal
for review:

- E-mail address for corresponding author,
- Full postal address,
- Telephone and fax numbers,
- All figure captions,
- All tables (including title, description, footnotes),
- Manuscript has been "spellchecked" and "grammar-checked",
- References are in the correct format for the journal,
- All references mentioned in the Reference list are cited in the text, and *vice versa*.

Submissions

Submissions should be directed to the Editor by e-mail: ***glasnik@pmf.unsa.ba***, or ***glasnikhtbh@gmail.com***. All manuscripts will be acknowledged on receipt (by e-mail) and given a reference number, which should be quoted in all subsequent correspondence.

Glasnik hemičara i tehnologa Bosne i Hercegovine

Bulletin of the Chemists and Technologists of Bosnia and Herzegovina

Print ISSN: 0367-4444
Online ISSN: 2232-7266

Zmaja od Bosne 33-35, BA-Sarajevo
Bosnia and Herzegovina
Phone: +387-33-279-918
Fax: +387-33-649-359
E-mail: glasnik@pmf.unsa.ba
glasnikhtbh@gmail.com

Sponsors

Glasnik hemičara i tehnologa Bosne i Hercegovine

Bulletin of the Chemists and Technologists of Bosnia and Herzegovina

Print ISSN: 0367-4444
Online ISSN: 2232-7266

Zmaja od Bosne 33-35, BA-Sarajevo
Bosnia and Herzegovina
Phone: +387-33-279-918
Fax: +387-33-649-359
E-mail: glasnik@pmf.unsa.ba
glasnikhtbh@gmail.com

www.elektroprivreda.ba/stranica/te-kakanj

Federalno ministarstvo obrazovanja i nauke

Zahvaljujemo se **Federalnom ministarstvu obrazovanja i nauke** na finansijskoj pomoći za izdavanje ovog broja ***Glasnika hemičara i tehnologa Bosne i Hercegovine***.

Redakcija GLASNIK-a